Lawrence Berkeley National Laboratory
Recent Work

Title

THERMAL IMPACT OF WASTE EMPLACEMENT AND SURFACE COOLING ASSOCIATED WITH GEOLOGIC DISPOSAL OF HIGH-LEVEL NUCLEAR WASTE

Permalink

https://escholarship.org/uc/item/1q14r9df

Authors

Mangold, D.C.
Tsang, C.F.

Publication Date

1986-12-01

eScholarship.org Powered by the California Digital Library
University of California

LBL-22615
Preprint

Lawrence Berkeley Laboratory
UNIVERSITY OF CALIFORNIA

EARTH SCIENCES DIVISION

RECEIVED
LAWRENCE
BERKELEY LABORATORY
JUN 2 1987
LIBRARY AND
DOCUMENTS SECTION

Submitted to Environmental Geology

THERMAL IMPACT OF WASTE EMPLACEMENT AND SURFACE COOLING ASSOCIATED WITH GEOLOGIC DISPOSAL OF HIGH-LEVEL NUCLEAR WASTE

J.S.Y. Wang, D.C. Mangold, and C.F. Tsang

December 1986

TWO-WEEK LOAN COPY

This is a Library Circulating Copy which may be borrowed for two weeks.

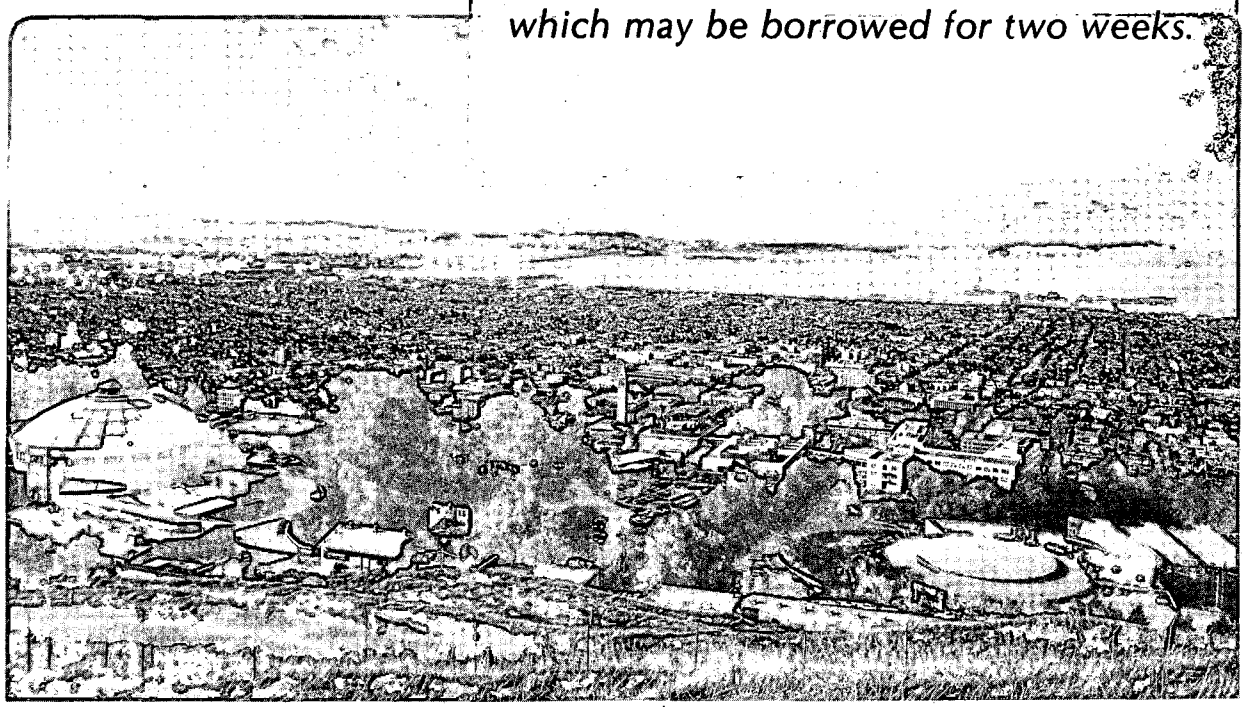

Prepared for the U.S. Department of Energy under Contract DE-AC03-76SF00098

LBL-22615

DISCLAIMER

This document was prepared as an account of work sponsored by the United States Government. While this document is believed to contain correct information, neither the United States Government nor any agency thereof, nor the Regents of the University of California, nor any of their employees, makes any warranty, express or implied, or assumes any legal responsibility for the accuracy, completeness, or usefulness of any information, apparatus, product, or process disclosed, or represents that its use would not infringe privately owned rights. Reference herein to any specific commercial product, process, or service by its trade name, trademark, manufacturer, or otherwise, does not necessarily constitute or imply its endorsement, recommendation, or favoring by the United States Government or any agency thereof, or the Regents of the University of California. The views and opinions of authors expressed herein do not necessarily state or reflect those of the United States Government or any agency thereof or the Regents of the University of California.

LBL-22615

THERMAL IMPACT OF WASTE EMPLACEMENT AND SURFACE COOLING ASSOCIATED WITH GEOLOGIC DISPOSAL OF HIGH-LEVEL NUCLEAR WASTE

J. S. Y. Wang, D. C. Mangold, and C. F. Tsang

Earth Sciences Division
Lawrence Berkeley Laboratory
University of California
Berkeley, California 94720

December 1986

Submitted to
Environmental Geology

Short title: Thermal Impact of Nuclear Waste Disposal

This work was supported by the U.S. Department of Energy under Contract No. DE-AC03-76SF00098.

ABSTRACT

This paper studies the thermal effects associated with the emplacement of aged radioactive high-level wastes in a geologic repository, with emphasis on the following subjects: the waste characteristics, repository structure, and rock properties controlling the thermally induced effects; the thermal, thermomechanical, and thermohydrologic impacts, determined mainly on the basis of previous studies that assume 10-year-old wastes; the thermal criteria used to determine the repository waste loading densities; and the technical advantages and disadvantages of surface cooling of the wastes prior to disposal as a means of mitigating the thermal impacts. The waste loading densities determined by repository designs for 10-year-old wastes are extended to older wastes using the near-field thermomechanical criteria based on room stability considerations. Also discussed are the effects of long surface cooling periods determined on the basis of far-field thermomechanical and thermohydrologic considerations. The extension of the surface cooling period from 10 years to longer periods can lower the near-field thermal impact but have only modest long-term effects for spent fuel. More significant long-term effects can be achieved by surface cooling of reprocessed high-level waste.

ABBREVIATIONS

BWR	boiling water reactor
DHLW	defense high-level waste
DOE	Department of Energy
EIA	Energy Information Administration
EIS	Environmental Impact Statement
EPA	Environmental Protection Agency
FBR	fast breeder reactor
GEIS	Generic Environmental Impact Statement
HLW	high-level waste
HTR	high-temperature reactor
HWR	heavy water reactor
INFCE	International Nuclear Fuel Cycle Evaluation
KBS	Karnbranslesakerhet, Swedish Nuclear Fuel Safety Program
LBL	Lawrence Berkeley Laboratory
LWR	light water reactor
MOX	mixed oxide fuel
MTHM	metric ton of heavy metal
NRC	Nuclear Regulatory Commission
NWTS	National Waste Terminal Storage Program
OCRD	Office of Crystalline Repository Development
ONWI	Office of Nuclear Waste Isolation
OWI	Office of Waste Isolation

PWR	pressurized water reactor
RH-TRU	remotely handled transuranic-contaminated waste
RRC-IWG	Reference Repository Conditions Interface Working Group
SF	spent fuel
SNL	Sandia National Laboratories
WIPP	Waste Isolation Project Plant

1. INTRODUCTION

Thermal loading is a principal consideration in the design and evaluation of a repository for geologic disposal of nuclear wastes. The age of the wastes--the length of time between their removal from the reactor cores and their final emplacement in a repository--is a significant factor in determining the waste's heat power at emplacement and the thermal effects on the waste's surroundings. Although many studies in the past decade have demonstrated the importance of thermal effects on all components involved--the waste canisters, the repository structure, and the surrounding geologic setting--most of the studies have focused on the effects of 10-year-old wastes. Because no nuclear waste repositories have yet been constructed, a substantial part of the wastes eventually placed in a given repository would have been stored on the surface much longer than 10 years. The emplacement of older wastes may also be preferred if the thermally induced effects are of major concern. Several European countries (Great Britain, West Germany, Sweden, Belgium) plan to allow their nuclear wastes to cool on the surface for longer periods (25, 40, or 100 years) before emplacing the material in a permanent site. The International Council of Scientific Unions Committee on the geologic disposal of high-level waste concluded that "interim storage of radwaste for periods of 100 years is desirable" (Fyfe and others 1984).

To evaluate the effects of different surface cooling periods and waste loading densities, it is important to specify the spatial scales and the time spans of concern. In the immediate vicinity of a waste

canister, it is desirable to maintain the structural integrity of the waste package and to limit the release of radionuclides. In the near-field, the thermomechanical stability of the shafts and underground openings may be adversely changed if the heat power and the density of wastes are too high. The stability of the repository structure is the main concern for the safety of underground operations during the excavation, emplacement, and retrieval periods. On the regional scale, the thermal impacts persist for thousands of years. Thermal loading of the rock formation may induce surface uplift and may change the hydrologic properties of the rocks. The thermally induced buoyancy gradient may cause vertical movement of the groundwater and thus accelerate the transport of radionuclides from the repository to the accessible environment.

The magnitudes of the thermal, mechanical, and hydrologic impacts depend on the heat power and waste loading density. The waste loading density is a key parameter in repository design. Although it is desirable to localize the wastes and minimize the size of a repository, it is also necessary to keep the waste loading low to limit the thermally induced impacts. The existing thermal design criteria are developed mainly on the basis of many years of research on salt and several recent investigations on hard rocks as possible geologic settings for a repository for 10-year-old wastes.

This study evaluates the thermal guidelines for optimal thermal loadings, emphasizing the effects of the surface cooling periods of the wastes. As part of this effort, a comprehensive review was made

of the available research literature on thermal effects, thermal criteria, and material properties of mined geologic repositories and their environment. Such a review of the sensitivity of the repository and the geologic setting to various parameters is aimed at elucidating the significance of these parameters in assessing the repository performance.

Since most of the early studies in the literature were based on the effects of 10-year-old wastes, additional calculations on the effects of different pre-disposal surface cooling times were performed to supplement the available data in the literature. The results lead to a clearer understanding of the importance of surface cooling in evaluating the overall thermal effects of a radioactive waste repository.

This paper is based on a report prepared for the U.S. Nuclear Regulatory Commission (NRC) (Wang and others 1983), with some condensation and literature update. In the United States, most of the recent repository studies have shifted from generic assessments to site-specific characterizations and experiments. The literature review in this paper is focused on the generic studies, especially the research works in support of the U.S. Department of Energy's (DOE) Environmental Impact Statements (EIS) in the period of the middle 1970's to the early 1980's. The vast amount of new data from on-going site characterization activities and field experiments will not be extensively reviewed. Many results from the current site-specific

studies are discussed in a series of 1986 DOE Enviromental Assessment reports (DOE 1986a,b,c,d,e). More detailed studies will be in DOE Site Characterization reports to be published in the late 1980's for the Deaf Smith salt, Hanford basalt, and Yucca Mountain tuff sites. In addition to site characterization, repository design and performance assessment are two other important tasks in high-level waste repository studies. With the delays in repository startups and the potential use of a Monitored Retrievable Storage facility before final storage in a geologic repository (DOE 1985, 1986f,g,h; NRC 1986), the study of the effects of surface cooling on repository thermal impacts remains an important topic in repository design and performance assessment.

In the remainder of this section, an overview of the thermally induced effects is given as an outline of this paper. In Section 2, the temperature rise, thermomechanical stability, and thermohydrologic perturbations due to the presence of a nuclear waste repository are reviewed. Most of these discussions are for the case of 10-year-old wastes, which have received the most attention. In Section 3, existing thermal criteria for nuclear waste repositories are summarized and evaluated. Both the conceptual and the experimental bases of the criteria are investigated. Section 4 presents a detailed examination of thermal calculations concerning different surface cooling periods. It is shown that the benefit of a longer surface cooling period is substantial for reprocessed high-level wastes but is marginal for spent fuel. Great care must be exercised if one attempts

to scale results of repository design studies and calculations based on 10-year-old wastes to older wastes.

1.1 THERMALLY INDUCED IMPACTS

To assess the thermal impacts in general, and the effects of different surface cooling periods in particular, it is important to specify the thermal loading, the repository design and operation, and the geologic setting. With the specification of these controlling parameters, one can then evaluate the perturbations of the temperature field, the rock deformation, and the fluid flow and radionuclide migration in the engineered structure and its surrounding environs.

1.1.1 Major Parameters

1.1.1.1 Thermal loading

In order to control the thermal effects in and around the repository, it is crucial to determine the thermal loading. The thermal loading is specified by the cooling and emplacement operations:

- duration of surface cooling periods before repository emplacement,
- waste types and heat power at emplacement, and decay thereafter,
- waste distribution and density within the repository, and
- loading sequence of waste emplacement.

Once these initial conditions have been specified, the thermal effects for a given rock type can be readily determined, at least in terms of bounding values from the known heat generation rates of the particular waste types and the available data on properties of the rock forma-

tions. Different surface cooling periods will induce different thermal impacts on the repository and its surrounding environment over time.

1.1.1.2 Repository structure and operation

The waste emplacement configuration depends on the repository structure. A repository will have several different shafts for the transportation of personnel, equipment, wastes, and the flow of air for ventilation. From the shafts, main corridors and long storage rooms extend into the surrounding rock formation. The important design parameters for thermal considerations are the geometrical dimensions of

- canister emplacement holes,
- hole pattern and arrays,
- room-and-pillar separation, and
- repository extension, shape, depth, and size.

The radius of the hole and the size of the gap between the canister and the rock are important for the determination of waste, canister, and hole temperatures. The hole pitch (separation distance between holes) and row separation determine the region of rock to be heated by each waste canister. The repository size, shape, and depth determine the waste emplacement capacity and the long-term thermal impact of a waste repository.

For the safety of operation during underground excavation and waste emplacement, ventilation will be maintained throughout the operational life of a repository. The ventilation will remove a fraction of the heat released by the waste. This underground cooling is an ex-

tension of surface cooling before emplacement. The requirement that the waste be maintained in a retrievable condition may extend the effective cooling period. The U. S. Nuclear Regulatory Commission's (NRC) proposed regulation (Code of Federal Regulations, Title 10, Part 60, 1983) would require that the geologic repository operations area be designed so that the entire inventory of waste could be retrieved on a reasonable schedule, starting at any time up to 50 years after waste emplacement operations are initiated. According to the same proposed regulation, a reasonable schedule is one that requires no longer than about the same overall period of time that was devoted to construction of the repository and emplacement of the wastes.

1.1.1.3 Geologic setting

Heat released from the wastes in the repository will be dissipated in the surrounding rock formations and will eventually be transferred to the ground surface. Depending on the location, the thermal impacts at a point in the rock formation will first increase and then slowly decrease, so that the host rock will eventually be returned to its original ambient condition, since the heat generation rate of the waste continuously decreases and the heat transfer processes slowly remove the heat. The spatial and temporal distribution of the thermal impacts depend on

- waste thermal loading in the repository,
- rock types,
- thermal, mechanical, and hydrologic properties,

- lithology and boundaries, and
- ambient conditions.

Bedded and domed salt, granite, basalt, shale, tuff, and alluvium are among the rock formations which have been considered for waste repositories. The geologic setting is the last barrier to prevent the escape of radionuclides to the accessible environment. Over the geologic time scale of thousands of years, the geologic setting could be effective in providing the required isolation if a stable formation is chosen and a suitable location is found. However, the uncertainties associated with formation inhomogeneity and variation in rock properties require that conservative and stringent criteria be imposed on the magnitude of thermal perturbations to be allowed in the ambient temperature field, the in situ stress field, and the regional groundwater movement.

1.1.2 Main Effects

1.1.2.1 Temperature rise, stress change, and buoyancy flow

The main concern in the assessment of the thermal impact of the wastes is on the thermally induced phenomena at different locations and various periods of time:

- temperature rise in the very-near-field of the canister-borehole region,
- thermomechanical stability in the near-field of room-and-pillar structure, and
- thermohydrologic perturbation in the far-field over the groundwater basin and the recharge-discharge flow pattern.

After the emplacement of a waste canister, the temperatures of the waste, the canister, and the borehole wall increase very rapidly to quasi-steady values that are maintained over long periods. The primary concern about these elevated temperatures is the maintenance of the integrity of the engineered containment. The stability of the room roof and the pillar support is essential for the safety of operations during the excavation, emplacement, and retrieval periods. The development of a buoyancy gradient over thousands of years is directly related to the effectiveness of the geologic setting in isolating the radionuclides.

1.1.2.2 Couplings between heat, fluid, and rocks

Before proceeding with a quantitative discussion of the findings in the literature on these thermal, mechanical, and hydrologic effects, it is appropriate to point out that most of the studies evaluate waste impact on heat, rock, and fluid in a stepwise, uncoupled approach. For the low-permeability, small-deformation effects expected for the waste impact, the simple approach is usually justifiable. However, it should also be realized that studies employing coupling are needed for better understanding of the physical and chemical processes involved, especially in the near-field (Tsang 1980; Carnahan 1983; LBL 1984; de Marsily 1985; Cook 1985). The coupling processes of primary concern are

- thermal-buoyancy flow coupling,
- thermal-stress coupling, and
- flow-stress coupling.

Both water and rocks exhibit a certain number of temperature-dependent properties. The density and viscosity of water are well-known functions of temperature. The gravitational force imbalance between the hot fluid near the repository and the ambient cold fluid in the surrounding formation induces a vertically upward driving gradient on the fluid flow. This may perturb the existing pattern of groundwater flow driven by pressure gradients. Also, the various rock types show varying degrees of expansion and deformation behavior as functions of temperature. Different rock formations may respond in a variety of ways to a thermal-stress coupling; for example, salt flows plastically, granite fractures absorb thermal stress nonlinearly, and shale shrinks above the boiling point. This in turn may have implications for fluid flow through a permeability-stress coupling. The counterbalance between the fluid pressure and the rock stress gives rise to the coupling between fluid behavior and rock deformation.

The coupling effects may be more easily appreciated in schematic form, which includes solute (for example, dissolved salt) and radionuclide transport (Fig. 1.1). The thermal loading is clearly the main source for the heat transfer, which influences the rock stress, fluid flow, and chemical processes. In these relationships, the fluid flow is likely to have a rather small effect on the temperature field. Except for the near-field, rock formations chosen for the repository should be nearly impermeable. The rock stress may significantly affect the fluid flow through the operation of the permeability-stress

coupling, especially for fractured media. In addition, heat may have a strong influence on the rock stress.

The couplings involving chemical solute transport and reactions are important, but will not be included within the scope of this study. The geochemical reactions and corrosion effects on the waste packages are highly temperature-dependent. The effect of temperature on solubility, sorption, and rates of reaction may be generally known, but further investigation is required to discover their precise degree of influence on the rocks, water, and radionuclides involved in nuclear waste isolation. The couplings between fluid flow and chemical processes are likewise quite important. Fluid flow transports the chemical species, and any dissolution or precipitation will affect the geometry of flow paths, such as the fracture aperture, which in turn will have a significant effect on fluid flow. The heat-rock-fluid-solute-radionuclide couplings are probably critical at the canister-borehole scale. They may also be important at the regional scale, although the processes could be much slower.

1.1.2.3 Effect on radionuclide transport

The focus of all of these interactive processes is the transport of radionuclides through the geologic setting to the accessible environment by fluid flow. It is generally recognized that the principal means of radionuclide transport is the movement of groundwater into, through, and out of the repository. Even though rock stress is important to the understanding of the thermal effects in and around the repository, its influence on radionuclide transport is largely through

its effect on permeability for fluid flow. Also, although several chemical processes are quite significant in radionuclide transport (solubility, complexing, sorption, etc), they basically determine only the extent to which radionuclides can be dissolved and how well they are retarded while being carried by the groundwater. Thus the most conservative way of estimating travel times of the waste to the accessible environment is to calculate the time for the fluid to reach the surface from the repository, assuming perfect solubility of the waste and negligible retardation by complexing, sorption, precipitation, etc.

Fluid transport of the radioactive wastes has important implications for the repository's thermal criteria. Even though the host rock may have a very low permeability, the thermal pulse from the decaying wastes will produce a buoyancy gradient in the groundwater surrounding the repository. The effect of this gradient is to create a driving force for water movement from the repository to the surface at rates above the typical regional flow. Travel paths may become more vertical, and therefore shorter than unperturbed regional flow paths. An important point of the present study is to bring these thermohydrologic effects into consideration and to discuss their implications for the thermal criteria of a nuclear waste repository.

2. THERMAL, THERMOMECHANICAL, AND THERMOHYDROLOGIC EFFECTS OF 10-YEAR-OLD WASTES

The need to manage existing and projected radioactive wastes is noted in many studies. Although the effects of the duration of surface cooling periods have been considered in several parametric studies (which are reviewed in Section 4), most studies treat 10-year-old waste as the baseline case. Therefore, this section is devoted mainly to the review of the effects of storing 10-year-old wastes. Since the decay heat characteristics are important for the assessment of waste impacts, several aspects of decay heat generation are discussed in Section 2.1. Section 2.2 reviews relevant features of the mined repository design, and Section 2.3 summarizes the thermal, mechanical, and hydrologic properties of the rock formations being considered as hosts for waste repositories. Following this are detailed reviews of the thermal impact of 10-year-old wastes on the temperature rise at the canister-hole scale in Section 2.4, the thermomechanical stability of the room-and-pillar structure in Section 2.5, and the thermohydrologic perturbation of groundwater movement at the regional scale in Section 2.6. This survey of thermal impacts not only summarizes results of waste heat studies, but also serves as a basis for discussing the effects of different surface cooling periods in later sections.

2.1 WASTE HEAT SOURCE CHARACTERIZATION

The magnitude of thermally induced impacts is controlled by the spatial and temporal distributions of waste heat sources. The amount of heat for a given amount of waste depends on the waste composition, which in turn depends on the nuclear fuel cycle employed, waste content, and waste age.

2.1.1 Decay Heat Generation of Nuclear Fuel Cycles

In the United States, the commercial nuclear reactors used are principally light water reactors (LWR), which use ordinary (light) water both as a circulating coolant and as a neutron moderator. There are two types of LWR: the pressurized water reactor (PWR) and the boiling-water reactor (BWR). Different reactors with alternative fuel compositions, cooling fluids, and moderating materials have also been developed. The International Nuclear Fuel Cycle Evaluation Conference (INFCE 1980) compares the thermal impacts of the different fuel cycles.

After a specified "burnup" time, the fuel is removed from the reactor, and the remaining uranium or plutonium, or both, can be recycled by fuel reprocessing if desired. Three cycles for LWR have been studied extensively by the NRC, the Environmental Protection Agency (EPA), and the Department of Energy (DOE) for their impact on commercial high-level waste management:

- Spent Fuel Cycle: This is the "throwaway" or once-through cycle. The irradiated fuel assemblies from an LWR core are disposed of directly as waste after being removed from the reactor. The spent fuel (SF) contains both uranium and plutonium as waste components.

- Uranium-only Recycle: This is a "partial" recycle operation. The spent fuel from an LWR is reprocessed by removing most of the uranium and plutonium in order to recycle the uranium for further use as fuel. The reprocessed high-level waste (HLW) contains only trace amounts of uranium and plutonium.
- Uranium and Plutonium Recycle: This is a "total" recycle, in which both uranium and plutonium are recovered from the spent fuel to form a "mixed oxide (MOX) of UO_2 and PuO_2 for further use as fuel. With effectively more extensive burnup in a MOX cycle, the trace amounts of uranium and plutonium remaining in the MOX reprocessed waste are higher than those contained in the U-only recycle.

These fuel cycles produce waste types of different composition and decay heat generation rates. Figure 2.1 shows the power densities for each of the three cycles. The wastes all originate from the same amount of fuel, 1 metric ton of heavy metal U (MTHM), charged to a pressurized water reactor (PWR).

Radioactive waste from any of the nuclear fuel cycles is composed of two main components: fission products (such as Sr-90 and Cs-137) and transuranic actinides (such as Pu, Am, and Cm). For the first few hundred years, the fission products are the principal contributors to the decay heat generation. This fission product activity is largely independent of the fuel mix, and the heat generation is similar for all three cases of the nuclear fuel cycle. However, the quantities of actinides vary widely according to the fuel cycle. After the first

few hundred years, these relatively long-lived heavy transuranic actinides become the major contributors to the decay heat generation. Therefore, in the long term it is the decay heat characteristics of the actinides and their daughters that control the heat generation of the radioactive wastes.

In Figure 2.1 the solid curves are plotted from tabulated data given in Kisner and others (1978). The U-only recycle contains only the reprocessed high-level waste (HLW) without the plutonium. The U + Pu recycle is based on the assumed 1:3 blend of MOX fuel and UO_2 fuel. For comparison, Figure 2.1 also includes points plotted from the tabulated data in reports by the EPA (1977) and the DOE (1980a). The spent fuel data are consistent among all three data sets. For the U + Pu HLW cycle, the EPA report assumed a 1:2 MOX:UO_2 ratio. The total MOX cycle is not expected to be used in the near future. The MOX:UO_2 ratio of 1:2 in the EPA (1977) study and the 1:3 ratio in the GEIS study (Science Applications Inc 1976) reflect the likelihood that a low percentage of the MOX cycle will be used for electricity generation. The differences in Figure 2.1 among the results of the three reports reflect the sensitivity of the contents of long-lived plutonium in the wastes to different assumptions in fuel mix, reactor burnup, and reprocessing treatment. Storch and Prince (1979) discuss the different source term data sets and other potential fuel cycles.

2.1.2 Waste Packages

The individual spent fuel canister usually contains one fuel assembly. For a PWR, the waste content of one fuel assembly is 0.4614

MTHM. This means that for 10-year-old wastes, the heat power is 0.55 kW/canister. For a BWR, the waste content is 0.1833 MTHM, and the 10-year-old heat power is 0.18 kW for each spent fuel assembly (Kisner and others 1978). The possibility of packing more than one fuel assembly into one canister was also considered (EPA 1977; Altenbach 1978).

For reprocessed HLW, the waste content in each canister can be controlled in the reprocessing procedure. Indeed, the maximum canister load is a design parameter that can be determined by a very-near-field thermal criterion. For 10-year-old HLW, high emplacement heat-power values have been used in earlier studies; for example, a 5-kW/canister value in Cheverton and Turner (1972) and Callahan and others (1975), and 3.95-kW/canister in EPA (1977). However, there is a general trend to lower the canister heat power, reflecting the concern over the waste heat impacts. The Reference Repository Conditions Interface Working Group (RRC-IWG) in the National Waste Terminal Storage (NWTS) Program (RRC-IWG 1980, 1983), used the values of 2.16 kW/canister and 1.0 kW/ canister.

The spent fuel waste form consists of an assembly of fuel rods coated with zircalloy cladding. With low thermal power per canister, high cladding thermal conductivity (Science Application Inc 1978), and additional radiative heat transfer among the fuel rods (Cox 1977), the spent fuel temperature rise is lower in most of the cases studied than the reprocessed HLW temperature rise.

The reprocessed HLW waste form depends on the solidification process employed. The thermal conductivity and leach resistance of HLW can be improved upon by the vitrification process, which incorporates HLW in a glass or ceramic form. Embedding waste-containing beads within a metallic matrix has been suggested to improve the thermal conductivity of reprocessed wastes.

In addition to carbon steel and stainless steel, titanium and copper are potential candidates for canister material. The canister wall may also be thickened to resist corrosion and to withstand the high temperatures. Most studies assume that the canister is a cylinder. However, rectangular-shaped canisters for spent fuel assemblies have also been considered. Outside the canister, an overpack can be added for additional protection. In addition to metals, ceramics, graphite and carbon materials, a wide variety of glasses and specially selected cements are being studied as potential overpack materials (DOE 1980a).

2.1.3 Waste Quantities and Ages

Projections of the amounts of radioactive waste are required in order to determine the number and size of waste repositories. The projections are determined by the growth rate of nuclear power generation capacity. The U.S. nuclear growth capacity has been lowered substantially in recent years with changes in national energy plans, environmental and regulatory constraints, and electricity demands. For example, the projection at year 2000 was 480 Gw(e) by Kisner and others (1978); 250 Gw(e) in DOE (1980a) and 123 GW(e) in DOE (1985).

The DOE Energy Information Administration (EIA) periodically forecasts nuclear power capacities.

With different projections, the estimates of cumulative spent fuel discharged from nuclear reactors varies. The cumulative spent fuel value in the DOE Environmental Impact Statement (EIS) Case 3 was 239,000 MTHM at year 2040 (DOE 1980a). The 1984 EIA middle-case value is 130,000 MTHM at year 2020 (DOE 1985). Two repositories are currently being considered in the United States, each having a capacity to receive 70,000 MTHM of wastes (DOE 1985).

The waste ages arriving at a repository depend on the repository startup date, the repository receiving capacity, and the backlog of the wastes. The EIS analyses for three assumed repository startup dates are shown in Figure 2.2 (DOE 1980a). With repository startup at year 2010, most of the spent fuel received by the repository will be much older than 10 years. For the case of a 2030 startup, the minimum age is 19 years.

2.2 MINED REPOSITORY DESIGN

The initial United States repository design study was Project Salt Vault in Lyons, Kansas (Bradshaw and McClain 1971; Cheverton and Turner 1972). Experiments and design studies in the 305-m (1000-ft) deep bedded salt repository were conducted for reprocessed HLW storage. Since then, modeling studies have been performed to characterize the thermal environment in different media for the storage of spent fuel and reprocessed HLW. These include the engineering design studies

of a reprocessed HLW repository in domed salt (Stearns-Roger Engineering Co 1979), a spent fuel repository in bedded salt (Kaiser Engineers 1978a,b), and a spent fuel repository in basalt (Kaiser Engineers and others 1980), as well as generic and scoping studies for granite (Lindblom and others 1977), shale (Thomas and others 1981), tuff (Bulmer and Lappin 1980; see also SNL 1986), and alluvium (Smyth and others 1979). Reference repository conditions for the first five rock types have been developed in a DOE/NWTS study (RRC-IWG 1980).

2.2.1 Emplacement Hole Description

Most repository designs specify placing waste canisters in vertical holes drilled into the storage room floors. One canister per hole is usually assumed. Horizontal emplacement with multiple-canister strings in long holes between corridors has been considered (Stinebaugh and others 1986). After canister emplacement, the hole is plugged with either concrete or backfill material. Engineered backfill and a liner can provide additional protection for the waste package and maintain the retrievability option; this will usually require a larger diameter hole. The main thermal concern is to design engineered structures with high thermal conductivities in order to avoid excessive temperature rises in the canister and waste. Crushed rock and small air gaps are poor thermal conductors. Typically, the thermal conductivity of crushed rock is one-tenth that of the uncrushed materials.

2.2.2 Room-and-Pillar Design

The geometrical dimensions of the storage rooms and the separation of the tunnels are two important factors in determining the stability of the excavation and its convenience for underground operations. Safety concerns have increased the pillar width from the 7.6-m value considered in Cheverton and Turner (1972) for a bedded salt HLW repository to 18-30 m in RRC-IWG (1980). The main concerns of room-and-pillar design have been the room deformation (roof sag, wall convergence, floor heave) in soft rocks and the possibility of rock fracturing in hard rocks during the repository operation-retrievability periods. These are the main factors considered in determining the allowable thermal loading in a repository.

2.2.3 Repository Configuration

The areal thermal loading and the repository depth below surface for the NWTS reference repositories are shown in Table 2.1. The average areal loading includes shafts and drifts, whereas the local areal loading refers only to the space within the storage area. The thermal loading value of 25 W/m^2 (100 kW/acre) for salt, granite, and tuff is two-thirds of the 37-W/m^2 (150-kW/acre) value that was considered in the mid-1970s. The latter value is adjusted downward from the maximum permissible thermal loading of 39 W/m^2 (158 kW/acre) based on salt temperature considerations (Cheverton and Turner 1972). The NWTS values for salt and other rocks, however, are high, especially for spent fuel repositories.

Table 2.1. NWTS Areal Loading.

Rock	Salt		Granite		Basalt		Shale		Tuff	
Waste	SF	HLW	SF	HLW	SF	HLW	SF	HLW	SF	HLW
Depth (m)	600	600	1,000	1,000	1,000	NA	600	600	800	800
Local Areal Thermal Loading (W/m^2)	25	25	20	25	12.3	NA	10	10	25	25
Average Areal Thermal Loading (W/m^2)	15	<25	<20	<25	8.2	NA	8	8	<25	<25

(RRC-IWG 1980)

Table 2.2 presents the GEIS values (Science Applications Inc 1978) based on a thermomechanical analysis during the 25-year retrievability period for spent fuel and the 5-year retrievability period for HLW. Long-term, far-field concerns for surface uplift have also imposed a constraint on the allowable thermal loading for salt (Lincoln and others 1978; Llewellyn 1978). Areal thermal loading is the most important parameter in determining the repository design. In Section 3, we discuss the controlling factors for determining the allowable thermal loading and present the detailed results on allowable thermal loadings in the draft GEIS and final EIS studies.

A single mined layer at a given desirable depth has been considered in most of the repository design studies. Such a configuration is ideal for layered formations (such as bedded salt), which are relatively thin but areally extensive. For intrusive formations, such as salt domes and granitic plutons, the lateral extension is limited, and either a multilayer repository structure or deeper boreholes with stacked canisters may be required (Just 1978; Kevenaar and others 1979).

The repository depths considered in most of the studies range from 300 m to 1000 m. The areal extensions are typically 1-3 km. A disk with a 1.61 km radius covers an area of 8.1 km^2 (2,000 acres). The 8.1 km^2 (2,000-acre) repository has been considered in a number of studies (EPA 1977; Kaiser Engineers 1978a; Stearns-Roger Engineering Co 1979; DOE 1980a).

Table 2.2. GEIS Areal Loading Based on Near-Field Thermomechanical Stress Studies.

Rock	Salt		Granite		Basalt		Shale	
Waste	SF[a]	HLW[b]	SF[a]	HLW[b]	SF[a]	HLW[b]	SF[a]	HLW[b]
Areal Loading (W/m^2)	9	37	20	47	20	47	14	30

(Science Applications Inc 1978)

[a] 25-year retrievability.

[b] 5-year retrievability.

2.3 ROCK FORMATION PROPERTIES

In addition to the waste heat source and repository dimensions, the thermal impacts depend on the rock properties of the geologic formations surrounding the repository. This section discusses the thermal, mechanical, and hydrologic parameters controlling the waste impacts.

2.3.1 Thermal Properties

The baseline thermal properties of four major rock types (salt, granite, basalt, and shale) considered in the GEIS (DOE 1979b) and the ranges of values of tuff considered by Tyler (1979) and of alluvium considered by Smyth and others (1979) as candidate repository host rocks are summarized in Table 2.3. Preliminary site-specific data tabulated in recent DOE reports are also included in parentheses for comparison. For conductive heat transfer, the controlling parameters are the thermal conductivity and the volumetric heat capacity (specific heat times density). The simple analytic results summarized in the Appendix indicate that the short-term temperature rises near the canister-rock interface are mainly determined by the thermal conductivity. For the average temperature rise at the repository level, the temperature rise is determined by the product of thermal conductivity and volumetric heat capacity for simple analytic solutions. The long-term, far-field thermal responses are related to the heat content in the rock which is described by the volumetric heat capacity. The rate of transient heat conduction is governed by the thermal diffusivity, that is, the ratio of thermal conductivity to volumetric heat capacity.

Table 2.3. Thermal Properties of Rocks.

Rock	Thermal Conductivity (W/m-°C)	Specific Heat (J/kg-°C)	Density (kg/m^3)
Salt	2.08-6.11[a] (3.15±0.54)[f]	840-920[b] (902.9±5.0)[f]	2,128[c] (2,190±60)[f]
Granite	1.99-2.85[a]	880-960[b]	2,640[c]
Basalt	1.16-1.56[a] (1.51±0.15)[g]	710-920[b] (847.6±9.3)[g]	2,880[c] (2,840±20)[g]
Shale	1.47-1.68[a]	800-880[b]	2,560[c]
Tuff (welded)	1.2 -1.9[d] (1.6-1.8±0.04)[h]	800-900[d]	2,000-2,400[d]
(nonwelded)	0.4 -0.8[d] (1.0-1.4±0.05)[h]	800-1,700[d]	1,500-2,100[d]
Alluvium (indurated unsaturated)	1.0 -1.2[e]	1,000[e]	1,700[e]

[a] Over the temperature range 0-400°C (DOE 1979b).

[b] Over the temperature range 0-200°C (DOE 1979b).

[c] DOE (1979b).

[d] Tyler (1979).

[e] Smyth and others (1979).

[f] At 100°C, Palo Duro Basin core samples (Lagedrost and Capps 1983; DOE 1986a).

[g] Cohassett Flow, Hanford (DOE 1985, 1986b).

[h] Saturated - dry values, Topopah Spring welded, Calico Hill nonwelded units, Yucca mountain (Tillerson and Nimick 1984; DOE 1985).

The thermal properties of the rocks around the canisters can be determined by in situ heating experiments. In most cases, the in situ values agree with the values measured in the laboratory. These thermal properties can be functions of temperature. Examples of the temperature-dependence of the thermal conductivities and volumetric heat capacities of four different rocks are shown in Figures 2.3 and 2.4. In comparison with thermal conductivities, the volumetric heat capacities are less sensitive to both the temperature and the rock types. The temperature-dependence of the thermal properties is considered in most detailed calculations of the very-near-field temperatures, where the spatial variation (temperature gradient) is high at early times.

The thermal properties of the rocks depend on their mineral compositions. For example, a salt-shale mixture containing 20 percent shale has a thermal conductivity of 3.2 W/m°C at 100°C compared to 4.2 W/m°C for pure salt at the same temperature (Cheverton and Turner 1972). The granite in Stripa, Sweden, with its high quartz content, has a high value of 3.23 W/m°C for thermal conductivity at 100°C (Pratt and others 1977; Chan and others 1980).

The thermal properties of the rocks also depend on their water content. For example, a nonwelded tuff, which has a high water content, generally has a lower thermal conductivity and higher heat capacity than a welded tuff, which has less porosity and a more dense and compacted structure (Tyler 1979; Moss and Haseman 1983). The unsaturated rocks usually have lower thermal conductivity because the air that replaces water in the pores is less conductive.

The thermal properties of rocks may also correlate with their mechanical behavior. For example, it was observed in the Eleana Near-Surface Heater Experiment (Lappin and others 1981) that above 100°C the thermal conductivity of shale decreases as a result of dehydration more than expected on the basis of matrix properties. This result suggests that there is a strong coupling of thermal behavior and volumetric contraction for this rock type, which contains appreciable amounts of expandable clays.

2.3.2 Mechanical Properties

The mechanical properties of five rocks are given in Table 2.4. The values given for the first four rocks are estimates used in the GEIS study (DOE 1979b). The range of values of the two tuff types illustrates the variability of mechanical properties with rock texture. For densely welded tuff, the strength may approach that of hard rocks like granite and basalt. Table 2.4 also includes some site-specific data from recent DOE reports.

Most of the thermomechanical stress analyses assume linear elastic behavior with either isotropic or orthotropic elastic properties. The dependence of elastic properties on temperature, pressure, and time is ignored. However, for realistic representation of the thermomechanical behavior, the nonlinearity of the rocks must be taken into account. The plasticity and creep-flow behavior of salt has received some attention in the literature (for example, Wahi and others 1977). Yet the effects of joints and fractures on repository structures in hard rocks have not been well established. One of the

Table 2.4. Mechanical Properties of Rocks.

Rock	Young's Modulus (GPa)	Poisson's Ratio	Unconfined Compressive Strength (MPa)	Tensile Strength (MPa)
Salt	11.0[a] 27.1±2.8)[c]	0.35[a] (0.32±0.02)[c]	22.1[a]	0.34[a]
Granite	7.2[a]	0.18[a]	131.0[a]	0[a]
Basalt	2.4[a]	0.26[a] (0.25±0.02)[d]	24.0[a]	0[a]
Shale (horizontal)	4.1[a]	0.15[a]	27.6[a]	0[a]
(vertical)	2.1[a]	0.15[a]	27.6[a]	0[a]
Tuff (welded)	23-41[b] (26.7±7.7)[e]	(0.14±0.05)[e]	117.0[b] (95.9±35.0)[e]	NA
(nonwelded)	7-9[b] (8.1±2.3)[e]	< 0.1-0.25[b] (0.16±0.06)[e]	7-30[b] (30.6±11.1)[e]	0.1-1.4[b]

[a] DOE (1979b).

[b] Tyler (1979).

[c] Palo Duro Basin (DOE 1985).

[d] Cohassett Flow, Hanford, intact rock value, size effect not taken into account (DOE 1985).

[e] Topopah Spring welded, Calico Hill nonweld units, Yucca Mountain (Tillerson and Nimick 1984; DOE 1985).

difficulties in assessing these effects is the lack of data and the corresponding incomplete understanding of the fracture behavior under normal and shear stresses. Even though hard rock mining experience is extensive, the effects of thermal loading on fracture stability are poorly understood.

Mainly because of fractures, the thermomechanical properties of a large rock mass cannot be represented by the elastic parameters determined by small core samples measured in the laboratory. A rock mass consists of intact blocks of rock separated by sets of fractures. The spacing, width, orientation, extent, filling material, etc, of the fracture sets determine the correction factor that scales the intact block value to the rock mass value of a large volume. The values of the elastic properties of granite, basalt, and shale shown in Table 2.4 have been modified by correction factors to approximate these size effects. In the GEIS values, a 1.5-m (5-ft) cube specimen was assumed to be large enough to represent the rock mass, with the effects of minor joints taken into account for all rock properties. The effects of major fractures are not incorporated in the GEIS study (Dames and Moore 1978a).

In addition to the size effects, the temperature dependence of the mechanical properties may also be an important consideration, especially for the cases in which the strength of the rock mass reduces with increasing temperature. The temperature dependence of mechanical properties, together with the thermally induced stress from thermal expansion, couples the mechanical processes with the thermal

behavior of the rock. The mechanical processes also couple with the hydrologic behavior because of the interaction between rock stress and fluid pressure. The compressibility of the rock matrix affects the storage capacity of the fluid in the rock mass.

2.3.3 Hydrologic Properties

The GEIS study (DOE 1979b) produced a generic description of the hydrologic stratigraphic sections, including hydrologic properties, for four major rock types. Hydrologic data for tuff and alluvium have also been compiled (Smyth and others 1979; Tyler 1979; Bulmer and Lappin 1980). Table 2.5 lists a typical value and the range for both the permeability and the porosity of the repository host interval or layer of the particular rock type. The table does not properly represent the geologic environments of a repository, since the layers both above and below the host rock intervals are also important in determining the hydraulic flow patterns. The regional groundwater movement also depends on the distant recharge and discharge areas and on the overall regional gradient. Consequently, the generic hydrogeologic conditions are difficult to determine.

The uncertainty and variation in hydrologic properties, especially permeability, is much higher than in thermal and mechanical properties. The permeability value is highly site specific, and the size effect is drastic. The laboratory measurements of intact rock samples are much lower than the borehole measurements, and the borehole measurements may be obscured by the small volume of rock surrounding the borehole.

Table 2.5. Hydrologic Properties of Rocks.

Rock Type	Permeability (m^2)		Porosity	
	Typical	Range	Typical	Range
Salt	nil	10^{-17} - 2×10^{-30}	0.005	NA
Granite	5×10^{-17}	10^{-13} - 10^{-17}	0.004	NA
Basalt	10^{-17}	2.7×10^{-14} - 10^{-18}	0.006	NA
Shale	7.1×10^{-16}	10^{-12} - 10^{-19}	0.16	NA
Tuff (welded)	10^{-17}	$\leq 1.4 \times 10^{-15}$	0.10	0.02 - 0.25
(nonwelded)	10^{-16}	10^{-15} - 10^{-18}	0.35	0.25 - 0.55
Alluvium	3×10^{-18}	2.4×10^{-14} - 1.2×10^{-21}	0.31	0.16 - 0.42

(Dames and Moore 1978c,d; DOE 1979b; Smyth and others 1979; Tyler 1979)

The sampling of a large volume of rock, especially a low-permeability rock formation suitable for a repository, is a major challenge and a significant source of uncertainty in the assessment of repository impact.

2.4 THERMAL ENVIRONMENT OF THE WASTE PACKAGE

The key factors in determining the very-near-field thermal environment are

- canister thermal loading,
- details of canister-borehole design,
- thermal properties of the wastes, canister-borehole components, host rock, and
- average canister spacing.

The maximum temperature and temperature gradient occur within the waste package and in the immediate vicinity of the waste canisters. The principal problems associated with the high temperatures are

- waste canister integrity for effective containment of the radionuclides, and
- canister recoverability during the retrievability period.

The following subsections discuss the maximum temperature rises in the waste, canister, and borehole; the structural instability of the various components in the very-near-field; and the long-term hydrological environment expected for the waste package.

2.4.1 Maximum Temperature Rises of Waste, Canister, Borehole

Many studies have been made to model the very-near-field temperatures in various rock formations. As an illustrative example, the results of Claiborne and others (1980) and RRC-IWG (1983) for the temperature histories in salt containing HLW and SF are shown in Figures 2.5 and 2.6 for temperatures at the waste centerline, the canister surface, and the wall of the emplacement hole. The centerline temperature of HLW peaks at about 320°C between 1 and 2 years after emplacement and decreases to about 120°C at 100 years. The canister temperature peaks at 260°C, and the maximum salt temperature peaks at less than 160°C. These temperatures correspond to a 2.16-kW vitrified waste in a stainless steel canister with an areal loading of 25 W/m^2 (100 kW/acre). The canister is emplaced in a 0.54-m diameter hole with crushed salt backfill between the carbon steel canister overpack and the hole liner. The SF results, with an emplacement power of 0.55 kW have lower salt, canister, and cladding temperatures, and the peaks are later in time than those for HLW (Fig. 2.6). These peaks occur within 60 years after emplacement. Similar calculations have been made for reference repositories in salt, granite, basalt, shale, and tuff as summarized in Table 2.6 (RRC-IWG 1980).

Many other studies have been made to model the very-near-field temperature. The rock temperature is relatively independent of the detailed waste package design. The heat flux from the waste package and the heat conduction into the rock determines the temperature

Table 2.6. Reference Peak Near-Field Temperatures (°C)[a].

Host Rock	Location	SF[c]	HLW	DHLW
Salt	Host rock	140	160	80
	Canister wall	145	260	90
	Waste[b]	175	320	100
Granite	Host rock	150	165	105
	Canister wall	170	205	115
	Waste[b]	190	225	120
Basalt	Host rock	165	NA	NA
	Canister wall	170	NA	NA
	Waste[b]	185	NA	NA
Shale	Host rock	125	140	125
	Canister wall	140	210	135
	Waste[b]	165	235	140
Tuff	Host rock	185	225	NA
	Canister wall	190	260	NA
	Waste[b]	230	295	NA

(RRC-IWG 1980)

[a] Assumes initial formation temperature of 34°C for salt, 20°C for granite, 57°C for basalt, 38°C for shale, and 35°C for tuff.

[b] Maximum centerline temperature for HLW and DHLW; maximum cladding temperature for SF. The canister loadings of 10-year-old wastes are 0.55 kW/canister for SF, 2.16 kW/canister for HLW in salt and tuff, 1.00 kW/canister for HLW in granite and shale, and 0.31 kW/canister for DHLW. The area loadings are 25 W/m^2 (100 kW/acre) for SF and HLW in salt and tuff and HLW in granite; 20 W/m^2 (80 kW/acre) for SF in granite; 12.3 W/m^2 (50 kW/acre) for SF in basalt; 10 W/m^2 (40 kW/acre) for SF, HLW, and DHLW in shale; 11.6 W/m^2 (47 kW/acre) for DHLW in salt; and 13.5 W/m^2 (55 kW/acre) for DHLW in granite.

[c] Results for 1 PWR element per canister waste package configuration.

rise. For the approximate analytic solutions summarized in the Appendix, the very-near-field temperature rise is approximately proportional to the waste power, is inversely proportional to the rock thermal conductivity, and has weak (logarithmic) dependence on the thermal diffusivity and well-bore radius. The temperature rise at the wall may affect the structural integrity of the borehole.

The temperature rise at the canister surface depends sensitively on the thermal properties and heat transfer modes in the gap between the rock and the canister. With crushed, low-thermal-conductivity rocks backfilling the gap, a high-temperature gradient is induced. The peak canister temperature of a 4.61-kW HLW canister with a 0.076-m (3-inch) crushed salt backfill has been modeled to be 194°C (350°F) hotter than would result if the gap were left unfilled (Davis 1979). If the gap is unfilled, the heat transfer across the gap depends not only on conduction but also on heat transfer by radiation and convection. If there is a large air gap, the significant contribution of air convection and radiation may result in higher equivalent conductivity than if there were perfect thermal contact between the canister and the rock medium. For a small air gap, the equivalent thermal conductivity of the dead air is low. It has been shown that a small gap on the order of 0.025 m (1 inch) should be avoided, since the canister temperature as a function of the gap size is highest at this critical value (Lowry and others 1980).

2.4.2 Wall Decrepitation and Canister Retrievability

With waste emplacement, the highest thermally induced compressive stresses from rock expansion are expected at the heater borehole wall. When the maximum axial and/or tangential stresses are approaching the compressive strength, spalling of the rock around the borehole will most likely occur, especially in brittle rocks. Decrepitation can also occur in salt at elevated temperatures (>250°C), but in the long term, plastic flow may heal the crushed salt.

The stability of the boreholes has been examined through in situ experiments. For example, the borehole walls surrounding a 5-kW heater in the granite experiment at a depth of 384 m in Stripa, Sweden, did not begin to fail until a temperature in excess of 300°C was reached (Witherspoon and others 1981). In the near-surface experiment on shale at 23 m depth, no borehole failure was observed for its 3.8-kW heater up to 350°C (Lappin and others 1981).

At Project Salt Vault (bedded salt), closure was observed along with deterioration of the hole surface due to migrating brine. The maximum hole closure was approximately 0.0127 m (0.5 inch) over the time of the heater experiment, about one and a half years (Bradshaw and McClain 1971). The heater power varied during the experiment, ranging from 1.6 kW/canister to 4.8 kW/canister, with the average at approximately 3.2 kW/canister.

In order to retrieve the waste, it may be necessary to install liners for the boreholes in bedded or domed salt repositories. The same effect can be achieved by reinforcing the hole by grouting, as

has been suggested for the case of the basalt reference repository (Kaiser Engineers and Parsons, Brinckerhoff, Quade and Douglas 1980). For granite, the inherent strength of the rock may make retrievability relatively easier to attain for long periods of time, so that special measures may not be required.

2.4.3 Brine Migration and the Canister Environment

In the presence of heat, saturated (all-liquid) brine trapped in small pockets or inclusions in the salt will migrate up the temperature gradient toward the canister. Waste package corrosion from brine accumulation is one of the isolation concerns in salt media, especially bedded salt. This phenomenon has been studied in Project Salt Vault in bedded salt (Bradshaw and McClain 1971), in the Asse salt mine experiment in a salt anticline (Rothfuchs and Durr 1980; Schlich and Jockwer 1985), in the Avery Island salt mine experiment in domed salt (Krause and others 1980), and in Sandia's salt block experiment with samples from the Waste Isolation Pilot Plant (WIPP) site (Hohlfelder and Hadley 1979.)

Jenks (1979) developed a phenomenological model based on the experimentally observed migration rate in single salt crystals. Jenks and Claiborne (1981) reviewed early brine migration studies and evaluated the accumulated influx of brine for canisters in domed and bedded salts (Jansen and others 1983). Figure 2.7 illustrates the dependence of total flow into a canister hole on the waste emplacement densities for 10-year-old SF and reprocessed HLW (Rickertsen 1980). The spent-fuel inflow continues to increase after 1,500 years because

of the slow decay rate of spent fuel. For reprocessed HLW with its higher power at emplacement, the inflow is higher, especially at early times. The total inflow is approximately 3% of the annulus volume.

If an all-liquid inclusion migrates to a heated canister, it can be transformed into a two-phase gas-liquid inclusion which moves in the opposite direction down the temperature gradient (Olander and others 1980). This mechanism may reduce further the total brine inflow but provides a means of dispersing radionuclides from a canister. The inclusions migrating up and down the temperature gradient may also be trapped along crystal grain boundaries. It was observed that more than 90 percent of the brine in Project Salt Vault and 40 percent of the brine in the salt block experiment were released after the heater was shut down. When the thermal stresses were released upon cooling, the trapped water in the salt was allowed to break free (Bradshaw and McClain 1971; Hohlfelder and Hadley 1979). In addition to the fluid inclusions and entrapments, the water chemically bound to clay minerals in the rock can be released upon heating. Gas release upon heating is also of concern (Jockwer and Gross 1985).

The pressure around a waste canister depends on the borehole seal. The pressure in an imperfectly sealed hole will be essentially equal to the near-atmospheric (0.1 MPa) pressure in the room during repository operations. The pressure in a perfectly sealed hole will change as a function of time in response to temperature and rate of brine inflow. For HLW in salt at an areal loading of 25 W/m^2 (100 kW/acre), the pressure peaks at about 3.2 MPa at 10 years after emplacement. For

SF at 10 W/m^2 (40 kW/acre), the pressure steadily increases up to 0.45 MPa at 50 years after emplacement (Claiborne and others 1980). Similar calculations have been made for other nonsalt rocks (RRC-IWG 1980, 1984). A repository located below the water table in these rocks is expected to be slowly filled with water. If the repository excavation is reflooded, the pressure would then rise to hydrostatic. The long-term effects of pressure are likely to be smaller than those induced by chemical and thermal influences on the canister integrity.

2.5 THERMOMECHANICAL ENVIRONMENT OF THE EXCAVATION

Key factors in determining the near-field thermomechanical impacts are

- thermal loading density,
- sizes of rooms and pillars and canister depth relative to the storage rooms,
- thermal and mechanical properties of the rocks, and
- ventilation and heat transfer in the drift.

The main concerns in underground operations are

- adequacy of the thermal environment for the function of personnel and equipment, and
- mechanical stability of the rock for safe operations during the excavation, emplacement, and retrieval periods.

The safety of personnel and maintenance of operating conditions were the focus of earlier design studies. As shown in a later section, the existing maximum allowable thermal loadings in the repository designs were determined primarily by thermomechanical stability

considerations. The thermomechanical analyses are generally more complex than heat transfer calculations. We first discuss the thermal field in the room-and-pillar region and then present an outline of the thermomechanical analyses and the approximations associated with these analyses. In the last subsection, we briefly review the effects of ventilation in underground cooling.

2.5.1 Temperature Field Surrounding the Storage Room

Following the emplacement of wastes, the rock in the immediate vicinity of the canister heats up. As the heat slowly transfers into the rock mass, heat flows from neighboring canisters interact and the temperatures of the rock masses above and below the canister horizon increase. The temperature evolution surrounding a storage room for the GEIS 47-W/m^2 (190-kW/acre) HLW repository in granite is shown in Figure 2.8 (Science Application Inc 1978; see also Osnes and others 1984).

The main interest in these near-field analyses is the temperature in the pillar center and around the room during the emplacement and retrieval periods. The two-dimensional unit cell was used to get the results shown in Figure 2.9. The repository is modeled as an infinite array of storage rooms with homogeneous heat sources buried below the storage room floors. The effects of surrounding storage rooms are taken into account by the insulating (adiabatic) side boundaries of the unit cell on the centerlines of the room and the pillar. Upper and lower boundaries of the model are sufficiently removed from the canister and room so that they have no effect on the near-field temperatures during the period of interest.

The temperature histories for three locations away from the canister are shown in Figure 2.9. These locations correspond to points near the upper corner of the storage room, mid-pillar at the storage floor level, and mid-pillar at the canister level, respectively. Ventilation in the storage room is not considered in these results. The GEIS report also presents modeling results for SF in salt, basalt, and shale. For the locations away from the waste canister, the two-dimensional temperature results agree fairly well with the three-dimensional results between the canisters.

These temperature distributions were used as input for the thermomechanical calculations. Most thermomechanical calculations to date for room stability have been two-dimensional. Because stress and strain are tensorial quantities, three-dimensional calculations are more complex than two-dimensional modeling (Loken 1983). The next subsection discusses two-dimensional thermoelastic results that represent the averages along the storage room and ignore the variations of stress and strain between canisters in the same row.

2.5.2 Rock Deformation and Stress Perturbation

The stability of the room-and-pillar structure depends on both the excavation and the thermal loading. The effects of excavation can be minimized by a small extraction ratio (the ratio of the volume removed to the volume remaining). For a radioactive waste repository, the extraction ratio will be in the 10-20 percent range, which is low compared to conventional mine operations for removal of mineral ore. The key question is whether the additional thermal loading will induce instability.

For soft rocks like salt, the main concern is for the room closure. Salt under stress can flow slowly, or "creep." With thermal loading, the creep rate increases. It is important to limit roof sag, floor heave, and wall convergence so that emplacement and retrieval equipment can be transported through the tunnel. The heated pillar experiment in Project Salt Vault measured in situ thermomechanical responses, and this data base has been used in model evaluation studies (Wahi and others 1978). In the design studies for salt (Stearns-Roger Engineering Co 1979; Kaiser Engineers 1978a,b), Lomenick's formula, based on laboratory salt pillar data, has been used to calculate creep. Lomenick's formula shows that strain is proportional to $T^{9.5}$, where T is the absolute temperature expressed in kelvins (K), which indicates the possible temperature dependence of the creep rate. More recent work has indicated that Lomenick's formula may be nonconservative for certain conditions and that the room closure predicted in both conceptual designs may have been underestimated (Stearns-Roger Services Inc 1980).

Although salt has been extensively studied for the past 20 years, further studies both in in situ experiments and modeling of creep are required to understand the important effects of thermal loading on the stability of a salt repository (Wagner and others 1986).

For hard rocks, creep is not a problem. The main concern is the presence of fractures. During excavation, drilling and blasting can shatter the rock around the perimeter of the tunnel. The stress concentration around the excavation may open existing fractures or create new ones. However, most of the modeling studies to date are based on

thermoelastic calculations, which neglect the effect of fractures. In addition to the GEIS study (Dames and Moore 1978a), thermoelastic analyses have been done in granite (Ratigan 1977), basalt (Hardy and Hocking 1978), and shale (Thomas and others 1981). The in situ granite experiment in Stripa, Sweden, shows that thermoelasticity cannot account for the rock displacements induced by the heater, as shown in Figure 2.10 (Hood and others 1979; Witherspoon and others 1981). The fractures can absorb the thermal expansion of rocks, and the thermomechanical responses are nonlinear. The significance of fractures for rock displacements in regions away from the heater canister has not yet been assessed, especially their significance for the stability of the storage room.

Although thermoelastic analyses neglecting fractures may not be quantitatively correct, they can qualitatively identify the zones of potential instability. In the GEIS study it was shown that the roof top is the most critically stressed area. Figure 2.11 is an example of thermally induced stresses for the 47-W/m^2 (190-kW/acre) HLW repository in granite. In this example, the maximum compressive stress parallel to the roof surface is 20.7 MPa (3,000 psi). The corresponding compressive stress induced at the same point by the excavation is 31.0 MPa (4,500 psi). (It is of interest to note that the in situ stress field without the excavation is assumed to be 13.8 MPa (2,000 psi) vertical and 20.7 MPa (3,000 psi) horizontal.) Therefore, at a roof temperature of 121°C (250°F), the total compressive stress at the roof top due to the sum of the stresses from thermal loading and ex-

cavation is 51.7 MPa (7,500 psi), one-half of the uniaxial compressive strength 103.4 MPa (15,000 psi). The above numerical example illustrates the procedure used in the GEIS to determine the maximum allowable thermal loading; thermal loading is adjusted so that induced stress is one-half the rock strength. For granite, this procedure gives the value 47 W/m^2 (190 kW/acre). In Table 2.7 the maximum area loadings from this procedure is given for granite, shale, and basalt.

In the Swedish Nuclear Fuel Safety Program (Karnbranslesakerhet, or KBS), the thermomechanical responses for a repository in granite were modeled (Ratigan 1977). Like the GEIS study, the KBS calculations were thermoelastic, and stresses were calculated without taking fractures into account. Fracture sets were assumed to exist in the rock mass, however, and after the stress calculations were made, the rock mass was assumed to fail along the fractures. A linear Mohr-Coulomb shear criterion was used to identify the regions of strength failure. This failure criterion is different from the compressive failure criterion used in the GEIS study.

Figures 2.12 and 2.13 illustrate the dependence of strength failure on joint orientation. Each figure shows the progressive failure due to the combined effects of thermomechanical and excavation-induced stresses. To control strength failure in locations where it may be undesirable, the characterization of joints must be carried out. Nonlinear stress analyses that take the inelastic responses of fractures into account should be performed to determine repository stability in hard rock.

Table 2.7. Maximum Areal Loadings Based on Near-Field Thermomechanical Stress Studies.

Rock Type	HLW and SF (5-year retrievability) W/m^2	(kW/acre)
Granite	47	(190)
Basalt	47	(190)
Shale	30	(120)

(Science Applications Inc 1978)

The Stripa experiment, the GEIS study, and the KBS calculations discussed above indicate that the thermoelastic analyses may be too simplistic and the effects of fractures should be studied and included in determining the allowable thermal loading. Since the thermomechanical stability tends to be the controlling criterion in determining the maximum allowable thermal loading, the uncertainties must be minimized in modeling studies. Also, the effects of engineering reinforcement should be studied. The safety of the excavation can be reinforced by engineering techniques. For example, the use of rock bolts has been included in design studies of bedded salt and basalt. Sound engineering reinforcement and careful monitoring will improve and maintain the margin of safety during the short period of repository operations.

2.5.3 Ventilation Cooling

The last topic to be discussed concerning excavation conditions is the effect of ventilation. To maintain the working environment, ventilation will be provided during the excavation and emplacement operations. The heat removed by air circulation effectively prolongs the cooling period of the wastes. If retrieval of the wastes were to be initiated after sealing the tunnel, recooling of the room would be required before the waste canisters could be reached. Both pre-emplacement and post-emplacement ventilation effects have been studied in the literature.

Heat transfer from the floors, roofs, and walls to the rooms and the natural and forced convection of the ventilating air through the rooms remove a large portion of the heat during the ventilation period.

Cheverton and Turner (1972) show that at about 5 years after burial, a maximum of 40 percent of the waste heat can be removed with room ventilation for a 39-W/m^2 (158-kW/acre) HLW repository in salt. Altenbach (1979) shows that up to 90 percent of the waste heat can be removed after 44 years for a 9-W/m^2 (36-kW/acre) SF repository in salt. The amount of cooling depends on a number of factors:

- flow rate, temperature and humidity of the air,
- thermal loading and the burial depth of the waste,
- heat transfer in the rock, and
- heat transfer in the room.

The last factor depends on the roughness of the rock wall (Boyd 1978). With ventilation, the excavation will experience less strength failure (Ratigan 1977). Ventilation can substantially lower borehole, canister, and waste temperatures, especially if the borehole is not backfilled with low-conductivity crushed rocks (Claiborne and others 1980).

When re-entry is desired, a waiting period is required to allow the room floor to cool to an acceptable temperature. Altenbach and Lowry (1980) show that it takes less than 6 months for the floor to cool down after 50 years' storage in a 9-W/m^2 (36-kW/acre) repository (see Fig. 2.14). Boyd (1978) shows that less than 10 years is required for the room temperature to drop to 49°C after 30 years in a 18.5-W/m^2 (75-kW/acre) WIPP drift. Forced ventillation may speed up the cooling (Svalstad 1983). The effects of recooling on room stability are not well known.

The principal advantage of ventilation is the cooling of storage rooms during the operations phase of the repository. However, the reduction in the accumulated thermal output of the waste during short periods of ventilation is expected to be small. Ventilation cannot be used to reduce significantly the problems caused by waste heat over thousands of years (Koplik and others 1979). The underground ventilation cooling is essentially an extension of surface cooling before waste emplacement.

2.6 THERMOHYDROMECHANICAL ENVIRONMENT IN ROCK FORMATIONS

The key factors in determining the far-field thermohydromechanical environment are

- time dependence of waste heat power and thermal loading density,
- repository depth, size, and shape,
- rock properties, and
- in situ environment and boundary conditions.

The main concerns in the geologic setting are

- groundwater buoyancy flow from the repository to the surface,
- surface uplift and integrity of the rock formation, and
- cumulative heat energy that remains in the formation.

The waste repository impact on the rock formation may persist for thousands of years over thousands of meters. Quantitative predictions of the long-term thermal, mechanical, and hydrologic perturbations can be made only through modeling of the repository and its geologic setting. With these predictions one can calculate the degree of long-

term isolation. In this section we review the results of far-field thermal modeling and parametric studies, discuss the surface uplift and stress changes, and analyze the hydrologic perturbations due to buoyancy flow.

2.6.1 Long-Term Thermal Perturbations in Rock Formations

Rock formations are poor thermal conductors. It takes hundreds to thousands of years for the waste heat to transfer from a 500- to 1000-m-deep repository to the ground surface. The waste releases heat continuously at a decreasing rate over thousands of years.

The long-term temperature variations and distributions in the rock formation surrounding a repository depend on the thermal loading, the repository characteristics, and the rock properties. The effects of these three controlling factors on the far-field temperature rise will be discussed in the following three subsections.

2.6.1.1 SF repository versus an HLW repository

Figure 2.15 illustrates the evolution of the temperature field in a 10-W/m^2 (40-kW/acre) SF disk-shaped repository in granite (Wang and others 1981). In this case, the heat leaks out to the atmosphere after 1,000 years, distorting the symmetry above and below the repository. The surface leakage and the decline of the waste heat output will eventually return the rock formation to its ambient condition.

The long-term, far-field thermal impact depends not only on the thermal loading power but also sensitively on the time dependence of the heat power. The heat power at long periods depends on the amount of actinides contained in the waste, as discussed in Section 2.1.

Comparing the contours of reprocessed HLW in Fig. 2.16 with those of SF in Fig. 2.15 demonstrates the sensitive dependence of the long-term, far-field thermal perturbations on the fuel cycle. Both wastes are initially emplaced with the same thermal loading.

Rather than the thermal power density at waste emplacement, the quantity that best characterizes the far-field thermal impact is the cumulative heat energy released by the wastes. The solid curves in Fig. 2.17 illustrate the dependence of the total heat released on the type of buried waste. The large thermal difference between the SF and the reprocessed HLW is responsible for the large difference between the long-term temperature contours in Fig. 2.15 and 2.16.

Since most of the long-lived actinides are removed from the reprocessed HLW, the overall environmental impact of HLW storage is far less than that of spent fuel, given the same quantity of waste. In order to have the same far-field impact, the spent fuel waste loading density should be reduced (Lincoln and others 1978; Llewellyn 1978; Science Applications Inc 1978).

2.6.1.2 Dependence of thermal impact on repository configurations

Figure 2.17 also illustrates the dependence of the cumulative heat remaining in the granite formation on the depth of a 3-km-diameter, disk-shaped repository (broken curves). When a repository is deeper, more heat will remain in the rock formation for a longer period of time. The rock formation between the repository and the ground surface can be regarded as a heat insulating layer. The deeper the repository, the thicker the layer and the more heat retained in the

rock. Both the thermomechanical perturbations (to be discussed in Section 2.6.2) and the thermohydrologic perturbations (to be discussed in Section 2.6.3) over the geologic settings depend on the amount of heat remaining in the rock formation. Although a deeper repository provides more physical protection and longer flow paths, the higher heat content remaining in the rock formation will induce larger and more persistent thermohydromechanical perturbations.

The repository size depends on the amount of waste to be stored and on its loading density. For ideal layered formations like bedded salt, the lateral extent of a repository can be great enough to accommodate a large amount of waste at a diluted density (that is, low thermal output). For domed salt or granitic plutons, the lateral extent of the host rock is limited, restricting in turn the repository size. Emplacing more than one canister in a deep borehole or using a multilevel repository have been considered for laterally limited rock formations (Hamstra and Kevenaar 1978; Just 1978; Tammemagi 1978). Table 2.8 compares the temperature increases in a single-level repository with a those of a three-level repository. Use of a multilevel burial concept reduces the repository temperature; the thermal interaction among adjoining layers delays the peak temperature. However, the total energy remaining in the formation will increase slightly.

In each of the above results, the repository is approximated by a disk heat source (assumed to be simultaneously loaded), with the waste uniformly distributed over the disk. In more detailed repository de-

Table 2.8. Peak Temperature of Single-Level and Three-Level Repositories.[a]

Number of Layers	Domed Salt		Granite	
	Temperature Increase (°C)	Time (years)	Temperature Increase (°C)	Time (years)
Single-level	37.0	60	48.1	70
Three-level	34.6	125	38.3	175

[a] Scaled from Just (1978) for a 10 W/m^2 (40 kW/acre) SF repository. The temperature is calculated from a far-field model.

signs, more realistic representations of the repository configuration and operations have been made.

For example, in the conceptual design study for the NWTS-1 repository in domed salt (Stearns-Roger Engineering Co and Woodward-Clyde Consultants 1978), the waste loading is not instantaneous and a more realistic rate of waste arrival at the repository is assumed. The repository shape is not a simple disk but a ring-shaped region with an inner radius of 344 m (1128 ft) and an outer radius of 1378 m (4522 ft). There is no waste emplacement in the inner-radius region in order to protect the centerline shaft for waste transportation. The repository is loaded from the outermost boundary toward the inner radius. Figure 2.18 shows the evolution of the temperature distribution along the radius of the repository. This result illustrates the sensitive dependence of short-term effects on sequential loading, as well as on repository configuration (Rickertsen and others 1982; Hahne and others 1985).

The repository configuration can have a far-field impact. For example, the surface uplift above a rectangular repository with a shaft pillar has been shown to be smaller than that above a disk repository (Dames and Moore 1978a). Surface uplift is discussed in detail in Section 2.6.2.1. In the remainder of this report, the repository is assumed to be a single-level disk for the far-field generic evaluation. It should represent the most compact configuration and induce the greatest impact in most cases.

2.6.1.3 Controlling rock properties for far-field temperatures

The temperature field in the repository and in the rock formation depends on

- the rock's capacity to sustain a temperature rise, and
- the heat transfer from the repository to the surrounding formation.

Figure 2.19 shows the dependence of the repository temperature history on the rock type, where temperature represents the areal temperature average between canisters. It produces a conservative estimate of the rock temperature in the pillar. For all rock types, this average repository temperature peaks before 100 years.

The maximum repository temperature rise is approximately proportional to the inverse square root of the product of thermal conductivity and volumetric heat capacity. (This is an exact result if the heat power is a single-term exponential decay function.) The high thermal conductivity of salt is compensated for by its low heat capacity. Table 2.9 summarizes the thermal properties used in Fig. 2.19.

The similarity of the calculated repository temperatures in granite, bedded salt, and domed salt was also noted previously in the EPA (1977) study. The vertical temperature profiles for granite and domed salt from the EPA study are shown in Fig. 2.20 and 2.21, respectively. Away from the repository, the temperature distributions are not very sensitive to the different rock types. At early times, the vertical temperature variation (gradient) is high and localized close to the repository. The temperature gradient at the repository level, related

Table 2.9. Thermal Properties of Rocks Used in the Far-Field Model.

Rock Type	Thermal Conductivity (K, W/m-°C)	Volumetric Heat Capacity (ρc, J/m^3-°C)	Thermal Diffusivity ($K/\rho c$, m^2/s)	Analytic Approximation[a] (°C$(W/m^2)^{-1}$)
Salt[b]	4.20	1.87×10^6	2.24×10^{-6}	4.02
Granite[b]	2.56	2.43×10^6	1.05×10^{-6}	4.52
Basalt[b]	1.26	2.30×10^6	0.547×10^{-6}	6.62
Shale[b]	1.54	2.15×10^6	0.716×10^{-6}	6.19
Tuff[c]	1.60	1.87×10^6	0.856×10^{-6}	6.52
Alluvium[d]	1.00	1.70×10^6	0.588×10^{-6}	8.65

[a] Analytic approximation for the temperature rise per areal loading in W/m^2 (see Eq. (A-6) in the Appendix): $\frac{0.305}{[K\rho c \ell n(2)/t_{1/2}]^{1/2}}$, $t_{1/2}$ = 30 years.

[b] GEIS values at 100°C (DOE 1979b).

[c] Typical values of welded tuff (Tyler 1979).

[d] Smyth and others 1979.

to the heat flux released by the waste, is monotonically decreasing. The temperature gradient at the surface, representing the heat flux leaked from the rock to the atmosphere, will be noticeably above its ambient value only after hundreds of years. When the heat flux from the waste is equal to the heat flowing out of the rock, the heat remaining in the rock is at its maximum and the temperature profile from the repository to the surface is nearly linear. This occurs at times on the order of thousands of years, depending on rock type and repository depth.

After this quasi-equilibrium state, the temperature rise from the repository to the surface is determined by the heat in the rock divided by the heat capacity. Although the heat transfer is determined by both thermal conductivity and volumetric heat capacity, the magnitude of the long-term, far-field temperature rise is more sensitive to the latter.

Many modeling studies have been done for different stratigraphies in various rock formations (EPA 1977; Science Applications Inc 1978; DOE 1980a). Although the rock layers in different stratigraphic models have very different thermal conductivities, the temperature profiles are all quite similar, with only mild kinks across the boundaries. The insensitivity of the temperature profiles to the heterogeneity of the rock layers has stemmed from the similarities among the heat capacities of the different rocks. Among all the rock properties discussed in Section 2.3 (see Tables 2.3 and 2.9), the heat capacity is the least site specific and the least rock specific.

This strongly suggests that we can easily model and understand the long-term temperature changes in the surrounding rock. The uncertainty associated with our incapability to measure rock properties in detail over large rock formations does not seriously limit our capability to assess the long-term temperature changes. A pessimistic viewpoint prevails in the literature that geologic settings are too complex and the uncertainty of the predicted results too great to give meaningful bounding values. However, a reserved optimism may be more appropriate, because, as we have seen above, a reasonable certainty can be assigned to our generic quantitative evaluation of the overall temperature changes in different rock formations.

2.6.2 Far-Field Thermomechanical Perturbations

One of the consequences of a temperature rise in the rock formation is the thermal expansion of the rock. When the rock mass expands, the ground surface rises. Of all the far-field perturbations, surface uplift has received the most attention, especially in salt, with its high thermal expansion coefficient. Thermal stress may also induce permeability changes. Surface uplift and rock displacement will be discussed in this section.

2.6.2.1 Surface uplift

The volumetric thermal expansion of the rock creates an uplift of the rock mass in which the waste is buried. The maximum thermal uplift will be above the center of the repository, where the maximum temperature rise within the strata will occur. Thermally induced rock displacements are pervasive and cumulative. Surface uplift depends on

temperature rise, or equivalently, on the waste heat energy in the whole rock formation. Conservative estimates can be made for surface uplift with rock movement constrained in the axial direction (Callahan and Gnirk 1978). Table 2.10 summarizes the results of maximum surface uplift for axisymmetric analyses in the GEIS study for salt (Callahan and Ratigan 1977; Russell 1979), granite, basalt, and shale (Dames and Moore 1978a). Also included are the linear thermal expansion coefficients and the Poisson ratio factor of the different rock types.

The thermal loadings in the table are determined by near-field, excavation stability analysis. The concern over large surface uplift for an SF repository in salt has resulted in a lowering of the waste loading from 37 W/m^2 (150 kW/acre) to 15 W/m^2 (60 kW/acre). This is the only case in the literature for which long-term far-field consideration of the waste impact has imposed a constraint on the thermal loading.

The surface uplift calculated by thermomechanical analyses did not include the opposite effect of subsidence. Subsidence is caused by the eventual closure of the excavation. Even if the repository is backfilled with crushed rock before decommissioning, the deformation of the rock to fill the void will lead to a lowering of the surface, especially in the case of salt, with its tendency to creep. This subsidence could cancel out part of the thermal uplift. Figure 2.22 shows such a phenomenon for an HLW repository in salt at 600 m depth (INFCE 1980).

Table 2.10. Surface Uplift.

Rock	Salt		Granite		Basalt		Shale	
Waste	SF	HLW	SF	HLW	SF	HLW	SF	HLW
Maximum Surface Uplift (m)	3.45	1.27	0.94	0.34	0.58	0.18	0.79	0.34
Time (years)	1,000	150	3,000	1,000	7,000	3,000	3,500	1,800
Thermal Loading W/m^2 (kW/acre)	37 (150)		47 (190)		47 (190)		30 (120)	
Linear Thermal Expansion Coefficient ($°C^{-1}$)	4×10^{-5}		8.1×10^{-6}		5.4×10^{-6}		8.1×10^{-6}	
Poisson Ratio Factor $(1+\mu/1-\mu)$	2.08		1.44		1.70		1.35	

(Dames and Moore 1978a; Russell 1979)

Both the uplift and subsidence processes are slow, their effects persisting over long periods of time. In comparison to the ground displacement predicted for the waste repository, much higher subsidence over shorter time periods has been observed in petroleum and geothermal fields. The main concern of surface uplift in repository studies is not the vertical displacement itself but the long-term stability of the geologic formations. This is discussed in the following subsection.

2.6.2.2 Stress perturbations and crack openings

The rock's volumetric thermal expansion can induce both axial and lateral stress changes. The development of thermally induced tensile stresses near the ground surface has been noted in thermomechanical analyses (Dames and Moore 1978a; Hodgkinson and Bourke 1980). The tensile stresses exist in the angular direction perpendicular to the radial-vertical (rz) plane. The horizontal components of tensile stress will reduce the normal stress across pre-existing vertical fractures, which will in turn increase their aperture and substantially change the rock mass permeability. If net tension is to be avoided, the rock mass must have large compressive horizontal in situ stresses to counter the induced tensile stresses.

The magnitude of the induced tensile stresses can be controlled by the thermal loading and repository depth. The analytic model of a spherical repository showed that the induced tensile stresses at the ground surface are inversely proportional to the cube of the mean repository depth (Hodgkinson and Bourke 1980).

The concern over the thermally induced tensile component is not limited to fractured hard rocks but exists also for salt. The large differential of the thermal expansion between bedded salt and the overlying shale layers, or between domed salt and its sheath, may cause a breach in the hydrologic barrier protecting the salt.

Although the significance of the tensile stresses has been noted in thermoelastic analyses, the quantitative assessment of their impact is difficult. The opening of fractures will redistribute the load and stress. The displacement field will be different from continuum analyses. As we noted earlier, the heater experiments in Stripa, Sweden, indicate that fractures under compression can absorb the thermally induced rock displacements in the near-field at early times. It is not clear to what degree the pre-existing fractures in the far-field under thermally induced tensile stress will alter the displacement of the fractured rock mass.

The main concern of thermomechanical perturbations, both in the near- and far-field, is the induced permeability changes in the rock mass (Wilkins and others 1985). Permeability may decrease with fracture closure in the compressive regions and increase with fracture opening in the tensile zones. Neither the temperature-stress nor the stress-permeability relationships are well known, especially for large volumes of rock mass. These considerations in coupled processes have contributed somewhat to the uncertainty in the evaluation of long-term, far-field effects. In the next section, other uncertainties in the assessment of hydrologic perturbations will

be discussed. It is essential that we understand the origin of these uncertainties in order to base our evaluation and criteria on quantities that can be accurately calculated.

2.6.3 Long-Term, Far-Field Thermohydrologic Perturbations in the Rock Formations

The thermally induced movement of groundwater from the repository to the surface may be the dominant mechanism for radionuclide transport at a particular site. The magnitude of the fluid velocity is difficult to determine because of the variations of the hydrologic parameters in the surrounding rock formations. This section discusses the significance and uncertainty of the thermohydrologic perturbations over thousands of years.

2.6.3.1 Variations in hydrologic conditions

The fluid flow is proportional to the permeability of the rock formation. Permeability may vary over six orders of magnitude even for the same rock type, as shown in Section 2.3.3. The permeability value depends on the scale of the rock volume measured (Brace 1980). Typically, the value measured in the field is larger than the value measured with small samples in the laboratory.

The velocity of water within the flow channels (fractures or connected pores) is inversely proportional to the porosity of the rock. Of the total void space measured in the laboratory, only a small fraction corresponds to the continuous flow paths (Norton and Knapp 1977). The uncertainty associated with porosity may be as high as two to three orders of magnitude. Fracture apertures estimated from flow

experiments may differ by orders of magnitude from that derived from tracer experiments (Abelin and others 1983) and the fracture flow is only through continuous channels (Neretnieks 1985; Tsang and Tsang 1986).

Scale dependence and the heterogeneity of the rock hydrologic properties largely originate from the presence of fractures. Most of the modeling studies use either a porous medium model to represent the average behavior of fractured rock masses (Dames and Moore 1978b; Hardy and Hocking 1978; Burgess and others 1979; Hodgkinson 1980; Bourke and Robinson 1981) or a simple fracture model for worst-case studies (Wang and Tsang 1980; Wang and others 1981). In view of the uncertainty of the hydrologic properties, these deterministic modeling studies must eventually be supplemented by statistical analyses in order to assess the effectiveness of the rock formation to isolate radionuclides.

2.6.3.2 Buoyancy flow

Although many different generic representations of the hydrologic conditions have been assumed in various modeling studies, they all demonstrate the significance of the vertical buoyancy flow, which has been shown to persist over thousands of years.

Figure 2.23 shows a sketch of a vertical fracture that is assumed to extend from a 10-W/m^2 (40-kW/acre) repository to the surface. The hydraulic aperture of the fracture is assumed to be 1 μm, corresponding to a fracture permeability of 8.3×10^{-19} m^2, and the lateral width of the fracture is assumed to be smaller than the diameter of the repository. The inlet of the fracture at the repository level is assumed to be in direct contact with ambient groundwater. This model

represents a very bad hydrologic condition for vertical buoyancy flow, with a continuous fracture connecting the repository to the surface and instant recharge at the repository level. The instant recharge can be maintained only with an effectively infinite permeable zone at the repository level. Although the fracture model is very simple, it illustrates some characteristics of buoyancy flow which are similar to that of the more complex systems in fractured rock masses.

Figure 2.24 illustrates the temporal dependence of the water velocity in such a vertical fracture as a function of fuel cycle and depth. It shows that the maximum buoyancy flow occurs at thousands of years for SF repositories and at hundreds of years for reprocessed HLW repositories. For the same thermal loading at waste emplacement, the magnitude of the buoyancy flow induced by SF is much larger than that by reprocessed HLW.

Figure 2.24 also shows that the maximum buoyancy flow occurs at a later time for a deeper repository. The buoyancy flow is determined by the integrated temperature distribution from the repository to the ground surface. For a deeper repository, it will take longer for the waste heat to reach the surface. The average temperature rise, or equivalently the amount of heat remaining in the rock formation, reaches its maximum value when the heat flowing out of the rock on the ground surface is equal to the heat released by the waste. The time of occurrence of the maximum value is approximately proportional to the square of the repository depth.

The maximum vertical velocity corresponds to the minimum transit time from the repository to the surface, called in the GEIS study the "minimum surface approach time." In that investigation a porous medium model was used to represent the average hydrologic properties of a fractured rock mass. The results are tabulated in Table 2.11 along with the estimated times of occurrence of these minimum approach times. The porous-medium results agree qualitatively with the calculations from the single-fracture model above, indicating that buoyancy flow can be an important effect regardless of the particular approximation for the flow paths in the rock mass.

It is of interest to note the similarity between buoyancy flow predictions discussed here and the surface uplifts described in Section 2.6.2. Both effects have maximum values at long times. Both effects are determined by the cumulative heat remaining in the rock formation. The buoyancy flow originates from the thermal expansion of the water, and the surface uplift originates from thermal expansion of the rock.

2.6.3.3 Distortion of convection cells

The repository represents a heat source of finite size embedded in the host rock. The temperature rise is localized around the repository. The density contrast between the hot water in the repository vicinity and the cold water away from the repository causes the formation of convection cells. The convection cells in an extended vertical fracture (see Fig. 2.25) at 1,000 years are illustrated in Fig. 2.26. Two convection cells have developed around the edges of the repository.

Table 2.11. Minimum Surface Approach Time.

Rock	Granite	Basalt	Shale
Minimum Surface Approach time (years)[a]	100	144-168	80-100
Time of Occurrence (years)	1,000-5,000	5,000-10,000	1,000-5,000

(Dames and Moore 1978b)

[a] The results are normalized to 25 W/m^2 (100 kW/acre).

Heated water flows up from the central area of the repository, and incoming water is drawn from the recharge zones on the two sides (5 km from the repository center) and from the ground surface far away from the center of the repository. The diameter of the cells are of the same order as the depth of the repository at 1,000 years. At much earlier times, the convection cells are localized in the regions of high temperature gradients in the immediate repository vicinity. The buoyancy flow and the convection cells grow as the cumulative heat increases in the rock formations. These thermally induced phenomena will eventually disappear when the heat is removed by the atmosphere and the rock returns to its original condition after tens of thousands of years.

The shape of the convection cells depends not only on the heat in the rocks but also on the regional groundwater flow driven by the pressure gradient between the recharge zone and the discharge zone. Fig. 2.27 shows the distortion of the cells with a horizontal gradient of 0.001 m/m. The regional groundwater flow suppresses the convection cell on the recharge side of the repository and distorts the cell on the discharge side. However, the vertical component of water velocity is only weakly coupled to the horizontal regional flow. The flow pattern in Fig. 2.27 is essentially a superposition of the horizontal regional groundwater flow upon the flow of the unperturbed cells in Fig. 2.26 (Wang and Tsang 1980).

The stratigraphic sections and the depth dependence of permeability also distort the convection cells (Dames and Moore 1978b; Burgess and others 1979). The water particles move slowly in low-permeability zones and accelerate when entering high-permeability zones. In the GEIS and KBS studies on granite, permeability decreases monotonically with depth. For shale and basalt (Dames and Moore, 1978b; Hardy and Hocking 1978), the possibility of high-permeability layers below the repository has also been considered. For unsaturated, fractured tuff with liquid flows through the matrix and gas flows through the fractures (Wang and Narasimhan 1985; Pruess and others 1986), high convective gas velocities can be induced by repository thermal loading.

2.6.3.4 Thermohydrologic effects: Further study needed

In waste repository studies, modeling of the long-term thermohydrologic impacts has only recently received attention in regard to the possibility of storing waste in hard rocks. Partly because of the uncertainty associated with hydrologic properties, and partly because of the historical focus on room closure in salt, the long-term consequences of hydrologic perturbation and the resulting impacts upon radionuclide migration have not been regarded as controlling factors in determining the repository thermal loading limit. Generic studies have shown that long-term buoyancy perturbation is significant. In future site-specific studies, the anticipated response of the bulk thermohydrologic system to the maximum design thermal loadings should be carefully evaluated to determine if the long-term buoyancy perturbation is significant enough to be a limiting consideration in thermal loading designs.

3. REPOSITORY WASTE LOADING CRITERIA

A number of research studies have developed thermal criteria for geologic radioactive waste repositories. These criteria cover all three levels of barriers in waste isolation: very-near-field (canister scale), near-field (repository scale), and far-field (geologic setting and accessible environment). They include both temperature limits and thermomechanical strength-to-stress ratios. These criteria have been gathered in the EIS document for the management of commercially generated radioactive waste (DOE 1980a) and its supporting technical report (DOE 1979b). Section 3.1 reviews these criteria, the data on which they are based, and the thermal loading limits computed with criteria for salt, granite, basalt, and shale. Section 3.2 addresses the issue of radionuclide transport through the geologic setting by thermally induced buoyancy flow, and discusses the restriction on the repository thermal loadings if a thermohydrologically derived limit is also used as a far-field criterion to supplement the thermal and thermomechanical criteria.

3.1 EIS THERMAL CRITERIA FOR NUCLEAR WASTE REPOSITORIES

3.1.1 Brief Description and Summary Tables

The EIS thermal criteria for repository design studies are given in Table 3.1. They are grouped according to the general scale of operation. These criteria are continuously updated with research and design studies (Fossum 1983; OCRD 1985).

3.1.1.1 Very-near-field criteria

Typical borosilicate waste glasses have a transition temperature of approximately 500°C, with a slightly higher softening temperature. Above the softening temperature, plutonium and other heavy waste elements embedded by vitrification may migrate and form separate phases in the glass. Significant increases in cracking and in leach rates might occur. For calcined and sintered glass ceramic, the maximum acceptable temperatures of waste are 700°C and 800°C, respectively (Jenks 1977). For spent fuel, the maximum pin temperature of 300°C was specified from stress rupture considerations.

Structural integrity of the waste package is also an important consideration. The austenitic stainless steel, probably 304L, that has been proposed for HLW canisters is known to undergo structural changes when heated above 400°C (Mecham and others 1976; Atlantic Richfield Hanford Co and Kaiser Engineers 1977); it also exhibits increased susceptibility to stress cracking when exposed to water.

The maximum rock temperatures suggested will vary with the specific rock type. Generally, approximately 250°C may be appropriate for salt and shale, and 350°C may be acceptable for basalt (Kaiser Engineers and Parsons, Brinckerhoff, Quade and Douglas 1980) and granite. However, since these properties depend on the site-specific characteristics of the hard rock, only a general range of temperature has been given.

The limit on maximum fracture of nonsalt rock raises further problems related to the presence or absence of a canister backfill. The conceptual waste package is frequently described as a canister

Table 3.1. Thermal and Thermomechanical Limits for Conceptual Design Studies.

Event	Limits
Very-Near-Field Considerations	
Maximum HLW temperature as vitrified waste	500°C (Jenks 1977)
Maximum spent fuel pin temperature	300°C (Blackburn and others 1978)
Maximum canister temperature	375°C (Jenks 1977)
Maximum rock temperature	250°C to 350°C
Maximum fracture of nonsalt rock	15 cm annulus around canister (Russell 1979)
Near-Field Considerations	
Room closure during ready retrievability period--salt	10 to 15 of original room opening (Russell 1979)
Room stability--granite, basalt rock strength-to-stress ratio	2 within 1.5 m of openings (Dames and Moore 1978a)
Room stability--shale with continuous support rock strength-to-stress ratio	1 within 1.5 m of openings (Dames and Moore 1978a)
Pillar stability--nonsalt strength-to-stress ratio	2 across mid-height of pillar (Dames and Moore 1978a)
Far-Field Considerations	
Maximum uplift over repository	1.2 to 1.5 m (Russell 1979)
Temperature rise at surface	0.5°C (Science Applications Inc 1976)
Temperature rise in aquifers	6°C (Science Applications Inc 1976)

(DOE 1979b, 1980a)

with sleeve surrounded by a backfill that may include materials for sorption of radionuclides, inhibiting water invasion, etc (EPA 1977; DOE 1979b, 1980a; Klingsberg and Duguid 1980). However, such a crushed-rock zone is likely to have a thermal conductivity an order of magnitude lower than that of solid rock, which could lead to unacceptably high canister wall temperatures. Lowry and others (1980) have discussed the possible dangers of a crushed-rock annulus, whether from backfill or decrepitation. They stated that crushed rock should be avoided because of its effect on canister temperatures and that even a sleeve could have a deleterious effect. In the EIS criteria, the annular zone of crushed rock or backfill is limited to less than 15 cm to control the canister temperature and to limit the susceptibility of the canister to aqueous solutions.

3.1.1.2 Near-field criteria

At the room-and-pillar scale, certain thermomechanical considerations must be taken into account to ensure safety in operation and to maintain retrievability of the waste if a decision on waste retrieval were made. These limits vary according to the thermal and mechanical properties of the host rock types. The retrieval operation can proceed if the rooms and tunnels remain accessible and the excavation is stable.

For salt, calculated room closures of less than 10-15 percent of the original room height imply that the repository will generally remain structurally stable throughout the retrieval period (Russell 1979); however, local rock conditions not accounted for in the analysis may result in some local failure.

The stresses around granite or basalt excavations are limited to no greater than one-half of the rock mass strength to ensure that no minor instabilities occur (Dames and Moore 1978a). If any minor failures were to occur, they would probably take place instantly and give rise to additional and larger failures before repair could be made.

Shale is weaker and more ductile than granite and basalt. Engineered supports may be required to construct excavations and assure stability. With proper and continuous support, the strength/stress ratio of the perimeter of the opening may be less than 2 but should be greater than 1.0 within a 1.5 m skin around the excavation.

To ensure pillar stability, the average stress across the mid-height of the pillar should be less than one-half of the uniaxial compressive strength. This criterion was established from past mining experience in hard rocks (Jaeger and Cook 1979). If the edges of the pillar are subjected to stresses greater than one-half of its rock mass strength, reinforcement of the excavation sidewalls is required to maintain the integrity of the pillar.

3.1.1.3 Far-field criteria

On the regional scale it is necessary to limit the surface uplift over the repository centerline. A number of modeling studies have shown that 1.2 to 1.5 m would be the maximum uplift to be expected over a repository in domed salt (DOE 1980a). This range of surface uplift was obtained by linear thermomechanical expansion studies for a 37-W/m^2 (150-kW/acre) repository. In the same study, similar

calculations for granite and basalt for loadings of 47 W/m^2 (190 kW/acre) and for shale for 30 W/m^2 (120 kW/acre) show less than 0.4 m of surface uplift. This limit is one that must be evaluated at a specific site, since the effects of the rock mass movement on the hydrology and geology of the region will vary according to the site.

To avoid problems with the biota (both flora and fauna), the temperature rise should be less than 0.5°C at the repository centerline surface. This is also site specific.

The temperature rise in aquifers is limited to less than 6°C to prevent thermal pollution in the region overlying the repository. There have also been proposals to limit the temperature rise in stagnant aquifers 30 and 90 m deep to 8°C and 28°C, respectively (Cheverton and Turner 1972). This limit must be re-evaluated for each specific site because of variations in geohydrologic and geochemical conditions.

3.1.2 Repository Thermal Load Limits Based on Thermal Criteria

In the DOE literature, a seven-step iterative procedure has been employed using the above thermal criteria to determine acceptable thermal loads for a conceptual repository. The local areal thermal load is first adjusted so that room-and-pillar stability is maintained during a readily retrievable period of at least five years. For reprocessed HLW, the canister load is kept low enough to stay within the very-near-field limits of Table 3.1. Calculations are then made to ensure that the far-field thermal and surface uplift criteria are fulfilled. In these calculations, reasonable estimates were made for the properties of the engineered barriers and geologic formations.

Several simplifying assumptions were also made: (1) the repository is loaded simultaneously and instantaneously, (2) the presence of water is neglected, and (3) only the spent fuel (once through) and U + Pu HLW (total recycle) fuel cycles are considered. The results are tabulated in Table 3.2. The thermal load limit and its controlling thermal criterion are given for each scale of operation and for each type of the four geologic media selected as possible repository environments. (Particular attention should be given to the notes below Table 3.2.) The age of the spent fuel and reprocessed HLW are assumed to be 6.5 years.

The thermal load limits given in the table for vitrified HLW are widely accepted values for the canister loading in each geologic media. The areal thermal loading limits are dominated mainly by the criteria for room closure, with the exception of salt. The parameter of surface uplift is strongly restrictive for spent fuel in salt because the additional heat generated by its actinides operates over the long term. Thus, in a spent fuel repository in salt, a thermal loading of 15 W/m^2 (60 kW/acre) is needed to control the surface uplift in the far-field. Without the surface uplift criterion, the near-field limit would be 37 W/m^2 (150 kW/acre).

Some additional adjustments have been applied to the above figures on the basis of engineering and operational constraints. In order to ensure a conservative estimate of repository capacity, design areal thermal loadings were taken at two-thirds of the value of Table 3.2. Moreover, assuming 6.5-year-old waste rather than 10-year-old waste provided an additional degree of conservatism, since the thermal

Table 3.2. Thermal Load Limits for Conceptual Repository Designs.

	Thermal Load Limit (controlling factor)[a]			
	Salt	Granite	Basalt	Shale
Canister Limits During Retrieval Period (kW)[b]				
Vitrified glass HLW	3.2(A)	1.7(A)	1.3(A)	1.2(A)
Calcined HLW	2.6(A)	1.6(A)	1.1(A)	1.1(A)
Near-Field Local Areal Thermal Loading Limits (W/m^2)[c]				
5-year retrieval - HLW	37(B)	47(B)	47(B)	30(B)
5-year retrieval - SF	[e]	47(B)[f]	47(B)	47(B)[f]
Far-Field Average Repository Thermal Loading Limits (W/m^2)[d]				
HLW	37(C)	47(B)	47(B)	30(B)
SF	15(C)	47(B)	47(B)	30(B)

(DOE 1980a)

[a] Controlling factors: A = canister temperature limit, B = room closure, C = earth surface uplift.

[b] Analysis assumes 15-cm annulus of crushed rock around waste package.

[c] Area includes rooms and adjacent pillars, but not corridors, buttress pillars, and receiving areas. To convert to kW/acre, multiply by 4.05.

[d] Area includes storage area for waste, including corridors and ventilation drifts, but does not include area for shafts or storage areas for other waste types if separate. To convert to kW/acre, multiply by 4.05.

[e] In salt, the emplacement of spent fuel and HLW with plutonium is controlled by the more restrictive 15 W/m^2 (60 kW/acre) far-field thermal limit. Otherwise the near-field limit would be 37 W/m^2 (150 kW/acre).

[f] In order to maintain spent fuel cladding temperatures within the 300°C limit with these areal thermal loadings, the annulus around the canister is left open (no backfill). Heat is transferred across this air space more readily than through crushed backfill material and results in cooler canister and cladding temperatures.

criteria were based on 10-year-old waste with lower thermal output. The resulting thermal loadings are given in Table 3.3. In each case an asterisk denotes the limiting thermal parameter for the given loading and emplacement medium.

From the table it is apparent that in nearly all cases, the near-field structural limitations are the limiting parameters. Only for spent fuel in salt is the far-field criterion of surface uplift a restriction. The conceptual designs consider both PWR and BWR canisters in the spent fuel repository and both reprocessed HLW and remotely handled transuranic waste (RH-TRU) for the recycling option repository. In the case of BWR in shale and RH-TRU in nonsalt media, structural limitations on canister placement limit thermal loading.

These tables demonstrate the use of thermal criteria in establishing design limits for a nuclear waste repository.

3.2 THERMOHYDROLOGIC CONSIDERATIONS ON WASTE LOADING

3.2.1 Needs in Far-field Criteria

Although the thermohydrologic perturbations to the ambient groundwater movement are among the important considerations for repository evaluation, the vertical buoyancy flow from the repository to the surface has not been considered as a bounding criterion in the determination of repository loading densities. This section focuses on the long-term thermohydrologic factors that may limit the waste loading design and discusses a generic thermohydrological criterion (Wang and others 1983a).

Table 3.3. Thermal Loadings Achieved at Conceptual Repositories.

Cycle	Thermal Loading at Emplacement	Salt	Granite	Basalt	Shale
Once through	PWR				
	kW/canister	0.72	0.72	0.72	0.72
	Near-field local (W/m^2)[a]	12	32*	32*	20*
	Far-field average (W/m^2)[a]	10*	25	25	16
	BWR				
	kW/canister	0.22	0.22	0.22	0.22
	Near-field local (W/m^2)[a]	12	32*	32*	14
	Far-field average (W/m^2)[a]	10*	25	25	11
U and Pu Recycle	HLW				
	kW/canister	3.2	1.7	1.3	1.2
	Near-field local (W/m^2)[a]	25*	32*	32*	20*
	Far-field average (W/m^2)[a]	19	23	23	15
	RH-TRU (hulls)				
	kW/canister	0.32	0.32	0.32	0.32
	Near-field local (W/m^2)[a]	25*	23	19	10
	Far-field average (W/m^2)[a]	19	17	15	8

(DOE 1980a)

[a] To convert to kW/acre, multiply by 4.05.

* Denotes limiting thermal parameter.

As shown in Table 3.1, only three stated far-field criteria have found acceptance so far. Two of the criteria are temperature-rise limits. The 0.5°C surface-temperature limit to avoid problems with biota appears to be reasonably achievable (Cheverton and Turner 1972; Science Applications Inc 1976; EPA 1977). The 6°C limit on temperature rise in fresh-water aquifers is to prevent thermal pollution in shallow, near-surface aquifers which are within the region easily accessed by man.

The important existing far-field criterion is the 1.2-1.5 m limit on uplift over the repository. The concern for uplift over the repository originated from the consideration of potential fracturing in the rock. For salt, especially domed salt, the thermal expansion of the salt may lead to fracturing in the over-burden and opening of channels for shallow water to reach the salt formation. The EPA report (1977) points out the significance of this criterion. Geologic stresses could cause a breach of repository integrity.

The primary concern for waste isolation is limiting the radionuclide transport from the repository to the accessible environment. The existing far-field criteria for repository thermal loadings have only an indirect bearing on radionuclide transport. The limits on the temperature rise in stagnant, shallow aquifers do not directly address the movement of groundwater. These limits mainly stem from an environmental concern over thermal pollution in near-surface soils. The issue of radionuclide transport from the repository to the accessible environment through the geologic setting cannot be quantified by the temperature rise near the surface. The uplift criterion indirectly

addresses the potential perturbation to the hydrologic properties of the rock formation, but not the perturbation of the movement of water and radionuclides. An important driving mechanism of radionuclide transport is the thermally induced buoyancy flow. The thermohydrologic effects between the repository and the accessible environment should be included in the criteria for determining waste loading densities.

To directly address the key concerns over thermal impacts on groundwater movement and radionuclide transport, a generic thermohydrologic consideration is discussed below. The thermohydrologic factor is expressed in terms of the allowable buoyancy gradient produced by the cumulative heat released by the waste to the surrounding geologic setting. The buoyancy perturbation to groundwater flow is determined by the thermal expansion of the water, while the surface uplift is determined by the thermal expansion of the rock. The allowable surface uplift has been accepted in the literature as a far-field criterion limiting the repository waste loading density. Preliminary analyses based on buoyancy considerations indicate that thermohydrologic considerations could be even more restrictive in limiting waste loading density than the surface-uplift criterion.

3.2.2 Controlling Factors in Radionuclide Transport

The movement of each individual radionuclide depends on its release rate, the groundwater movement, its adsorption/desorption on the rock surfaces, its diffusion in the rock matrix, the radioactive decay chains, and the chemical processes (reactions, ion exchange, complexing, etc) with other aqueous components. If the velocity field

as a function of space and time can be determined, the path of the radionuclide can be traced and the contribution to the concentration and radiotoxicity of radionuclides in the accessible environment can be evaluated.

Both the geochemical and hydrologic factors in determining the radionuclide velocity in the groundwater are complex. However, lumped factors can describe the velocity as a product of a conductance factor and a driving gradient.

The conductance factor can also be decomposed into the hydrologic and geochemical components:

$$\text{conductance} = \frac{\text{hydraulic conductivity}}{\text{porosity}} \times \frac{1}{\text{retardation}} .$$

The hydraulic conductivity represents the drag on the viscous fluid flow from the porous medium. To determine the water velocity within individual pores and fractures, the fluid flux is corrected by the porosity. The retardation factor is related to the equilibrium sorption coefficient K_d which accounts for the adsorption and other radionuclide-rock interactions in a lumped manner.

The hydraulic conductivity has a high degree of uncertainty with a very wide range in value (four orders of magnitude or more) even for a given rock type (Brace 1980); see Table 2.5 in Section 2.3.3. The porosity may also contribute to the uncertainty because not all the voids are necessarily flow paths for the fluid (Norton and Knapp 1977). The uncertainty in the radionuclide retardation factor depends not only on the rock properties, but also on the geochemical conditions

and radionuclide species in the groundwater. The overall conductance factor for radionuclides, then, will be difficult to determine with certainty, and must be carefully measured on a site-specific basis over the large scale of rock masses.

In contrast to the conductance factor, the driving gradient for the fluid flow and radionuclide transport can be determined with less uncertainty. There are two mechanisms for inducing a hydraulic gradient: the pressure gradient and the buoyancy gradient.

The pressure gradient is determined by the topography and groundwater table near the surface, and by the regional distribution of recharge and discharge zones at depth. The water table and the regional pressure variations can be measured with well-known hydrogeologic techniques. It is expected that the repository will be located in regions with a low regional pressure gradient: for example, 0.001 m/m or 1 m of water table difference over 1 km distance.

The mechanism of buoyancy flow is also well known. With increased temperature, the density of water decreases. The density contrast between the hot fluid near the repository and the cold fluid in the surrounding formation induces the buoyancy gradient in the vertical direction. The magnitude of the buoyancy gradient depends on the change of water density with temperature and on the temperature rise in the rock formation. The former factor has been measured with a high degree of accuracy. The latter factor can be calculated for different rock formations. Away from the repository, the temperature distributions are not very sensitive to the rock types (see for example the compari-

son of granite, bedded salt and domed salt temperature profiles in the EPA report (1977) and previous discussions in Section 2.6. The long-term, far-field temperature rise depends mainly on the rock heat capacity which is fairly insensitive to the different rock types. This allows us to evaluate and predict long-term thermal effects with cautious optimism.

3.2.3 Thermohydrologic Effects Quantified by the Buoyancy Gradient

The magnitude of the buoyancy gradient can be a measure for the thermohydrologic effects. Thermal impact with waste emplacement should not perturb the ambient hydrologic condition excessively. The thermohydrologic perturbations could be limited by requiring that the thermally induced buoyancy gradient be less than the ambient pressure gradient.

When the hydrogeologic conditions around a suitable site have been evaluated and the rock formations have been shown to be tight enough to have slow ambient groundwater flow, it is imperative that the waste emplacement does not breach the effectiveness of the isolation provided by the geologic setting. If we want to maintain the hydrologic integrity of the rock formation in order to contain the radionuclides, the perturbation induced by the waste should be as small as possible. Otherwise, the long, favorable flow paths from the repository to the discharge zone may be short-circuited by the vertical flow paths. With drastic flow pattern changes, there is no longer a guarantee that the hydrologic conditions favorable for isolation can be preserved. If the ambient groundwater flow is horizontal, the thermally induced upward tilting of the water velocity through the

repository should be less than 45° (for the effects of 45° tilting, see the study in Bourke and Robinson 1981). If the ambient groundwater movement is downward, for a repository located below a recharge zone, the buoyancy gradient should be limited to ensure that the water will not reverse its direction during the thermal period.

Depending on one's viewpoint, the requirement that "the buoyancy gradient be less than the ambient pressure gradient" may be regarded as either not conservative enough or too restrictive. On the one hand, one may argue that a tilting of 45° is too large a distortion to the ambient groundwater flow pattern. According to this view, if the distance between the repository and the discharge zone is ten times the depth of the repository, the allowable buoyancy gradient should be one-tenth of the regional pressure gradient. On the other hand, one may argue that the host formation has low enough permeability and high enough retardation that the buoyancy gradient can be much larger than the present ambient gradient. Therefore, the allowable magnitude of the buoyancy gradient is best left as an open question at present. As a preliminary suggestion, we have suggested that the maximum buoyancy gradient be less than the ambient pressure gradient, a proposition that is balanced between the different viewpoints.

A further requirement for a useful criterion is that it must allow meaningful quantitative evaluations with minimal assumptions and uncertainty. An essential feature of using the buoyancy gradient as a measure of thermohydrologic effect is that it is expressed in terms of the magnitudes of the gradient components rather than the magnitudes of the velocity components. The buoyancy and pressure components of

the hydraulic gradient can be determined with reasonable precision by current hydrogeologic techniques and are free from the uncertainty associated with the hydrologic and geochemical parameters of the rocks.

3.2.4 Allowable Thermal Loading from Buoyancy Considerations

In all the existing studies, the repository thermal loading is mainly determined by thermomechanical criteria. If the thermohydrologic consideration is less restrictive than the existing criteria, it will be of limited interest as an additional check. The simple analysis presented below shows that the buoyancy consideration turns out to be more restrictive in many cases than the existing criteria in determining the allowable thermal loading.

We will base our analysis on the results of the generic EIS (GEIS) study (Dames and Moore 1978a). In the GEIS, surface uplift has been evaluated for SF repositories and HLW repositories in salt, granite, basalt, and shale. These results are tabulated in Table 3.4. Both the surface uplift ΔZ and the buoyancy gradient i_B are determined by the temperature rise $\Delta T(z)$ from the repository to the surface. Assuming a homogeneous rock medium and treating the level at repository depth D as a stationary boundary for rock movement and an ambient boundary for buoyancy flow,

$$i_B \frac{D}{\alpha_{water}} = \Delta Z \frac{1}{\alpha_{rock}} \frac{1-\mu}{1+\mu} = \int_{-D}^{0} \Delta T(z)\, dz \ .$$

This equation is discussed in detail in the Appendix. The values of the buoyancy gradient deduced from the corresponding values of surface

Table 3.4. Surface Uplift and Buoyancy Gradient.

Rock	Salt		Granite		Basalt		Shale	
Waste	SF	HLW	SF	HLW	SF	HLW	SF	HLW
Maximum surface uplift, m	3.45	1.27	0.94	0.34	0.58	0.18	0.79	0.34
Time, years	1,000	150	3,000	1,000	7,000	3,000	3,500	1,800
Loading, W/m^2	37		47		47		30	
Thermal expansion coeff. α_{rock}, $°C^{-1}$	4.0×10^{-5}		8.1×10^{-6}		5.4×10^{-6}		8.1×10^{-6}	
Poisson ratio factor, $1+\mu/1-\mu$	2.08		1.44		1.70		1.35	
Buoyancy gradient, m/m	0.026	0.0097	0.051	0.018	0.040	0.013	0.046	0.019

(Science Applications Inc 1976; Dames and Moore 1978a)

Thermal expansion coefficient of water $\alpha_{water} = 3.85 \times 10^{-4}$ $°C^{-1}$.

Repository depth D = 610 m (2,000 ft).

uplift are also tabulated in Table 3.4, together with the rock and water parameters needed for the conversion.

For the 37 W/m^2 (150 kW/acre) repositories in salt, the 47 W/m^2 (190 kW/acre) repositories in granite and basalt, and the 30 W/m^2 (120 kW/acre) repositories in shale considered in the GEIS, the buoyancy gradients are in the range of 0.01 to 0.05 m/m. These values are 10 to 50 times larger than the typical ambient pressure gradient of 0.001 m/m. The 0.001 m/m value has been used in most of the recent thermohydrologic studies in waste repositories (Dames and Moore 1978b; Hardy and Hocking 1978; Burgess and others 1979; Hodgkinson 1980; Wang and Tsang 1980).

If we require that the thermal loading will not induce a buoyancy gradient larger than 0.001 m/m, then the GEIS thermal loading values based on the room stability criterion must be reduced. The thermal loadings based on this buoyancy consideration are tabulated in Table 3.5.

Thus, if we adopt this buoyancy gradient limit, it is clear from Tables 3.4 and 3.5 that the thermal loadings have to be much smaller than all the values considered in the past. The implication is obviously a dramatic one. To limit the long-term thermohydrologic perturbation and to preserve the integrity of the rock formation as a waste barrier, either we have to use 10 to 50 times more repositories to accommodate the same amount of wastes, or to extend the area of each repository in design 10- to 50-fold. These preliminary results therefore indicate that the thermohydrologic considerations could be very restrictive and are a key area that requires further study.

Table 3.5. Loading Based on Buoyancy Considerations.

Rock	Salt		Granite		Basalt		Shale	
Waste	SF	HLW	SF	HLW	SF	HLW	SF	HLW
Allowable Waste Density, MTHM/m^2	0.0012	0.0037	0.0008	0.0025	0.0010	0.0036	0.0005	0.0015
Allowable thermal loading, W/m^2	1.4	3.8	0.9	2.7	1.2	3.7	0.6	1.5

One additional factor to consider with regard to thermohydrologic effects is the time when the maximum buoyancy gradient occurs. The maximum surface uplift and buoyancy effects occur between 1,000 and 10,000 years. If the existing thermal loading is still used, the waste must be contained or at least the rate of release must be controlled before the peak of the buoyancy gradient. Otherwise, when the 1,000-year containment time is over and the radionuclides are released from the canisters, it will coincide with a peak of the buoyancy gradient and radionuclides could be transported relatively quickly to the surface. In the GEIS study, the minimum surface approach time is in the range of 100 years.

3.2.5 Discussion on Buoyancy Gradient Considerations

For the long-term prediction of radionuclide transport, we need to know the absolute magnitude of the movement of the water and radionuclides, which the buoyancy gradient consideration does not include. It does not impose an absolute limitation on the magnitude of the movement of water and radionuclides. In addition to the gradient, the movement of individual water particles and dissolved radionuclides also depends on the conductance factors for each flow path in the rock formation. In essence, the gradient criterion factors out the hydrologic and geochemical parameters which are highly heterogeneous and difficult to measure. By comparing only the gradient components, most of the uncertain factors in assessing the thermal impact are lumped together and thereby avoided. The buoyancy gradient consideration addresses only the change of the flow pattern, not the absolute magnitude of the velocity and travel time.

Imposing a limit on the buoyancy gradient does ensure that the thermally induced vertical groundwater environment will not overwhelm the ambient groundwater flow. An understanding of long-term, far-field thermohydrologic effects is necessary to relate the site characterization studies to the repository designs. In the existing siting criteria for geologic formations, the focus is on the characterization of ambient hydrologic and geochemical conditions to identify a tight formation with long travel times to the accessible environment. The determination of the thermal loading by using thermohydrologic considerations in repository design is to ensure that the additional perturbation will not upset the ambient conditions excessively and will preserve the features of a site which make it useful for the effective isolation of nuclear wastes. Thus this buoyancy consideration complements the already-established criteria in the literature for the proper design of the repository in a suitable geologic setting.

4. EFFECTS OF THE SURFACE COOLING PERIOD ON THERMAL IMPACTS

For a given amount of waste, a long surface cooling period allows the short-lived radionuclides to decay and the heat power to decrease. In the United States, 10 years has been regarded as the standard cooling period. The basis for the choice of a 10-year cooling period is briefly discussed in Section 4.1. With longer surface cooling periods, the very-near-field temperature rises around the waste canister will be lower, as shown in Section 4.2. The effects of surface cooling on the near-field temperature rise in the repository depend sensitively on the waste density and thermal loading schemes, as discussed in Section 4.3. There is a growing consensus, especially in the European countries considering permanent disposal of reprocessed HLW, that an extension from 10 years to 40 years or even up to 100 years of cooling time may be beneficial. Section 4.4 discusses the trade-off between a longer surface cooling period and a higher waste loading density as determined by existing near-field thermomechanical criteria. Section 4.5 addresses the question of the cooling period and thermal loading from the long-term, far-field point of view.

4.1 ECONOMIC CONSIDERATIONS OF THE SURFACE COOLING PERIOD

Temporary storage of waste above ground allows heat generation rates and radiation intensities to decrease, thereby reducing subsequent treatment and disposal expenses. However, the maintenance of surface facilities can be expensive. For reprocessed HLW, the cost of waste solidification and waste transportation to and from the processing site depends on the waste age (Dillon and others 1971). The summation of the predisposal and disposal expenses as a function

of waste age at burial was shown to have a minimum of 3 to 10 years, and likely closer to 10 years because of increases in estimated expenses for the repository (Cheverton and Turner 1972). Most of the subsequent thermal analyses have taken the work of Cheverton and Turner as the benchmark and considered 10 years as the optimal cooling period.

Several factors have since contributed to the uncertainties of the economics of mined geologic repositories. One factor is that SF is now being considered as a potential waste form. Currently, most of the discharged SF assemblies are stored in cooling ponds at reactor sites. Away-from-reactor monitored retrievable storage facilities are being considered to accommodate the SF when the on-site capacities are saturated (DOE 1979a, 1980a, 1984, 1985, 1986f,g,h; NRC 1986). With the delay in the repository start-up dates, the fraction of older wastes to be emplaced in the repository will increase (see Section 2.1.3). The waste form, thermal loading, and time delays are among the key variables in determining the expense of a repository. Uncertainties in repository costs are expected to be quite large (Forster 1979).

The sensitivity of the expense of a repository to its design parameters has been evaluated in a number of studies (Kaiser Engineers 1978b; Stearns-Roger Engineering Co 1979; DOE 1980a,b). The choices of rock type, thermal loading, and repository size all influence repository costs significantly. Table 4.1 gives representative cost figures for basalt and granite repositories for each of two thermal loadings. The total expenses per repository decrease with lower thermal loading. However, undiscounted unit costs increase sharply,

indicating that the total cost reductions achieved are not in proportion to the decrease in waste receipts. Table 4.2 shows the effects of the repository size on the expenses for domed salt repositories. The total expenses per repository are insensitive to repository size. The undiscounted unit costs decrease as size increases.

The representative results given in Table 4.2 illustrate the sensitivity of repository expenses. It is important to point out that in the examples of economic analyses presented above, and in the repository design considerations discussed previously in Sections 2 and 3, the repository capacities are expressed in terms of areal thermal loadings. The thermal loading values are referred to a fixed waste age. When wastes of different ages (cooling periods) are considered, the corresponding thermal loading values change drastically (see description in Section 4.2). If the economic analyses of repository design based on 10-year-old wastes are used for different waste ages, the results must be carefully scaled to avoid nonconservative and erroneous conclusions. As will be shown in Sections 4.3-4.5, nonconservative conclusions could be made if long-term, far-field environmental considerations are not included in the economic analyses and design studies. Dippold and Wampler (1984) discussed the implications of older wastes on the design and cost of a salt repository.

4.2 REDUCTION OF VERY-NEAR-FIELD THERMAL IMPACTS

In the very-near-field, the short-term rises in temperature around the waste canisters are very sensitive to the duration of the surface cooling period. If the structural integrity of the waste package and

Table 4.1. Estimated Repository Expenses for Varying Thermal Loadings.

Item	Basalt 25 W/m^2 (100 kW/acre)	Basalt 10 W/m^2 (40 kW/acre)	Granite 25 W/m^2 (100 kW/acre)	Granite 10 W/m^2 (40 kW/acre)
Canisters of SF Stored	400,000	160,000	400,000	160,000
MTHM Stored	170,000	68,000	170,000	68,000
Repository Area, km^2 (acres)	8.1 (2,000)	8.1 (2,000)	8.1 (2,000)	8.1 (2,000)
MTHM/m^2 (MTHM/acre)	0.021 (85)	0.0083 (34)	0.021 (85)	0.0083 (34)
Canisters/m^2 (per acre)	0.05 (200)	0.02 (80)	0.05 (200)	0.02 (80)
Years of Operation	32	14.9	32	14.9
Total Expense (M)	3950	3150	3940	3130
Undiscounted Unit Cost (/kg)	23.20	46.30	23.20	46.00

(DOE 1980c)

Note: All expenses in 1980 dollars, unescalated, undiscounted.

Table 4.2. Effects of Size on Salt Dome Repository Expenses.

Item	Standardized Repository Size 4.9 km^2 (1,200 acre)	8.1 km^2 (2,000 acre)	11.3 km^2 (2,800 acre)
Assumed Heat Loading W/m^2 (kW/acre)	10 (40)	10 (40)	10 (40)
Canisters of SF Stored	96,000	160,000	224,000
MTHM Stored	41,000	68,000	96,000
MTHM/m^2 (MTHM/acre)	0.0083 (34)	0.0083 (34)	0.0083 (34)
Canisters/m^2 (per acre)	0.02 (80)	0.02 (80)	0.02 (80)
Years of Operation	10.4	14.9	19.5
Total Expense (M)	2470	2490	2850
Undiscounted Unit Costs (/kg)	60.20	36.60	29.70

(DOE 1980c)

Note: All expenses in 1980 dollars, unescalated, undiscounted.

emplacement borehole is the primary concern, it is advantageous to allow the highly active waste elements to decay and the temperature to decrease.

4.2.1 Decay of Fission Products

Radioactive decay and neutron-induced nuclear reactions in the waste elements determine the radioactivity and the heat generation rate of the stored wastes. Table 4.3 shows the contributions from the principal radionuclides to the heat power of SF 10 years after being discharged from a PWR. The heat of 10-year-old waste is released mainly by the short-lived fission products. The time dependence of the heat power between 10 and 100 years will be determined mainly by Sr-90 and Cs-137, with half-lives of 28 and 30 years, respectively.

The main effect of a long surface cooling period is to reduce the concentration of the short-lived radionuclides. The heat released by the long-lived actinides Pu-239, Pu-240, and Am-241 will not be reduced significantly with the extension of cooling from 10 years to 100 years. The composition of waste content depends on the fuel cycles discussed in Section 2.1.1. Table 4.4 summarizes the heat generation rates for different waste ages and different fuel cycles from a given amount of waste (1 MTHM). Among the three fuel cycles, reprocessed HLW with both U and Pu recycled contains the highest concentration of fission products, and SF contains the highest concentration of actinides. The contrast in the waste compositions among different fuel cycles must be taken into account in studying the effects of different surface cooling periods.

Table 4.3. Radionuclide Heat Generation Rates for 10-year-old PWR SF.

Principal Radionuclides	Half-life (years)	Heat Power W/MTHM	Heat Power of Total
Fission Products			
Kr-85	10.76	7.4	0.6
Sr-90	28	71	6
Y-90[a]	7.39×10^{-3}	330	28
Sb-125	2.7	2.5	0.2
Cs-134	2.1	95	8
Cs-137	30	89	7
Ba-137[a]	4.94×10^{-6}	320	27
Pr-144[a]	3.29×10^{-5}	1.1	0.1
Pm-147	2.6	2.7	0.2
Eu-154	16	50	4.2
Actinides			
Pu-238	89	73	6.1
Pu-239	2.4×10^{4}	10	0.8
Pu-240	6.6×10^{4}	15	1.3
Pu-241	13	3.3	0.3
Am-241	458	59	5.0
Cm-244	18.1	47	3.9
Others		14	1.2
	Total	1190.0	100.0

(Arbital and others 1979)

[a] Short-lived daughter products.

Table 4.4. Initial Heat Generation Rates for Different Waste Ages and Types.

	Heat Power (W/MTHM)		
Years after Discharge	Spent Fuel PWR	HLW: U + Pu Recycle	HLW: No Recycle
1	10,430	11,542	10,274
2	5,640	6,177	5,500
5	2,011	2,256	1,867
10	1,189	1,340	1,032
40	625	540	431
100	289	139	109

4.2.2 Decreases in Temperature Rise

When heat power decreases, the temperature rise decreases. Figure 4.1 illustrates the sensitive dependence of the very-near-field temperature rise on the duration of the surface cooling period. The temperature rises are for the point located at 0.26 m from the canister axis in the midplane of a single HLW canister measuring 0.162 m in diameter and 3 m in length and containing 2.09 MTHM of waste. If the thermal interaction from neighboring canisters is neglected, the very-near-field temperature rises in different rocks are approximately proportional to the inverse of the thermal conductivities, and the times are scaled by the thermal diffusivities controlling the heat conduction. The thermal properties in Table 2.9 are used in the scaling in Fig. 4.1.

The very-near-field temperature rise is approximately proportional to the canister emplacement heat power, which decreases sharply with surface cooling duration. The short cooling periods are therefore especially effective in lowering the very-near-field thermal impacts. By applying the very-near-field thermal criteria (Section 3.1), the waste content in each reprocessed HLW canister can be determined. For an SF canister containing one fuel assembly, the waste content (0.4614 MTHM for PWR, 0.1833 MTHM for BWR) is lower than for a reprocessed HLW canister, and the very-near-field temperature rises around a single SF canister will be lower than those shown in Fig. 4.1.

For a more concentrated SF canister, the very-near-field temperature rises are correspondingly higher. Table 4.5 lists the unit-cell results of Altenbach (1978) for the maximum salt temperature around a concentrated SF canister containing 650 fuel rods (or approximately 3 PWR fuel assemblies). (The area of the unit cell occupied by one canister is 5.5 m (18 ft) by 23.8 m (78 ft).) To show that the very-near-field temperature rise is approximately proportional to emplacement power, the ratio of borehole temperature rise to initial canister power is also included in Table 4.5. The unit-cell results also take into account the thermal interaction among neighboring canisters. For cases with high areal waste density and close canister spacing, the thermal interaction is an important factor in determining the maximum rock temperature. As a result of thermal interaction, the temperature rise from the combined contribution of the canister array is higher than that induced by a single canister.

These analyses illustrate that the sensitive thermal effects near the waste package at short times are approximately proportional to the emplacement heat power. With a long surface cooling period, the heat power at emplacement decreases and the temperature rise decreases correspondingly. The potential advantage of a long surface cooling period is to lower the likelihood of undesirable thermally induced effects such as canister cracking and borehole degradation.

4.3 WASTE DENSITY AND THERMAL LOADING

If the waste content of each canister and the spacing between the canisters are fixed, it is obvious that longer surface cooling will reduce the thermal impact at all scales of operation and over all

Table 4.5. Peak Salt Temperature for Various Emplacement Times.

Surface Cooling Period (years)	Emplacement Power (kW/canister)	Maximum Temperature Rise (°C)[a]	Temperature to Power Ratio (°C/kW)	Time of Maximum (years)
0.4	28.8	510	18	0.26
1.4	11.6	221	19	0.46
3.4	4.61	88	19	0.59
5.4	2.81	57	20	1.02

[a] Ambient temperature 37°C (98°F) was subtracted from the results of Altenbach (1978).

times. However, economic considerations may require that the repository design take advantage of the lower thermal impact by utilizing a more concentrated emplacement scheme. Sections 4.3.1-4.3.3 discuss and compare the results of different loading schemes.

4.3.1 Loading at Constant Waste Density

For a standard repository with 10-year-old SF stored at a thermal loading of 10 W/m^2 (40 kW/acre), the corresponding waste density is 0.0083 $MTHM/m^2$ (33.6 MTHM/acre). Figure 4.2 illustrates the dependence of the repository temperature increase on the surface cooling period if this waste density is held fixed.

Each curve in Fig. 4.2 has several peaks or bumps at different times. The 1-year cooling curve shows this structure most clearly. These features appear before 10 years and around 10^2, 10^3, and 10^4 years. The short-time features diminish rapidly with longer surface cooling periods. The earlier peaks originate from the short-lived radionuclides. The long-lived radionuclides control the long-term thermal impact. Although the surface cooling periods drastically change the repository peak temperature, the repository will nevertheless have a significant temperature rise above the ambient for over 10^4 years, even for a surface cooling period of 100 years.

The results in Fig. 4.2 are calculated with a uniform disk repository model in granite and scaled to other rock formations by the inverse square root of thermal conductivity-volumetric heat capacity products (see Equation (A-6) in the Appendix). This scaling is exact if the heat power is a single-term exponential decay function. The small differences in the shapes of the temperature rise curves among

different rocks (see, for example, Fig. 2.19) are neglected in the scaling used in Fig. 4.2-4.7.

If reprocessed HLW instead of SF is stored with the same waste density, extending the cooling time from 10 years to 100 years can lower the repository temperature much more effectively. This is shown in Fig. 4.3. Reprocessed HLW has most of its long-lived actinides removed, and the repository temperature can therefore return to ambient much faster. If an effective half-life of 30 years is assumed for the reprocessed wastes, a 40-year cooling will reduce the activity of 10-year-old waste by half and a 100-year cooling period will lower the heat power of 10-year-old waste by a factor of 8.

If the waste density is fixed, the results for both SF and reprocessed HLW indicate that surface cooling can lower the peak temperature at early times. The long-term thermal impact depends on the actinide content, which is not sensitive to the duration of the surface cooling period.

4.3.2 Loading at Constant Emplacement Power Density

In this section, we will consider the same repositories but with a constant thermal power density instead of a constant waste density. Two reasons have prompted us to present these results. First, the results of most economic analyses and repository design studies are presented in terms of areal thermal loading. It is interesting to study the effects of surface cooling by treating the familiar areal thermal loading (W/m^2 or kW/acre) as a fixed parameter. Second, the very-near-field analysis discussed in Section 4.2 indicates that the rises in temperature around the waste package scale with emplacement

heat power. If only the very-near-field impacts are considered, a constant heat power will induce the same thermal impact, independent of the waste age.

Figure 4.4 illustrates the dependence of temperature increase on the surface cooling period of an SF repository with a constant emplacement power density of 10 W/m^2 (40 kW/acre). With the same emplacement power density, the repository temperature rises do not stay the same with different cooling periods. With longer cooling periods, the repository temperature increases. This anomalous trend is especially drastic for surface cooling periods changing from 10 to 40 to 100 years.

By imposing the same emplacement heat power density, the 100-year-old waste, with most of the short-lived fission products already decayed, will contain a substantially larger amount of actinides per unit acre. Therefore, the long-term thermal impact increases accordingly. For reprocessed HLW, the anomalous difference between 10-year cooling and 100-year cooling is less drastic, as shown in Fig. 4.5.

Unlike the very-near-field impacts which scale approximately with emplacement heat power alone, the near-field and far-field thermal impacts depend on both the initial power and the subsequent time decay. Since the heat power decay depends sensitively on the waste content, the effects of surface cooling must be assessed for each different fuel cycle.

4.3.3 Comparison of Different Loading Schemes

The results of Section 4.3.1 for constant waste density and the results of Section 4.3.2 for constant power density are summarized in Fig. 4.6 and 4.7, respectively. These results illustrate that entirely different conclusions can be made about the effects of surface cooling periods, depending on the parameters chosen and the waste type considered. Comparing the 10-year results with the 100-year results leads to the following conclusions.

- With constant waste density, surface cooling reduces the thermal impacts significantly for reprocessed HLW but modestly for SF.
- With constant emplacement power density, surface cooling increases the thermal impact significantly for SF but very modestly for reprocessed HLW.

We emphasize these points because the thermal loading density has been the most frequently used parameter in the literature. The relationship between thermal loading and waste density has been recognized implicitly in some of the literature. We hope that the above explicit comparison will call attention to this simple but important difference.

4.4 OPTIMIZATION OF WASTE LOADING WITH NEAR-FIELD CRITERIA

Waste loading density is one of the key parameters in the design of a repository. Near-field thermomechanical criteria have been used to determine the optimal waste loading density for 10-year-old wastes (see Sections 2.5.2 and 3.1.2). With longer surface cooling periods to lower the heat power per unit waste, it seems logical to allow a more concentrated waste loading scheme. Section 4.4.1 discusses the

allowable waste loading densities based on the temperature rise criteria. In Section 4.4.2, the existing thermomechanical criteria for different rock types are used to extend the design densities for 10-year-old wastes to older wastes.

4.4.1 Allowable Loading with Near-Field Temperature Criteria

In the classical conceptual design study for salt, Cheverton and Turner (1972) used the 1 percent and 25 percent salt temperature criteria to determine the maximum permissible loading density. Between the canisters, no more than 1 percent of the salt was allowed to have a temperature above 250°C and no more than 25 percent of the salt was allowed to have a temperature above 200°C. The results for a room 4.6 m wide are shown in Fig. 4.8. The results were calculated with 1- , 4- , and 10-year-old reprocessed HLW and extrapolated to 100 years on the assumption that the effective half-life of the waste is 30 years. (A constant half-life results in a constant maximum permissible emplacement power level per waste package.) For a waste age of less than 4 years, the 1 percent salt criterion (very-near-field) becomes limiting and the permissible loading depends on the pitch along a canister row. For older wastes, the 25 percent salt criterion (near-field) determines the loading.

For older wastes with near-field instead of very-near-field criteria controlling the permissible loading density, we could use a simpler model that assumes a uniform waste loading to calculate the maximum repository temperature and determines the allowable waste densities accordingly. For example, Table 4.6 illustrates the acceptable waste

Table 4.6. Waste Density and Thermal Loading for Repository Temperature Rise of 47°C in Granite.

	Spent Fuel		Reprocessed HLW	
Surface Cooling Period (years)	MTHM/m^2 (MTHM/acre)	W/m^2 (kW/acre)	MTHM/m^2 (MTHM/acre)	W/m^2 (kW/acre)
10	0.0083 (33.6)	10.0 (40)	0.0117 (47.2)	12.0 (49)
40	0.0118 (47.7)	7.4 (30)	0.0240 (97.2)	10.3 (42)
100	0.0142 (57.5)	4.1 (17)	0.0921 (373)	10.1 (41)

density and the corresponding thermal loading in granite if a 47°C temperature rise limit is imposed as a criterion. The 47°C temperature rise is specified for a granite repository containing 10-year-old spent fuel loaded at a thermal density of 10 W/m^2 (40 kW/acre). With longer surface cooling, it is shown that the same repository can accommodate more waste, but only if emplacement power density is lower.

The maximum repository temperature determines the thermomechanical stability of the mined repositories. In the current thermal design criteria for different rock types, the maximum allowable temperature-rise limits are replaced by thermomechanical criteria. The results of the extension of thermomechanical analyses for 10-year-old wastes to older wastes are discussed in the next section.

4.4.2 Allowable Waste Density with Near-Field Thermomechanical Criteria

The existing thermomechanical criteria are expressed in terms of strain of room closure for salt and strength-to-stress ratios for hard rock repositories (shown earlier in Table 3.1). Imposing these existing criteria on older wastes enables allowable waste densities to be determined. The salt and nonsalt analyses are discussed in the following two subsections (Wang and others 1983b).

4.4.2.1 Reduction of strain for room convergence in salt

Room convergence in salt mines depends on the temperature, pillar stress, and time. In Project Salt Vault (Bradshaw and McClain 1971), the results of model pillar tests of rock salt from the Lyons mine were fitted with an analytic formula called Lomenick's formula (see Appendix, Section A.2). It has been used in the NWTS conceptual

designs for domed and bedded salt (Kaiser Engineers 1978a,b; Stearns-Roger Engineering Co 1979) and in the NWTS conceptual reference repository description (Bechtel 1981). In this section we extend the NWTS results for 10-year-old wastes to older wastes.

The NWTS reference salt repository contained 10-year-old wastes emplaced at 37 W/m^2 (150 kW/acre) at 640 m (2100 ft) depth with an average pillar stress of 14.5 MPa (2100 psi). The waste storage rooms were 6.1 m (20 ft) wide and 4.8 m (15 ft 9 in.) high. After 5 years, however, the roof height had shortened by 0.23 m (9 in.). Older wastes stored in the same room and at the same waste emplacement density have a lower average temperature rise at 5 years, thereby reducing the cumulative room convergence (Fig. 4.9). If 0.23 m of room convergence (5 percent linear strain) is acceptable for safe operations in the repository, the waste emplacement density can be increased. The allowable waste densities and the corresponding thermal densities are tabulated in Tables 4.7 and 4.8 along with the results for hard rocks, discussed in the following subsection.

4.4.2.2 Reduction of strength-to-stress ratios in granite, basalt, and shale

The stress fields around a room in hard rocks such as granite, basalt, and shale depend on the temperature, the in situ stress field, and the change in load due to excavation (see Section 2.5.2). The thermomechanical stability limits for mined repositories in hard rock were established in the GEIS study (Dames and Moore 1978a; DOE 1979b). These near-field criteria determine the repository loading density of 10-year-old wastes (see Section 3.1.2).

The near-field thermomechanical criteria are expressed in terms of strength-to-stress ratios, as shown earlier in Table 3.1. The repositories contain 10-year-old wastes stored at a thermal power density of 47 W/m^2 (190 kW/acre) in granite and basalt and 30 W/m^2 (120 kW/acre) in shale. At 5 years after waste emplacement, the sum of the thermally induced stress and the excavation-induced stress within 1.5 m of the openings is half the magnitude of the rock strength for granite and basalt and equal to the rock strength for shale. Older wastes stored at the same waste emplacement density have a lower average temperature rise after 5 years, and the thermally induced stress is less (Fig. 4.10). The temperature rises at the end of 5 years are used to determine the stress values. If the same strength-to-stress ratio criteria can be used for older wastes to ensure mine stability, the waste emplacement density can be increased to accommodate more wastes in the repository, as shown in Table 4.7. The temperature dependence of the rock strength is taken into account. The corresponding thermal loading densities are less sensitive to the surface cooling period, as shown in Table 4.8.

4.4.2.3 Increase of waste emplacement density

The ratios of allowable waste densities of older wastes (tabulated in Table 4.7) to the values of 10-year-old wastes are illustrated in Fig. 4.11. It shows that older wastes could be emplaced at more concentrated densities. These results are based on the assumption that the near-field thermomechanical criteria developed for 10-year-old wastes are acceptable independent of the surface cooling period. For reprocessed HLW with a small thermal contribution from the long-lived

Table 4.7. Allowable Waste Density Determined by the Near-Field Thermomechanical Criteria.

Surface Cooling Period (years)	Salt		Granite		Basalt		Shale	
	SF	HLW	SF	HLW	SF	HLW	SF	HLW
	$MTHM/m^2$ (MTHM/acre)		$MTHM/m^2$ (MTHM/acre)		$MTHM/m^2$ (MTHM/acre)		$MTHM/m^2$ (MTHM/acre)	
10	0.0311 (126.0)	0.0359 (145.2)	0.0394 (159.6)	0.0454 (183.9)	0.0394 (159.6)	0.0454 (183.9)	0.0249 (100.8)	0.0287 (116.1)
40	0.0534 (216.1)	0.0713 (288.7)	0.0797 (322.5)	0.1173 (474.6)	0.0699 (282.7)	0.1011 (409.2)	0.0441 (178.5)	0.0639 (258.4)
100	0.0786 (318.2)	0.1112 (450.0)	0.1759 (711.8)	0.4799 (1942)	0.1478 (598.1)	0.3966 (1605)	0.0933 (377.8)	0.2505 (1014)

Table 4.8. Allowable Thermal Loading Density Determined by the Near-Field Thermomechanical Criteria.

Surface Cooling Period (years)	Salt		Granite		Basalt		Shale	
	SF	HLW	SF	HLW	SF	HLW	SF	HLW
	W/m^2 (kW/acre)		W/m^2 (kW/acre)		W/m^2 (kW/acre)		W/m^2 (kW/acre)	
10	37 (150)	37 (150)	47 (190)	47 (190)	47 (190)	47 (190)	30 (120)	30 (120)
40	33 (135)	31 (124)	50 (201)	51 (204)	44 (177)	44 (176)	28 (111)	28 (111)
100	23 (92)	12 (49)	51 (205)	52 (212)	43 (173)	43 (175)	27 (109)	27 (111)

actinides, these conclusions may be valid. However, for spent fuel repositories, the long-term, far-field effects could become the limiting consideration. This is discussed in Section 4.5.

Figure 4.11 also shows that the increase in allowable waste density is modest for salt compared to the results for hard rocks. For salt, the increase in allowable waste density grows at a slower rate for the longer surface cooling times. Thus the option of a longer surface cooling period may be less attractive for salt than for hard rock repositories. The difference in the form of the curves for salt and for hard rocks results mainly from the different thermomechanical behaviors assumed in the analyses. For salt, the plastic creep strain is proportional to $(T_{amb} + \Delta T)^{9.5}$, where T_{amb} is the ambient temperature in kelvins and ΔT is the waste-induced temperature rise (see Lomenick's formula in the Appendix, Section A.2). For hard rocks, thermoelasticity is assumed for the stress changes, and the thermally induced stress is proportional to ΔT. As longer surface cooling periods lower the temperature rise, ΔT, the nonlinear temperature dependence of the creep for salt shows less sensitivity to ΔT, resulting in a smaller increase in allowable waste density.

The thermoelasticity assumed for hard rocks may be oversimplified in view of the potential nonlinear contributions from the presence of fractures. Additional research beyond the scope of this report is required to study the thermomechanical behavior of fractured rock masses. The temperature dependence of the elastic constants are also not taken into account in the calculations. The dependence of rock strength on temperature, however, is taken into account. Within the

temperature range of interest for these calculations (below 120°C or 250°F), granite exhibits a noticeable change in rock strength with temperature, whereas the basalt and shale strengths are almost temperature independent (Dames and Moore 1978a). For cooling periods of 10 to 100 years, this gain in strength with lower temperature permits an approximate increase of 20 percent in waste density for granite relative to its allowable limit for a fixed strength at 120°C. Since the mechanical properties and rock strengths are highly site specific, the quantitative conclusions in these calculations should be carefully re-evaluated for any specific rock type and any potential repository site.

4.5 LIMITATION OF LOADING BY LONG-TERM, FAR-FIELD CONSTRAINTS

The long-term, far-field thermohydromechanical effects depend on the temperature rise in the host rock, especially in the region between the repository and the surface. Before we present more detailed results for the loadings based on far-field considerations, it is of interest to present one example of the far-field temperatures in granite induced by a repository uniformly loaded with a constant mass density. Figure 4.12 illustrates the temperature rise at a point midway between the repository and the surface. Similar magnitudes of the maximum temperature rises are expected for other rocks, since the volumetric heat capacities controlling the far-field temperature are insensitive to the differences in rock types. Comparing these results with the near-field results shown earlier in Fig. 4.2 and 4.3 makes it evident that the far-field results are less sensitive to the surface cooling period, especially for the SF repository.

The temperature rise from the repository to the surface determines the surface uplift and the buoyancy flow. The repository loading density could be limited by these far-field constraints. These constraints are discussed in the following two sections.

4.5.1 Surface Uplift Considerations

To illustrate that the surface uplift considerations can determine waste loading densities, we will summarize the results of the final EIS (DOE 1980a) on the effect of waste age for salt, granite, basalt, and shale. The thermal criteria discussed in Section 3.1 were used to determine the maximum thermal loading for both SF and reprocessed HLW at 5, 10, and 50 years of age. The loading takes into account the temperature and thermomechanical limitations listed in Table 3.1. These limitations include the maximum allowable temperatures at waste centerline, canister surface, and borehole wall; the maximum room closure for salt; strength-to-stress ratios for hard rocks; and the maximum allowable surface uplifts.

The final thermal loadings used in the EIS study are shown in Table 4.9. The far-field average loading takes into account the unused passive areas for corridors, etc. A safety margin of two-thirds is included in the results. The limiting parameter is denoted by an asterisk. Usually the near-field criteria determine the thermal loadings; however, the far-field surface uplift is also a limiting factor in a number of cases, including not only the SF repositories in salt but also 50-year-old HLW in salt and 50-year-old SF in shale. These results indicate that for older wastes, the far-field criteria become more important in determining the repository loading.

Table 4.9. EIS Thermal Loadings for Waste Repositories (W/m^2).

Formation	Age of Waste at Emplacement (yr)	Spent Fuel		HLW	
		Near-Field Local Loading	Far-Field Average Loading	Near-Field Local Loading	Far-Field Average Loading
Salt	5	21	17*	32*	24
	10	12	10*	25*	19
	50	6	5*	17	13*
Granite	5	49*	40	35*	27
	10	32*	26	32*	25
	50	23*	19	30*	23
Basalt	5	49*	40	35*	27
	10	32*	26	32*	25
	50	23*	19	30*	23
Shale	5	30*	24	23*	17
	10	20*	16	20*	15
	50	13	10*	20*	15

(DOE 1980a)

* Denotes limiting parameters.

The repository waste capacities calculated for these loadings are plotted in Fig. 4.13 for SF and in Fig. 4.14 for reprocessed HLW for a 8.1 km^2 (2,000-acre) repository. The capacity of a salt repository for SF is substantially less than for reprocessed HLW and increases only about 10 percent from 5 to 50 years. Increases in capacity for the other media range from 30 percent for SF in shale to 100 percent for reprocessed wastes in granite.

The sensitive dependence of the repository capacity on fuel cycles and waste age was studied in detail at the International Nuclear Fuel Cycle Evaluation (INFCE) Conference. In the technical appendix of their proceedings, prepared by a joint effort of the Federal Republic of Germany, The Netherlands, and the United States (INFCE 1980), the waste densities and thermal loadings were calculated for seven fuel cycles and for 10-year-old and 40-year-old wastes in salt. Only the far-field criterion of maximum surface uplift of 1.5 m was used as the limiting parameter for all fuel cycles and waste ages. The near-field and very-near-field temperature profiles were calculated only to assure compliance with near-field and very-near-field temperature criteria.

The results of the INFCE study are shown in Table 4.10. A comparison of the 10- and 40-year-old waste data clearly illustrates the interesting features of allowed areal thermal loadings and emplacement densities that are impacted by surface cooling. Although the allowed thermal loading is reduced by aging the waste an additional 30 years prior to emplacement, the density of emplacement is increased. The increase in the amount of waste (number of canisters in Table 4.10) that can be emplaced per unit area varies from about 1.5 percent for

the SF of heavy water reactors (HWR) to about 103 percent for the HLW of HWR with both uranium (U) and thorium (Th) recycled. The corresponding enhancement percentages for the light water reactors (LWR), which are the main interest in the United States, are 7 percent for SF and 83 percent for HLW with U and Pu recycled.

4.5.2 Surface Cooling, Cumulative Heat, and Far-Field Thermal Effects

The controlling quantity in assessing the far-field thermal effects is the cumulative heat released by the emplaced wastes. Fig. 4.15 illustrates the dependence of total heat released by the buried waste in an 8.1-km^2 (2,000-acre) repository on the surface cooling period. The waste heat will remain in the rock formation for a long period of time. Although the curves in Fig. 4.15 are independent of rock type and characterize only the waste heat source, most of the results on far-field effects presented earlier in this section can be understood from these curves. SF releases more heat over a longer period of time than reprocessed HLW; extension of the surface cooling period removes only a small fraction of the cumulative heat released. On the other hand, the heat from reprocessed HLW is mainly released early. The cumulative heat of reprocessed HLW is much lower than that of SF; the heat removed by surface cooling is a significant fraction of the cumulative heat.

The ratios of cumulative heat released by 40- and 100-year-old wastes to that released by 10-year-old wastes are plotted in Fig. 4.16. This figure represents the relative dependence and sensitivity of surface cooling effects over the time range of interest. A lower ratio of cumulative heat energies indicates a greater advantage obtained from

Table 4.10. INFCE Canister and Repository Thermal Loadings and Waste Emplacement Density.

Fuel Cycle	10-Year-Old Waste			40-Year-Old Waste		
	Canister Thermal Loading (kW/canister)	Areal Thermal Loading (W/m^2)	Emplacement Density (canister/m^2)	Canister Thermal Loading (kW/canister)	Areal Thermal Loading (W/m^2)	Emplacement Density (canister/m^2)
#1 LWR Spent Fuel	0.56	15	0.027	0.30	9	0.029
#2 LWR U + Pu-Recycle	1.86	37	0.020	0.74	27	0.037
#3 FBR U + Pu-Recycle	1.26	16	0.013	0.64	10	0.016
#4 HWR Spent Fuel	.30	8	0.027	0.17	5	0.027
#5 HWR U + Pu-Recycle	2.29	25	0.011	0.95	14	0.015
#6 HWR U + Th-Recycle	1.56	35	0.022	0.77	35	0.045
#7 HTR U + Th-Recycle	1.09	32	0.029	0.53	29	0.055

(INFCE 1980)

longer surface cooling. It is clear from the figure that the effect of surface cooling is more significant for reprocessed wastes than for spent fuel in terms of long-term, far-field effect. The potential advantage of a 100-year cooling period for reprocessed waste is to lower the surface uplift and buoyancy flow to less than half the magnitude of a 10-year cooling period.

European countries, including Belgium, Sweden, the United Kingdom, and West Germany, have also considered longer cooling periods for reprocessed waste (Harmon and others 1980). The reasons range from near-field concerns over clay stability (Belgium), to backfill stability above 100°C (Sweden), to far-field buoyancy perturbation (United Kingdom). It is of interest to note that an unpublished United Kingdom report quoted by Bredehoeft and Maini (1981) states that "if waste is allowed to cool for 40 to 60 or 70 years, depending on the waste type, the heat would be reduced to the point where buoyancy-induced flow would not be significant."

4.5.3 The Importance of Surface Cooling Effects

In the evaluation of the thermal effects of waste repositories, waste age is an important parameter controlling waste heat. The heat released into the rocks by the waste is determined by the following three primary parameters: waste age, waste type, and waste loading density. From these parameters the thermal loading density at waste emplacement and the cumulative heat energy can be derived.

Although these derived quantities characterize the thermal effect for scales of operation ranging from the very-near-field to the far-field, and for times ranging from days to thousands of years, the primary waste parameters are more directly related to waste management and economic considerations. The waste loading density especially determines the size of the repository and the excavation costs. To determine the waste heat characteristics, waste age and type must also be specified. The review and evaluation in this study indicates that the effects of waste age (or surface cooling periods) should be carefully studied in repository design and evaluation.

5. SUMMARY

This study discusses the thermal effects that could result from the emplacement of radioactive waste in a geologic repository and the potential for mitigation of those effects by surface cooling of the waste prior to disposal. This summary lists the main points of the various key technical findings in five brief sections. Section 5.1 addresses the factors that control thermal effects. Section 5.2 covers the overall thermal, thermomechanical, and thermohydrologic impacts determined mainly on the basis of previous studies that assumed 10-year-old wastes. Since the waste loading density in a repository is determined by thermal criteria, thermal criteria and a generic thermohydrologically derived limit are discussed next in Section 5.3. Section 5.4 evaluates the mitigating effects of different surface cooling periods on thermal perturbations in the canister boreholes, at the repository level, and in the surrounding geologic setting. In a given waste disposal system, the surface cooling period would be determined by a combination of technical, economic, social, and environmental factors. This study examines mainly the technical factors and from that standpoint reviews the advantages and disadvantages of surface cooling in Section 5.5.

5.1 CONTROLLING FACTORS OF THERMAL EFFECTS

Thermally induced effects are determined by the waste characteristics, repository structure, and rock properties. Analyses in the literature show that:

- For the same waste loading density, spent fuel releases more heat at longer times than reprocessed wastes, which have most of the long-lived plutonium and uranium isotopes removed. Thus the spent fuel will induce much larger long-term thermal impacts than reprocessed high-level radioactive waste.
- Waste inventory studies indicate that a significant fraction of the wastes received by repositories will be more than 10 years old, especially if completion of fully operational repositories are delayed until close to the turn of the century.
- Many years of research on salt as a repository medium and several recent investigations on hard rocks are enabling investigators to develop detailed designs of the configurations of the emplacement holes and the room-and-pillar structures. Relatively simple repository geometries, however, have been used in most far-field models. Eventually, the exact depth, size, and shape of the repositories will be determined by the site-specific stratigraphic and regional constraints of the geologic setting as well as the environmental impacts of waste emplacement.
- Thermal properties of the rock formations can be measured fairly accurately in the laboratory and in the field. Mechanical properties measured in intact rock samples are not representative of those of fractured rock masses.

Hydrologic properties, especially permeability, have a wide range of uncertainty.

5.2 THERMAL EFFECTS DETERMINED MAINLY ON THE BASIS OF STUDIES OF 10-YEAR-OLD WASTES

The very-near-field, near-field, and far-field thermal effects have been extensively studied for 10-year-old wastes. The main findings are that:

- Waste package integrity and maximum waste and canister temperatures depend sensitively on the heat power of the emplaced waste and thermal conductivities of the various components, including backfill or air gaps surrounding the canister. Borehole degradation should be controlled to maintain retrievability for a prescribed period of time.
- Thermomechanical stability of the room-and-pillar structure is determined by the stress changes due to both excavation and thermal loading. Controlling thermal loading and ventilation, and utilizing mining engineering techniques, such as roof bolting, will help to ensure mechanical stability and maintain the safety of personnel during the waste emplacement and retrieval operations.
- The long-term, far-field temperature rise depends mainly on the heat capacity of the rock. Heat capacity is the least site-specific and rock-specific property. This allows us to evaluate and predict long-term thermal effects with cautious optimism.

- Surface uplift from thermal expansion of rock is largest for a spent fuel repository in salt. The surface uplift depends on the cumulative heat energy in the rock formation, which persists over thousands of years.
- Buoyancy flow will also persist for more than 1000 years. Distortion of the convection cells by a regional pressure gradient does not significantly change the travel time for water to move from the repository up to the surface.

5.3 RESEARCH NEEDS FOR THERMAL, THERMOMECHANICAL, AND THERMOHYDROLOGIC CRITERIA

Waste loading criteria used by the DOE in repository design have not included the following considerations.

- Thermohydrologic perturbation is not addressed in the existing far-field criteria. Although safety analysis requires including a description of the anticipated response of the bulk hydrogeologic system to the maximum design thermal loading, the repository loading density itself is not explicitly bounded by the considerations of vertical flow from the repository to the surface. Preliminary analyses based on buoyancy gradient considerations indicate that thermohydrological considerations could be very restrictive in limiting waste loading density. Further investigations are required to elucidate the dependence of design waste loading on thermohydrologic impacts and the predictability of long-term thermohydrologic responses.

- The very-near-field criteria are based on limits on the maximum temperature rises occurring at short times. The relationships between these early-time maxima and the long-term waste package integrity and radionuclide release rates should be carefully evaluated. For salt, brine inflow to the borehole has been observed to be low during the heating period and high after the heat power has been turned off. The potential long-term delay in brine migration due to entrapment in microcracks should be considered.
- Thermoelastic analyses do not predict the behavior of non-elastic fractured rock masses. The rock failure conditions should be evaluated with fracture models that consider the couplings of fracture deformation to thermal expansion of rock blocks and to fluid flow through the fractures.
- Thermomechanical instability induced by tension outside the heated zone should be considered in addition to compressive failure. This should be done for both the near-field room-and-pillar structure and the far-field rock formations. Thermally induced tensile stress may open the fractures and change the permeability.

5.4 EMPLACEMENT WASTE DENSITY AND THERMAL LOADING OF AGED WASTES

The effect of different surface cooling periods on thermal impact can be summarized as follows:

- For constant mass of emplaced material per unit area, surface cooling significantly reduces the thermal impact for reprocessed waste, but only modestly for spent fuel. The main effect of surface cooling is to allow a significant portion of the fission products to decay. For spent fuel containing long-lived actinides, the thermal impacts over thousands of years are not significantly changed by extending the period of surface cooling from 10 to 100 years.
- For constant power density at emplacement, longer surface cooling increases the thermal impact significantly for spent fuel, but only modestly for reprocessed waste. Since most of the design studies and economic analyses are expressed in terms of thermal power densities, conclusions based on 10-year-old waste should not be applied to older wastes unless careful re-evaluations are made.
- If a higher waste density is considered in the design of a repository for older wastes, limitations of loading should be carefully determined by imposing both near-field criteria based on thermomechanical stability considerations and far-field criteria based on thermohydrologic perturbation considerations.

5.5 ADVANTAGES AND DISADVANTAGES OF SURFACE COOLING FROM THE STANDPOINT OF THERMAL IMPACT

Repository design and environmental evaluation should carefully consider the effects of different surface cooling periods.

- Surface cooling allows more concentrated waste emplacement and lower thermal loading. The quantitative changes depend sensitively on the waste type and on the thermal criteria used in determining optimal loading.
- For the region in the vicinity of the waste package and the repository room-and-pillar, the lower thermal loadings associated with older wastes could reduce the short-term temperature rise and the thermomechanical instability.
- Reductions in the near-field thermomechanical perturbations are significant for older wastes in salt and especially in hard rocks. If the near-field criteria determine the waste loadings, the creep analyses for salt and the thermoelastic analyses for hard rocks should be carefully evaluated to determine the optimal waste-loading densities for older wastes.
- If far-field criteria are used, the extension of surface cooling periods will allow only a modest increase in waste density for spent fuel. The balance between a modest reduction in repository spatial requirements and the additional expense of the maintenance of surface storage facilities will be the determining factor in optimizing the duration of surface cooling.

- For reprocessed waste, long surface cooling can effectively lower the far-field thermal effects. From a technical standpoint, it may be advantageous to store reprocessed wastes above ground for up to 100 years to allow a significant fraction of the fission products to decay.

ACKNOWLEDGMENTS

The authors express their gratitude to Lois Armetta, June DeLaVergne, Barbara Jones, Ruthie Redic, Karla Savage, Robin Spencer, Ashok Verma, and Jean Wolslegel for their generous practical help in many details of the production of this report.

The material in this article is taken from the report NUREG/CR-2910 prepared for the U. S. Nuclear Regulatory Commission (Wang and others 1982). This work was supported by the High Level Waste Technical Development Branch, Division of Waste Management, Office of Nuclear Material Safety and Safeguards, U. S. Nuclear Regulatory Commission, Washington, D.C. 20555, through N.R.C. FIN No. B 3109-0 under Interagency Agreement DOE-50-80-97, through U. S. Department of Energy under Contract No. DE-AC03-76SF00098.
This report was prepared as an account of work sponsored by an agency of the United States Government. Neither the United States Government nor any agency thereof, or any of their employees, makes any warranty, expressed or implied, or assumes any legal liability of responsibility for any third party's use, or the results of such use, of any information, apparatus, product or process disclosed in this report, or represents that its use by such third party would not infringe privately owned rights.

APPENDIX: ANALYTIC FORMULAS

A number of analytic solutions for thermally induced effects are presented in this appendix. These formulas illustrate the functional dependence of temperature rise, thermomechanical deformation, and thermohydrologic perturbation on the thermal loading, rock properties, and repository dimensions.

Simple approximations are made in these solutions so that the controlling parameters in the very-near-field, the near-field, and the far-field can be easily identified.

A.1 VERY-NEAR-FIELD FORMULAS

The maximum temperature rise in the rock on the borehole wall surrounding a radioactive waste canister is approximately given by (Hodgkinson and Bourke 1978):

$$\Delta T_{rock}^{max} = \frac{q_c(0)}{\pi L K_{rock}} \left[A(L, r_w) - \frac{3L}{8} \left(\frac{8\lambda A(L, r_w)}{\pi L \kappa_{rock}} \right)^{1/3} \right] ,$$

with

$$A(L, r_w) = \frac{1}{2} \ln \left[\frac{L}{2r_w} + \left(1 + \left(\frac{L}{2r_w} \right)^2 \right)^{1/2} \right] , \qquad \text{(A-1)}$$

$q_c(0)$ = canister emplacement power, W/canister,

L = canister length, m,

r_w = borehole radius, m,

K_{rock} = thermal conductivity of the rock, W/m°C,

κ_{rock} = thermal diffusivity of the rock, m^2/s,

λ = radioactive decay constant, $\ln(2)/t_{1/2}$, 1/s.

The temperature rise across the cylindrical gap between the canister and the borehole wall may be computed with the steady-state solution

$$\Delta T_{gap} = \frac{q_c(0)}{2\pi L K_{gap}} \ell n \left(\frac{r_w}{r_c}\right), \qquad \text{(A-2)}$$

where

K_{gap} = effective thermal conductivity of the gap, W/m°C,

r_c = canister radius, m.

The temperature rise in the waste may be computed using the steady-state solution in an infinitely long cylinder of waste

$$\Delta T_{waste} = \frac{q_c(0)}{4\pi L K_{waste}}, \qquad \text{(A-3)}$$

where K_{waste} = thermal conductivity of the waste, W/m°C.

These steady-state solutions were used in the GEIS study (Science Applications Inc 1978) to validate numerical models.

Equations (A-1) and (A-3) illustrate that the very-near-field temperature rises are proportional to the waste emplacement power and inversely proportional to the thermal conductivities of the various waste components and of the surrounding rock.

A.2 NEAR-FIELD FORMULAS

The temperature rise at the pillar centerline between canister rows can be approximated conservatively by a model with wastes uniformly distributed along the rows at the repository level. The repository temperature in this model (Carslaw and Jaeger 1959) is given by

$$\Delta T_{repository} = \frac{1}{2\rho c_{rock}} \int_0^t \frac{Q_R(t')}{[\pi \kappa_{rock}(t - t')]^{1/2}} \quad , \qquad (A\text{-}4)$$

where

$Q_R(t')$ = heat power per unit area at time t', W/m^2,

ρc_{rock} = volumetric heat capacity of the rock, or product of the rock density and specific heat, $W/m^3°C$.

The repository temperature for a radioactive decay areal heat source (Beyerlein and Claiborne 1980; Hodgkinson and Bourke 1978) is

$$\Delta T_{repository} = \frac{Q_R(0)}{2K_{rock}} \left(\frac{\kappa_{rock}}{\lambda}\right)^{1/2} \mathrm{ImW}[(\lambda t)^{1/2}], \qquad (A\text{-}5)$$

where

$Q_R(0)$ = thermal loading density, W/m^2,

ImW = imaginary part of the error function of complex argument.

The maximum temperature rise is

$$\Delta T^{max}_{repository} = 0.305 \frac{Q_R(0)}{K_{rock}} \left(\frac{\kappa_{rock}}{\lambda}\right)^{1/2} = 0.305 \frac{Q_R(0)}{(K_{rock}\rho c_{rock}\lambda)^{1/2}} \qquad (A\text{-}6)$$

Equation (A-6) shows that the near-field maximum temperature rise is proportional to the areal thermal loading and inversely proportional to the square root of the product of thermal conductivity, heat capacity, and effective radioactive decay constant.

The temperature rise induces stress and strain changes in the rock medium surrounding the repository. If the rock medium is elastic, the thermally induced stress-strain changes are proportional to ΔT.

Thermoelastic analyses were used in the GEIS study (Dames and Moore 1978a) and in the results given in Section 2.5.2 for hard rocks (granite, basalt, shale). Lomenick's formula, deduced from creep studies in Project Salt Vault (Bradshaw and McClain 1971), was frequently used in repository designs for salt as a plastic rock medium. In SI units the formula is

$$E = CT^{9.5}\sigma^{3.0}t^{0.3}$$

where

E = cumulative strain, m/m,

$T = T_{ambient} + \Delta T$, absolute temperature, K,

σ = average pillar stress, Pa,

t = time, s,

C = 3.4 E-50.

The cumulative strain is therefore a nonlinear function of ΔT.

A.3 FAR-FIELD FORMULAS

The temperature rise around a disk-like repository at any point (r, z) (Carslaw and Jaeger 1959; Wang and others 1981) is given by

$$\Delta T(r,z,t) = \frac{1}{\rho c_{rock}} \int_0^t Q_R(t')\left[V_{-D}(r,z,t-t') - V_{+D}(r,z,t-t')\right] dt', \quad (A-7)$$

with

$$V_{\mp D}(r,z,t) = \frac{1}{4\left(\pi\kappa_{rock}^3 t^3\right)^{1/2}} \int_0^R \exp\left[-\frac{r^2+r'^2+(z\pm D)^2}{4\kappa_{rock}t}\right] I_0\left(\frac{rr'}{2\kappa_{rock}t}\right) r'dr',$$

where

$V_{\mp D}$ = instantaneous disk heat source of radius R in the plane $z = \mp D$, 1/m,

r = radial distance from the axis of the repository, m,

I_0 = zeroth-order modified Bessel function of the first kind,

z = vertical coordinate, negative below the ground surface, m,

t = time, s.

The areal heat power function $Q_R(t')$ could be expressed as a series of exponential decay terms. For each decay term, the temperature rise along the z-axis of the repository is

$$\begin{aligned}\Delta T(0,z,t) = {} & f\{[(z + D)^2/4\kappa_{rock}\, t]^{1/2},\, t\} \\ & - f\{[(R^2 + (z + D)^2)/4\kappa_{rock} t]^{1/2},\, t\} \\ & + f\{[(z - D)^2/4\kappa_{rock}\, t]^{1/2},\, t\} \\ & - f\{[(R^2 + (z - D)^2)/4\kappa_{rock}\, t]^{1/2},\, t\}\ , \end{aligned} \tag{A-8}$$

with

$$f(x,\, t) = \frac{Q_R(0)}{2K_{rock}} \left(\frac{\kappa_{rock}}{\lambda}\right)^{1/2} \mathrm{Im}W[(\lambda t)^{1/2} + ix]\ .$$

The surface uplift due to the thermal expansion of rock between the repository and the surface is given by

$$\Delta Z = \int_{-D}^{0} \left(\frac{1 + \mu}{1 - \mu}\right) \alpha_{rock}\, \Delta T\, dz, \tag{A-9}$$

where α_{rock} = thermal expansivity of the rock, 1/°C, and μ = Poisson's ratio of the rock.

The buoyancy gradient due to the thermal expansion of water for flow from the repository to the surface is approximately given by

$$i_B = \int_{-D}^{0} \alpha_{water} \Delta T \frac{dz}{D} , \qquad \text{(A-10)}$$

where α_{water} = thermal expansivity of water, 1/°C.

Both the surface uplift and the buoyancy gradient are therefore determined by the integrated temperature rise in the rock formation, which is related to the cumulative heat remaining in the rock.

REFERENCES CITED

Abelin, H., J. Grindlund, and I. Neretnieks, 1983, Migration experiments in a single fracture in the Stripa granite: preliminary results, in Proceedings, Workshop on Geological Disposal of Radioactive Waste in Situ Experiments in Granite, Stockholm, Sweden, 154-163, Organization for Economic Cooperation and Development, Paris.

Altenbach, T. J., 1978, Interim report on nuclear waste depository thermal analysis: Lawrence Livermore National Laboratory, Livermore, California, UCID-17865, 28 p.

Altenbach, T. J., 1979, Three-dimensional thermal analysis of a high-level repository: Lawrence Livermore National Laboratory, Livermore, California, UCID-17984, 32 p.

Altenbach, T. J., and Lowry, W. E., 1980, Advanced 3-D modeling of a baseline spent fuel repository: Lawrence Livermore National Laboratory, Livermore, California, UCID-18660, 55 p.

Arbital, J., Bettis, E., Myrick, T., Watts, H., Wilems, R., Yook, H., 1979, Considerations for development of specifications for subsurface waste handling equipment: Office of Nuclear Waste Isolation, Battelle, Columbus, Ohio, ONWI-75.

Atlantic Richfield Hanford Co. and Kaiser Engineers, 1977, Retrievable surface storage facility conceptual system design description: Atlantic Richfield Hanford Company, Richland, Washington, ARH-LD-140 Rev.

Bechtel Group, Inc., 1981, NWTS conceptual reference repository description (CRRD): Office of Nuclear Waste Isolation, Battelle, Columbus, Ohio, ONWI-258, v. 3.

Beyerlein, S. W., and Claiborne, H. C., 1980, Possibility of multiple temperature maxima in geologic repositories for spent fuel from nuclear reactors: Oak Ridge National Laboratory, Oak Ridge, Tennessee, ORNL/TM-7024.

Blackburn, L. D., Farwick, D. G., Fields, S. R., Jones, L. A., and Moen, R. A., 1978, Maximum allowable temperature for storage of spent nuclear reactor fuel--An interim report: Hanford Engineering Development Laboratory, Richland, Washington, HEDL-TME 78-37, 45 p.

Bourke, P. J., and Robinson, P. C., 1981, Comparison of thermally induced and naturally occurring waterborne leakages from hard rock depositories for radioactive waste: Radioactive Waste Management, v. 1, no. 4, p. 365-380.

Boyd, R. D., 1978, Forced air cooling of a WIPP mine drift: Sandia National Laboratories, Albuquerque, New Mexico, SAND-78-1122, 39 p.

Brace, W. F., 1980, Permeability of crystalline and argillaceous rocks: Int. J. of Rock Mechanics and Mineral Science, v. 17, no. 5, p. 241-251.

Bradshaw, R. L., and McClain, W. C., 1971, Project Salt Vault: A demonstration of the disposal of high-activity solidified waste in underground salt mines: Oak Ridge National Laboratory, Oak Ridge, Tennessee, ORNL-4555, 356 p.

Bredehoeft, J. D., and Maini, T., 1981, Strategy for radioactive waste disposal in crystalline rocks: Science, v. 213, no. 4505, p. 293-296.

Bulmer, B. M., and Lappin, A. R., 1980, Preliminary one-dimensional thermal analysis of waste emplacement in tuffs: Sandia National Laboratories, Albuquerque, New Mexico, SAND-79-1265, 26 p.

Burgess, A. S., Charlwood, R. G., Skiba, E. L., Ratigan, J. L., Gnirk, P. E., Stille, H., and Lindblom, U. E., 1979, Analyses of groundwater flow around a high-level waste repository in crystalline rock: presented at OECD Nuclear Energy Agency Workshop on Low-Flow, Low-Permeability Measurements in Largely Impermeable Rocks, Paris, France, 10 p.

Callahan, G. D., and Gnirk, P. F., 1978, Technical memorandum report RSI-0064, Analytical approximations to the thermoelastic behavior of repository configurations: Office of Waste Isolation, Oak Ridge, Tennessee, Y/OWI/SUB-78/22303/10, 35 p.

Callahan, G. D., and Ratigan, J. L., 1977, Thermoelastic analysis of spent fuel repositories in bedded and dome salt: Office of Waste Isolation, Oak Ridge, Tennessee, Y/OWI/SUB-7722303/4.

Callahan, G. D., Ratigan, J. L., Russell, J. E., and Fossum, A. F., 1975, Heat transfer analysis of the waste-container sleeve/salt configuration: Oak Ridge National Laboratory, Oak Ridge, Tennessee, ORNL/SUB/4269-7, 68 p.

Carnahan, C. L., 1983, Thermodynamic coupling of heat and matter flows in near-field regions of nuclear waste repositories, Proceedings, Scientific Basis for Nuclear Waste Management VII, North-Holland, p. 1023-1030.

Carslaw, H. S., and Jaeger, J. C., 1959, Conduction of Heat in Solids: 2nd ed., Oxford University Press, Oxford, United Kingdom.

Chan, T., Witherspoon, P. A., and Javandel, I., 1980, Heat transfer in underground heating experiments in granite, Stripa, Sweden: in Heat Transfer in Nuclear Waste Disposal, F. A. Kulacki and R. W. Lyczkowski, eds., Winter Annual Meeting of ASME, Chicago, Illinois, HTD v. 11, p. 1-8.

Cheverton, R. D., and Turner, W. D., 1972, Thermal analysis of the national radioactive waste repository: Progress through March 1972: Oak Ridge National Laboratory, Oak Ridge, Tennessee, ORNL 4789, 80 p.

Claiborne, H. C., Rickertsen, L. D., and Graham, R. F., 1980, Expected environments in high-level nuclear waste and spent fuel repositories in salt: Oak Ridge National Laboratory, Oak Ridge, Tennessee, ORNL/TM-7201, 188 p.

Code of Federal Regulations, Title 10 Part 60, 1983, Disposal of high-level radioactive wastes in geologic repositories: Federal Register 48(120), Rules and Regulations, 28194-28229.

Cook, N. G. W., 1985, Coupled processes in geomechanics, Proceedings, International Symposium on Coupled Processes Affecting the Performance of a Nuclear Waste Repository, Lawrence Berkeley Laboratory LBL-21850, p. 73-82.

Cox, R. L., 1977, Radioactive heat transfer in arrays of parallel cylinders: Ph.D. dissertation, University of Tennessee, Department of Chemical Engineering, Oak Ridge National Laboratory, Oak Ridge, Tennessee, ORNL-5239, 286 p.

Dames and Moore, 1978a, Technical support for GEIS: Radioactive waste isolation in geologic formations: Thermomechanical stress analysis and development of thermal loading guidelines: Dames and Moore, White Plains, New York, Y/OWI/TM-36/20.

Dames and Moore, 1978b, Technical support for GEIS: Radioactive waste isolation in geologic formations: Ground water movement and nuclide transport: Dames and Moore, White Plains, New York, Y/OWI/TM-36/21.

Dames and Moore, 1978c, Technical support for GEIS: Radioactive waste isolation in geologic formations: Baseline rock properties--granite: Dames and Moore, White Plains, New York, Y/OWI/TM-36/5.

Dames and Moore, 1978d, Technical support for GEIS: Radioactive waste isolation in geologic formations: Baseline rock properties--basalt: Dames and Moore, White Plains, New York, Y/OWI/TM-36/7.

Davis, B. W., 1979, Preliminary assessment of the thermal effects of an annular air space surrounding an emplaced nuclear waste canister: Lawrence Livermore National Laboratory, Livermore, California, UCRL-15014, 42 p.

de Marsily, G., 1985, An overview of coupled processes with emphasis on geohydrology, Proceedings, International Symposium on Coupled Processes Affecting the Performance of a Nuclear Waste Repository, Lawrence Berkeley Laboratory, LBL-21850, p. 68-72.

Department of Energy, 1979a, Spent fuel storage requirements--The need for away-from-reactor storage: U. S. Department of Energy, Washington, D. C., DOE/ET-0075.

Department of Energy, 1979b, Technology for commercial radioactive waste management: U. S. Department of Energy, Washington, D. C., DOE/ET-0028.

Department of Energy, 1980a, Management of commercially generated radioactive waste: U. S. Department of Energy, Washington, D. C., DOE/EIS-0046F, 320 p.

Department of Energy, 1980b, Spent fuel storage requirements--The need for away-from-reactor storage: An update of DOE/ET-0075: U. S. Department of Energy, Washington, D. C., DOE/NE-0002.

Department of Energy, 1980c, In the matter of proposed rulemaking on the storage and disposal of nuclear waste: Statement of position of the United States Department of Energy: U. S. Department of Energy, Washington, D. C., DOE/NE-0007, 720 p.

Department of Energy, 1985, Mission plan for the civilian radioactive waste management program, Office of Civilian Radioactive Waste Management, Washington, D.C. DOE/RW-0005.

Department of Energy, 1986a, Environmental Assessment Deaf Smith County Site, Texas, Office of Civilian Radioactive Waste Management, Washington, D. C., DOE/RW-0069.

Department of Energy, 1986b, Environmental Assessment Reference Repository Location, Hanford Site, Washington, Office of Civilian Radioactive Waste Management, Washington, D.C., DOE/RW-0070.

Department of Energy, 1986c, Environmental Assessment Davis Canyon Site, Utah, Office of Civilian Radioactive Waste Management, Washington, D. C., DOE/RW-0071.

Department of Energy, 1986d, Environmental Assessment Richton Dome Site, Mississippi, Office of Civilian Radioactive Waste Management, Washington, D.C., DOE/RW-0072.

Department of Energy, 1986e, Environmental Assessment Yucca Mountain Site, Nevada Research and Development Area, Nevada, Office of Civilian Radioactive Waste Management, Washington, D. C., DOE/RW-0073.

Department of Energy, 1986f, Waste management systems requirements and descriptions (SRD), Office of Civilian Radioactive Waste Management, Washington, D. C., DOE/RW-0063.

Department of Energy, 1986g, Report of the task force on the MRS/repository interface, Office of Civilian Radioactive Waste Management, Washington, D. C., DOE/RW-0044.

Department of Energy, 1986h, Monitored retrievable storage, submission to Congress, Office of Civilian Radioactive Waste Management, Washington, D.C., DOE/RW-0035.

Dillon, R. S., Perona, J. J., and Blomeke, J. O., 1971, A model for the economic analysis of high-level radioactive waste management: Oak Ridge National Laboratory, Oak Ridge, Tennessee, ORNL-4633.

Dippold, D. G. and J. A. Wampler, 1984, Spent fuel burnup and age: implications for the design and cost of a waste disposal system, Office of Nuclear Waste Isolation, Battelle Memorial Institute, Columbus OH, ONWI-561.

DuPont, 1980, Preliminary technical data summary no. 3: E. I. DuPont de Nemours and Co., DPSTD-77-13-3.

Environmental Protection Agency, 1977, Technical support of standards for high-level radioactive waste management: U. S. Environmental Protection Agency, Washington, D. C., EPA 520/4-79-007.

Forster, J. D., 1979, The economics of mined geologic repositories: TRW Energy Systems, Planning Division, Office of Nuclear Waste Isolation, Battelle, Columbus, ONWI-93.

Fossum, A. F., 1983, Room stability in salt repositories, Battelle Memorial Institute, Columbus OH, ONWI-315.

Fyfe, W. F., Babuska, V., Price, N. J., Schmid, E., Tsang, C. F., Uyeda, S., and Velde, B., 1984, The geology of nuclear waste disposal: Nature, v. 310, p. 537-540.

Hahne, K., M. Schlich and E. Korthaus, 1985, Numerical calculations of the time and space dependent temperature distribution in a HLW repository of finite extension and temporal step-by-step disposal procedure, Proceedings, Scientific Basis for Nuclear Waste Management IX, Material Research Society, Vol. 50, pp. 809-816,

Hamstra, J., and Kevenaar, J. W. A. M., 1978, Temperature calculations on different configurations for disposal of high-level reprocessing waste in a salt dome model: Stichting Energie-onderzdek Centrum Nederland, Petten, Netherlands, ECN-42, 57 p.

Hardy, M. P., and Hocking, G., 1978, Numerical modeling of rock stresses within a basaltic nuclear waste repository: Phase II - Parametric design studies: Rockwell Hanford Operations, Richland, Washington, RHO-BWI-C-23, 303 p.

Harmon, K. M., Kelman, J. A., Stout, L. A., and Hsieh, K. A., 1980, Summary of non-U. S. national and international radioactive waste management programs, 1980: Battelle Pacific Northwest Laboratory, Richland, Washington, PNL-3333, 89 p.

Hodgkinson, D. P., 1980, A mathematical model for hydrothermal convection around a radioactive waste depository in hard rock: Ann. of Nuclear Energy, v. 7, p. 313-334.

Hodgkinson, D. P., and Bourke, P. J., 1978, The far-field heating effects of a radioactive waste depository in hard rock: presented at OECD-NEA and SKBF Seminar on In Situ Heating Experiments in Geological Formations, Stripa, Sweden, p. 237-248.

Hodgkinson, D. P., and Bourke, P. J., 1980, Initial assessment of the thermal stresses around a radioactive waste depository in hard rock: Ann. of Nuclear Energy, v. 7, p. 541-552.

Hohlfelder, J. J., and Hadley, G. R., 1979, Measurements of water lost from heated geologic salt: Sandia National Laboratories, Albuquerque, New Mexico, SAND79-0462.

Hood, M., Carlsson, H., and Nelson, P. H., 1979, I: Some results from a field investigation of thermomechanical loading of a rock mass when heaters are emplaced in the rock, II: The application of field data from heater experiments conducted at Stripa, Sweden, to parameters for repository design: Lawrence Berkeley Laboratory, Berkeley, California, LBL-9492, SAC-26, 39 p.

International Nuclear Fuel Cycle Evaluation Conference, 1980, Waste management and disposal report of INFCE Working Group 7: International Atomic Energy Agency, Vienna, 288 p.

Jaeger, J. C., and Cook, N. G. W., 1979, Fundamentals of Rock Mechanics: 2nd ed., John Wiley and Sons, Inc., New York, New York, 585 p.

Jansen, G., Jr., G. E. Raines, and T. P. Kircher, 1983, Performance analysis of conceptual waste package designs in salt repositories, Proceedings, Scientific Basis for Nuclear Waste Management VII, Elsevier Science Publishing Co., Vol. 26, pp. 445-454.

Jenks, G. H., 1977, Maximum acceptable temperatures of wastes and containers during retrievable geologic storage: Office of Waste Isolation, Oak Ridge, Tennessee, Y/OWI/TM-42, 7 p.

Jenks, G. H., 1979, Effects of temperature, temperature gradients, stress and irradiation of migration of brine inclusion in a salt repository: Oak Ridge National Laboratory, Oak Ridge, Tennessee, ORNL-5526, 62 p.

Jenks, G. H. and H. C. Claiborne, 1981, Brine migrations in salt and its implications in the geologic disposal of nuclear waste, Oak Ridge National Laboratory, Oak Ridge, TN, ORNL-5818.

Jockwer, N. and S. Gross, 1985, Natural, thermal and radiolytical gas migration in rock salt as a result of disposed high-level radioactive waste, Proceedings, Scientific Basis for Nuclear Waste Management IX, Material Research Society, Vol. 50, pp. 587-594.

Joy, D. S., Hudson, B. J., and Anthony, M. W., 1980, Logistics characterization for regional spent fuel repositories concept: mechanical report: Office of Nuclear Waste Isolation, Columbus, Ohio, ONWI-124, 105 p.

Just, R. A., 1978, Heat transfer studies in salt and granite: Oak Ridge National Laboratory, Oak Ridge, Tennessee, ORNL/ENG/TM-14, 90 p.

Kaiser Engineers, 1978a, A national waste terminal storage repository in a bedded salt formation for spent unreprocessed fuel, conceptual design descriptions: Kaiser Engineers, Oakland, California, KE Report no. 78-58-R.

Kaiser Engineers, 1978b, A national waste terminal storage repository in a bedded salt formation for spent unreprocessed fuel, basis of design decisions: Kaiser Engineers, Oakland, California, KE Report no. 78-79-R.

Kaiser Engineers, Inc., and Parsons, Brinckerhoff, Quade and Douglas, Inc., 1980, Nuclear waste repository in basalt, project B-301, functional design criteria: Rockwell Hanford Operations, Richland, Washington, RHO-BWI-CD-38 Rev. 3, 127 p.

Kee, C. W., Croff, A. G., and Blomeke, J. O., 1976, Updated projections of radioactive wastes to be generated by the U. S. nuclear power industry: Oak Ridge National Laboratory, Oak Ridge, Tennessee, ORNL/TM-5427.

Kevenaar, J. W. A. M., Janssen, L. S. J., Ploumen, P., Winske, P., 1979, Comparisons of temperature calculations for an arbitrary high-level waste disposal configuration in salt formations: Stichting Energieonderzdek Centrum Nederland, Petten, Netherlands, ECN-63, 33 p.

Kisner, R. A., Marshall, J. R., Turner D. W., Vath, J. E., 1978, Nuclear waste projections and source-term data for FY 1977: Office of Waste Isolation, Oak Ridge, Tennessee, Y/OWI/TM-34, 80 p.

Klingsberg, C., and Duguid, J., 1980, Status of technology for isolating high-level radioactive wastes in geologic repositories: U. S. Department of Energy, Washington, D. C., DOE/TIC-11207 (draft), 127 p.

Koplik, C. M., Pollak, G. D., Ross, B. I., 1979, Supplementary analysis of nuclear waste management options: Lawrence Livermore National Laboratory, Livermore, California, UCRL-15048.

Krause, W. B., Van Sambeek, L. L., and Stickney, R. G., 1980, In situ brine migration experiments at the Avery Island salt mine: in Heat Transfer in Nuclear Waste Disposal, F. A. Kulacki and R. W. Lyczkowski, eds., Winter Annual Meeting of ASME, Chicago, Illinois, HTD v. 11, p. 27-33.

Lagedrost, J. F. and W. Capps, 1983, Thermal properties and density measurements of samples taken from drilling cores from potential geologic media, Battelle Memorial Institute, Columbus, OH, ONWI-522.

Lappin, A. R., Thomas, R. K., and McVey, D. F., 1981, Eleana near-surface heater experiment: Final Report: Sandia National Laboratories, Albuquerque, New Mexico, SAND-80-2137.

Lawrence Berkeley Laboratory, 1984, Panel report on coupled thermo-mechanical-hydro-chemical processes associated with a nuclear waste repository, LBL-18250, 82 p.

Lincoln, R. C., Larson, D. W., and Sisson, C. E., 1978, Estimates of relative areas for the disposal in bedded salt of LWR wastes from alternative fuel cycles: Sandia National Laboratories, Albuquerque, New Mexico, SAND-77-1816, 240 p.

Lindblom, U. E., Stille, H., Gnirk, P. F., Ratigan, J. L., Charlwood, R. G., and Burgess, A. S., 1977, Groundwater movements around a repository: Final Report: Karnbranslesakerhet, Stockholm, Sweden, KBS-TR-54-06, 127 p.

Llewellyn, G. H., 1978, Prediction of temperature increases in a salt repository expected from the storage of spent fuel or high-level waste: Oak Ridge National Laboratory, Oak Ridge, Tennessee, ORNL/ENG/TM-7, 83 p.

Loken, M. C., 1983, Preliminary investigation of the structural influence of entry-entry intersections and inhomogeneous initial stress fields on repository disposal rooms, Office of Nuclear Waste Isolation, Battelle Memorial Institute, Columbus OH, ONWI-197.

Lowry, W. E., Davis, B. W., and Cheung, H., 1980, The effects of annular air gaps surrounding an emplaced nuclear waste canister in deep geologic storage: in Heat Transfer in Nuclear Waste Disposal, F. A. Kulacki and R. W. Lyczkowski, eds., Winter Annual Meeting of ASME, Chicago, Illinois, HTD v. 11, p. 69-74.

Mecham, W. J., Seefeldt, W. B., and Steindler, M. J., 1976, An analysis of factors influencing the reliability of retrievable storage canisters for containment of solid high level radioactive waste: Argonne National Laboratory, Argonne, Illinois, ANL-76-82.

Moss, M. and G. M. Haseman, 1983, A proposed model for the thermal conductivity of dry and water-saturated tuff, Proceedings, Scientific Basis for Nuclear Waste Management VII, Materials Research Society, Vol. 26, pp. 967-974.

Neretnieks, I., 1985, Transport in fractured rocks, Proceedings, Memoires of the 17th International Congress of IAH, Tucson, AZ, vol. XVII, 301-318.

Norton, D., and Knapp, R., 1977, Transport phenomena in hydrothermal systems: The nature of porosity: Amer. J. of Science, v. 277, p. 913-936.

Nuclear Regulatory Commission, 1986, Staff evaluation of U.S. Department of Energy proposal for monitored retrievable storage, Office of Nuclear Material Safety and Safeguards, Washington, D.C., NUREG-1168.

Office of Crystalline Repository Development, 1985, Guidelines on interim performance constraints for radioactive waste disposal in crystalline rock, Office of Crystalline Repository Development, Battelle Memorial Institute, Columbus, OH, OCRD-19.

Osnes, J. D., G. K. Coats, K. B. DeJong, M. C. Loken, and R. A. Wagner, 1984, Expected repository environments in granite: thermal environment, Office of Crystalline Repository Development Battelle Memorial Institute, Columbus, OH, OCRD-7.

Pratt, H. R., Schrauf, T. A., Bills, L. A., and Hustrulid, W. A., 1977, Thermal and mechanical properties of granite: Stripa, Sweden: Terra Tek, Inc., Salt Lake City, Utah, TR-77-92.

Pruess, K., J. S. Y. Wang and Y. W. Tsang, 1986, Effective continuum approximation for modeling fluid flow in fractured porous tuff, Sandia National Laboratories, Report SAND86-7000, Albuquerque, NM.

Ratigan, J. L., 1977, Groundwater movements around a repository: Rock mechanics analyses: Karnbranslesakerhet, Stockholm, Sweden, KBS-TR-54-04, 50 p.

Reference Repository Conditions Interface Working Group: Raines, G. E., Rickertsen, L. D., Claiborne, H. C., McElroy, J. L., and Lynch, R. W., 1980, Development of reference conditions for geologic repositories for nuclear waste in the U.S.A.: in Scientific Basis for Nuclear Waste Management, Materials Research Society, Boston, Massachusetts, v. 3, p. 1-10.

Reference Repository Conditions Interface Working Group, 1983, Results of repository conditions study for commerical and defense high-level nuclear waste and spent fuel repositories in salt, Office of Nuclear Waste Isolation, Battelle Memorial Institute, Columbus, OH, ONWI-483, 37 p.

Reference Repository Conditions Interface Working Group, 1984, Typical repository conditions for generic commerical and defense high-level nuclear waste and spent fuel repositories in crystalline rock, Office of Crysatlline Repository Development, Battelle Memorial Institute, Columbus, OH, OCRD-12.

Rickertsen, L. D., 1980, Brine migration in a bedded salt nuclear waste repository: in Heat Transfer in Nuclear Waste Disposal, F. A. Kulacki and R. W. Lyczkowski, eds., Winter Annual Meeting of ASME, Chicago, Illinois, HTD v. 11, p. 101-104.

Rickertsen, L. D., J. G. Arbital, and H. C. Claiborne, 1982, Expected near-field thermal environments in a sequentially loaded spent-fuel or high-level waste repository in salt, Oak Ridge National Laboratory, ORNL TM-8083, 58 p.

Rothfuchs, T., and Durr, K., 1980, In-situ investigation of brine migration, temperature distribution, and convergence in salt in a high-level waste simulation experiment at the Asse salt mine: in Heat Transfer in Nuclear Waste Disposal, F. A. Kulacki and R. W. Lyczkowski, eds., Winter Annual Meeting of ASME, Chicago, Illinois, HTD v. 11, p. 35-41.

Russell, J. E., 1979, Areal thermal loading recommendations for nuclear waste repositories in salt: Office of Waste Isolation, Oak Ridge, Tennessee, Y/OWI/TM-37, 43 p.

Sandia National Laboratories, 1986, Repository conceptual design in support of site characterization, Sandia National Laboratories, Albuquerque, NM, SAND 84-2641.

Schlich, M. and N. Jockwer, 1985, Simulation of water transport in heated rock salt, Proceedings, Scientific Basis for Nuclear Waste Management IX, Materials Research Society, Vol. 50, pp. 577-585.

Science Applications, Inc., 1976, The selection and evaluation of thermal criteria for a geologic waste isolation facility in salt: Office of Waste Isolation, Oak Ridge, Tennessee, Y/OWI/SUB-76/07220, 92 p.

Science Applications, Inc., 1978, Technical support for GEIS: Radioactive waste isolation in geologic formations: v. 19 - Thermal analysis: Office of Waste Isolation, Oak Ridge, Tennessee, Y/OWI/TM-36/19, 266 p.

Smyth, J. R., Crowe, B. M., Halleck, P. M., and Reed, A. W., 1979, A preliminary evaluation of the radioactive waste isolation potential of the alluvium-filled valleys of the Great Basin: Los Alamos Scientific Laboratory, Los Alamos, New Mexico, LA-7962-MS, 22 p.

Stearns-Roger Engineering Co., 1979, Conceptual design, NWTS repository for storing reprocessed wastes in a dome salt formation, conceptual design descriptions: v. 2. Stearns-Roger Engineering Co., Denver, Colorado.

Stearns-Roger Engineering Co. and Woodward-Clyde Consultants, 1978, National waste terminal storage repository no. 1, conceptual design study no. 6, thermal analysis: Office of Nuclear Waste Isolation, Oak Ridge, Tenn., ONWI-LIB-0138, EY-77-C-05-5367, 69 p.

Stearns-Roger Services, Inc., 1980, Technical conservatisms in NWTS repository conceptual designs: National waste terminal storage repository no. 1 - special study no. 4: Office of Nuclear Waste isolation, Columbus, Ohio, ONWI-222, 88 p.

Stinebaugh, R. E., J. C. Frostenson, and I. B. White, 1986, A recommendation for the horizontal emplacement of radioactive waste in tuff, basalt, and granite, Sandia National Laboratories, Albuquerque, NM, SAND 84-2197.

Storch, S. N., and Prince, B. E., 1979, Assumptions and ground rules used in nuclear waste projections and source term data: Office of Nuclear Waste Isolation, Columbus, Ohio, ONWI-24, 124 p.

Svalstad, D. K., 1983, Forced ventilation analysis of a commerical high-level nuclear waste repository in salt, Battelle Memorial Institute, Columbus, OH, ONWI-383.

Tammemagi, H. V., 1978, Preliminary assessment of temperature distributions associated with a radioactive waste vault: Atomic Energy of Canada, Ltd., Chalk River, Ontario, AECL-6308, 46 p.

Thomas, R. K., Lappin, A. R., and Gubbels, M. H., 1981, Three-dimensional thermal and mechanical scoping calculations for underground disposal of nuclear waste in shale: Sandia National Laboratories, Albuquerque, New Mexico, SAND-80-2507, 46 p.

Tillerson, J. R., and F. B. Nimick, 1984, Geoengineering properties of potential repository units at Yucca Mountain, Southern Nevada, Sandia National Laboratories, Albuquerque, NM, SAND 84-0221.

Tsang, C. F., 1980, A review of the state-of-the-art of thermomechanical-hydrochemical modeling of a hardrock waste repository, Proceedings, Workshop on Thermomechanical-Hydrochemical Modeling for a Hardrock Waste Repository, Lawrence Berkeley Laboratory, Berkeley, CA, LBL-11204, p. 16-21.

Tsang, Y. W. and C. F. Tsang, 1986, Channel model of flow through fractured media, to be published in Water Resources Research.

Tyler, L. D., 1979, Evaluation of tuff as a waste isolation medium: Proceedings, State of Waste Disposal Technology and the Social and Political Implications, R. E. Post, ed., Univ. of Arizona, p. 199-215.

Wahi, K. K., Maxwell, D. E., and Hofmann, R., 1977, Simulation of the thermomechanical response of Project Salt Vault: Final Report: Office of Waste Isolation, Oak Ridge, Tennessee, Y/OWI/Sub-77/16519/1, 84 p.

Wahi, K. K., Maxwell, D. E., and Hofmann, R., 1978, Two-dimensional simulation of the thermomechanical response of Project Salt Vault including the excavation sequence: Final Report: Office of Waste Isolation, Oak Ridge, Tennessee, Y/OWI/SUB-78/16549/2, 70 p.

Wagner, R. A., M. C. Loken, H. Y. Tammemagi, 1986, Preliminary thermo-mechanical analyses of a conceptual nuclear waste repository at four salt sites, Office of Nuclear Waste Isolation, Battelle Memorial Institute, Columbus, OH, ONWI-512.

Wang, J. S. Y., Mangold, D. C., and Tsang, C. F., 1983a, Long-term thermomechanical and thermohydrological factors controlling the optimal design of a nuclear waste repository: in Scientific Basis for Nuclear Waste Management VI, D. G. Brookins, ed., Materials Research Society Symposia Proceedings, v. 15, Elsevier Science Publishing Co. p. 531-538.

Wang, J. S. Y., Mangold, D. C., and Tsang, C. F., 1983b, Effects of surface cooling on thermal impacts: in Waste Management '83, R. G. Post, ed., Proceedings of the Symposium on Waste Management, v. II, Univ. of Arizona, p. 243-247.

Wang, J. S. Y., Mangold, D. C., Spencer, R. K., and Tsang, C. F., 1982, Thermal impact of waste emplacement and surface cooling associated with geologic disposal of nuclear waste: Nuclear Regulatory Commission, Washington, D. C., NUREG/CR-2910, LBL-13341, 277 p.

Wang, J. S. Y., and T. N. Narasimhan, 1985, Hydrologic mechanisms governing fluid flow in a partially saturated, fractured, porous medium, Water Resources Research, v. 21, no. 12, p. 1861-1874.

Wang, J. S. Y. and Tsang, C. F., 1980, Buoyancy flow in fractures intersecting a nuclear waste repository: in Heat Transfer in Nuclear Waste Disposal, F. A. Kulacki and R. W. Lyczkowski, eds., Winter Annual Meeting of ASME, Chicago, Illinois, HTD v. 11, p. 105-112, (LBL-11112).

Wang, J. S. Y., Tsang, C. F., Cook, N. G. W., and Witherspoon, P. A., 1980, Long-term thermohydrologic behavior of nuclear waste repositories: in Predictive Geology, G. de Marsily and D. F. Merriam, eds., Computers and Geology, v. 4, Pergamon Press, Oxford, United Kingdom, p. 101-115.

Wang, J. S. Y., Tsang, C. F., Cook, N. G. W., and Witherspoon, P. A., 1981, A study of regional temperature and thermohydrologic effects of an underground repository for nuclear wastes in hard rock: J. of Geophysical Res., v. 86, no. B5, p. 3759-3770.

Wilkins, B. J., Y. Liner and G. L. Rigby, Estimations of changes in microcrack-population, elastic modulus, and permeability, due to differential-thermal expansion in plutonic rock surrounding a nuclear fuel waste disposal vault, Proceedings, Scientific Basis for Nuclear Waste Management IX, Materials Research Society, Vol. 50, pp. 99-105.

Witherspoon, P. A., Cook, N. G. W., and Gale, J. E., 1981, Geologic storage of radioactive waste: Field studies in Sweden: Science, v. 211, p. 894-900.

FIGURE CAPTIONS

Figure 1.1 Schematic diagram of major factors affecting radionuclide transport from geologic repositories.

Figure 2.1 Decay heat power from 1 MTHM of a PWR for each of three nuclear fuel cycles.

Figure 2.2 Age of fuel entering repository for the SF cycle in EIS Case 3 (DOE 1980a).

Figure 2.3 Thermal conductivity as a function of temperature for four major rock types (DOE 1979b).

Figure 2.4 Volumetric heat capacity as a function of temperature for four major rock types (DOE 1979b).

Figure 2.5 Salt temperature histories for HLW loaded at 25 W/m^2 (100 kW/acre) (Claiborne and others 1980).

Figure 2.6 Salt temperature histories for SF loaded at 25 W/m^2 (100 kW/acre) (Claiborne and others 1980).

Figure 2.7 Flow into a single hole as a function of time for different waste types and areal thermal loadings (Rickertson 1980).

Figure 2.8 Near-field isothermal profiles (°C) for a 47-W/m^2 (190-kW/acre) HLW repository in granite (Science Applicatons Inc 1978).

Figure 2.9 Near-field temperature histories for a 47-W/m^2 (190-kW/acre) SF and HLW repository in granite (Science Applicatons Inc 1978).

Figure 2.10 Predicted and measured vertical displacements between anchor points 3 m above and 3 m below heater midplane (Hood and others 1979).

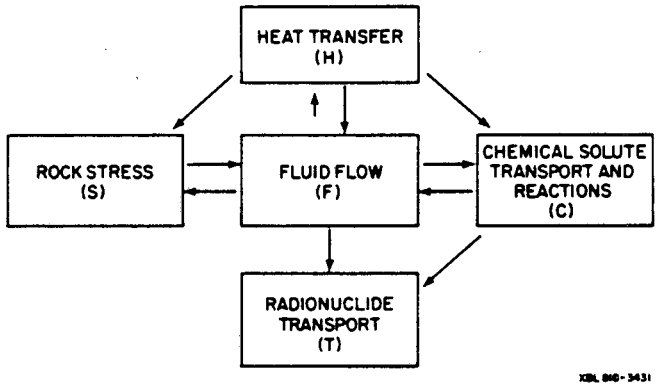

Figure 1.1 Schematic diagram of major factors affecting radionuclide transport from geologic repositories.

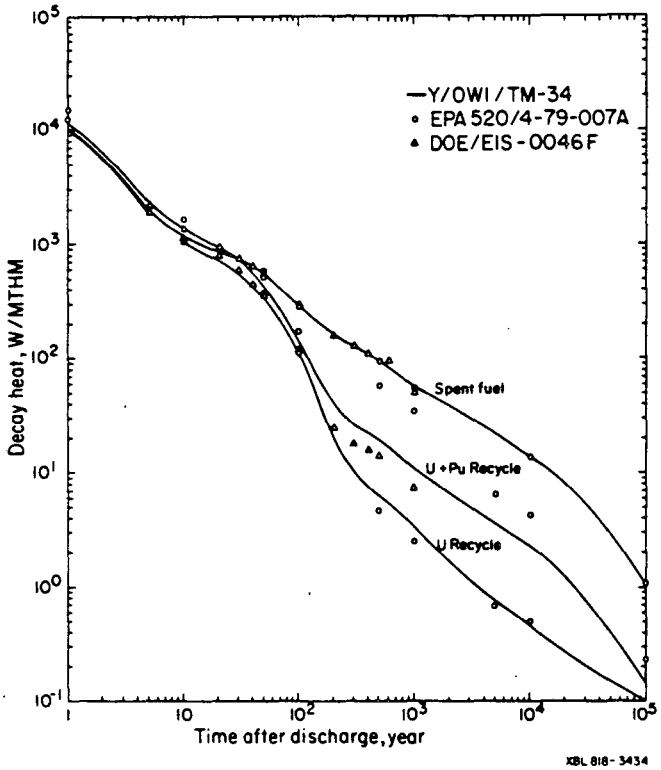

Figure 2.1 Decay heat power from 1 MTHM of a PWR for each of three nuclear fuel cycles.

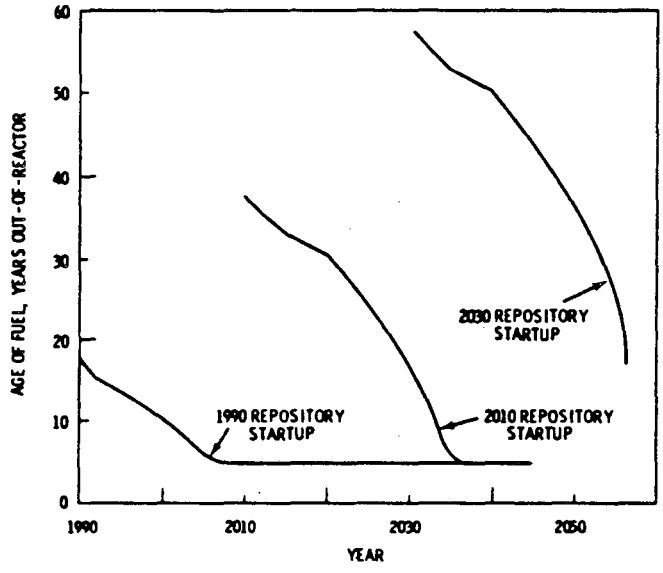

Figure 2.2 Age of fuel entering repository for the SF cycle in EIS Case 3 (DOE 1980a).

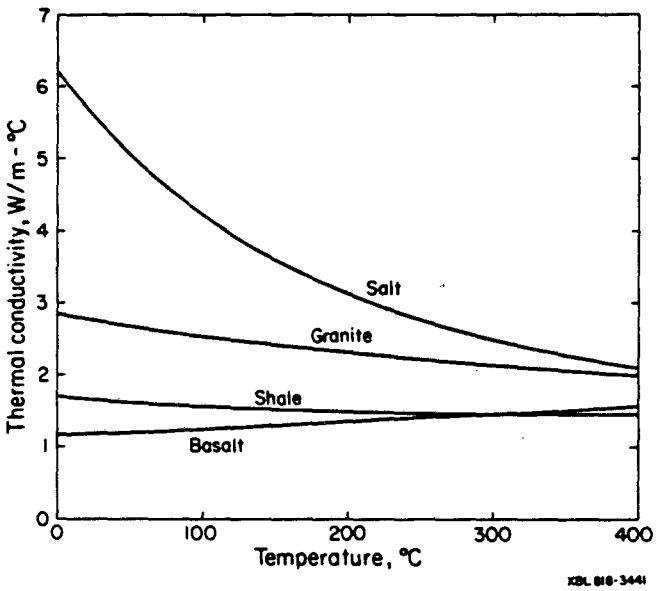

Figure 2.3 Thermal conductivity as a function of temperature for four major rock types (DOE 1979b).

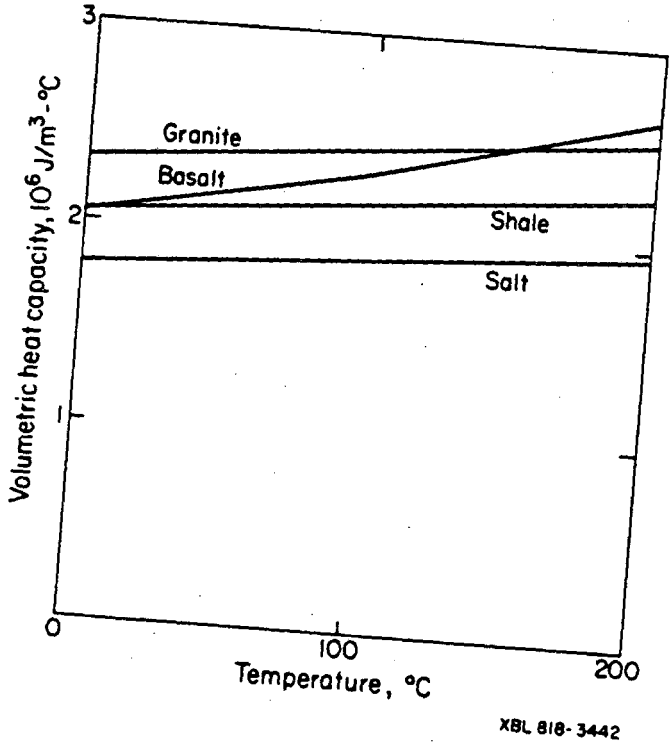

Figure 2.4 Volumetric heat capacity as a function of temperature for four major rock types (DOE 1979b).

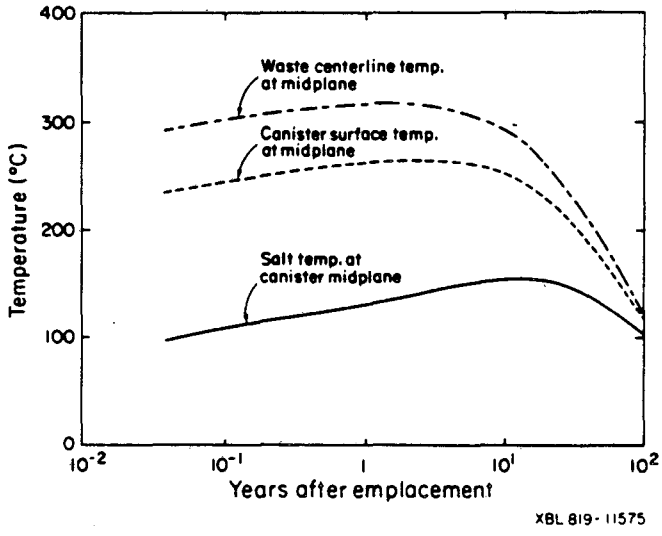

Figure 2.5 Salt temperature histories for HLW loaded at 25 W/m^2 (100 kW/acre) (Claiborne and others 1980).

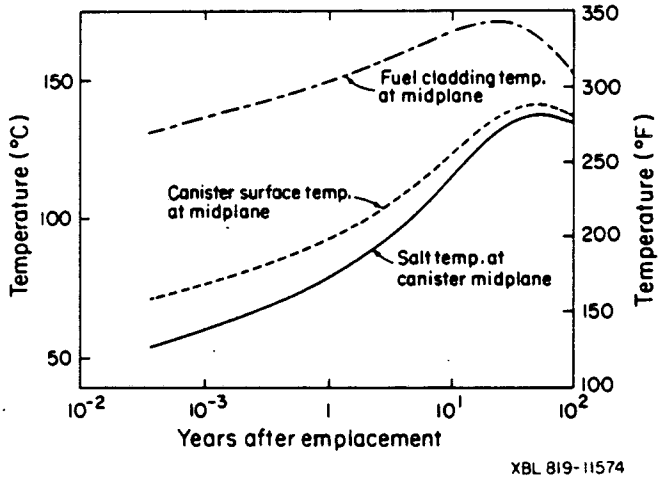

Figure 2.6 Salt temperature histories for SF loaded at 25 W/m^2 (100 kW/acre) (Claiborne and others 1980).

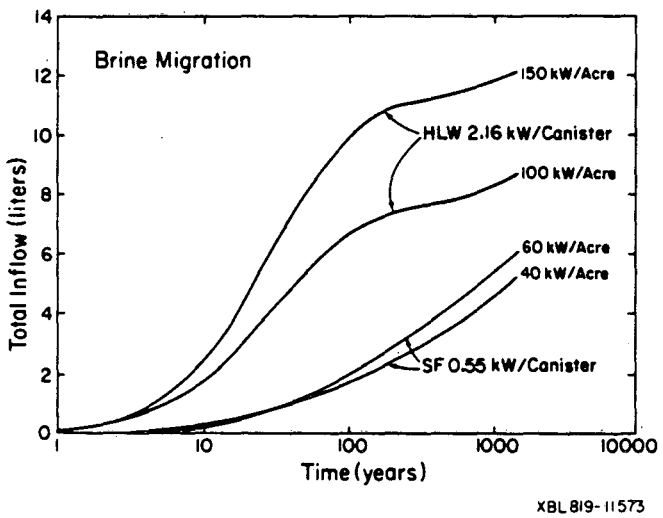

Figure 2.7 Flow into a single hole as a function of time for different waste types and areal thermal loadings (Rickertson 1980).

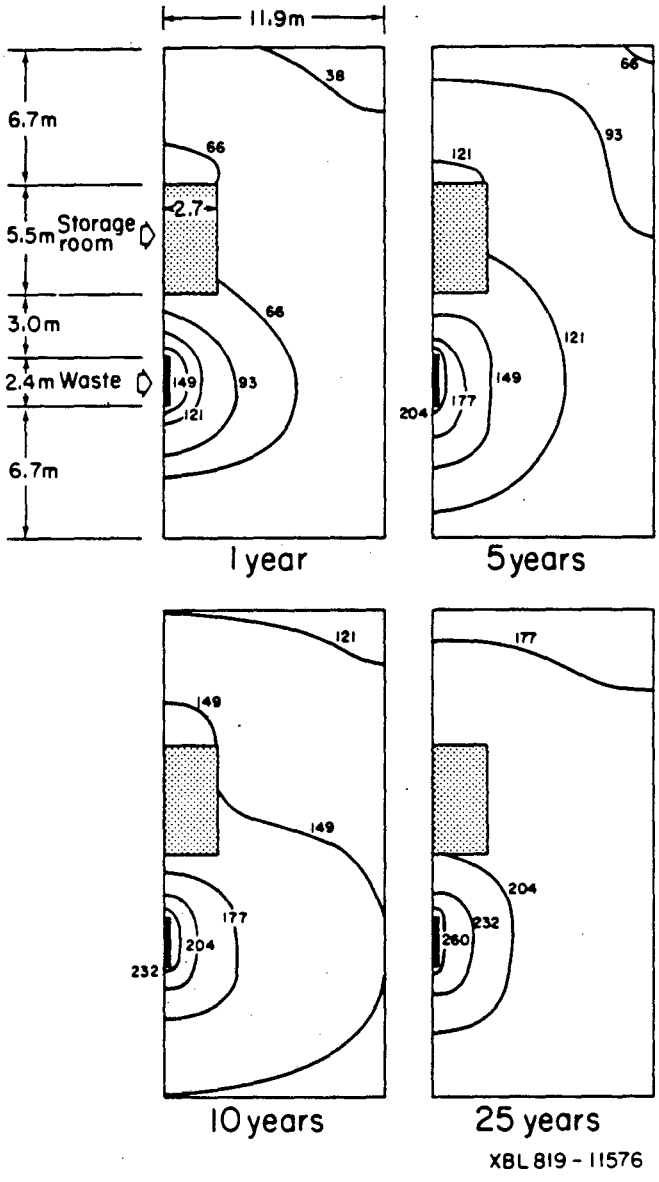

Figure 2.8 Near-field isothermal profiles (°C) for a 47-W/m^2 (190-kW/acre) HLW repository in granite (Science Applicatons Inc 1978).

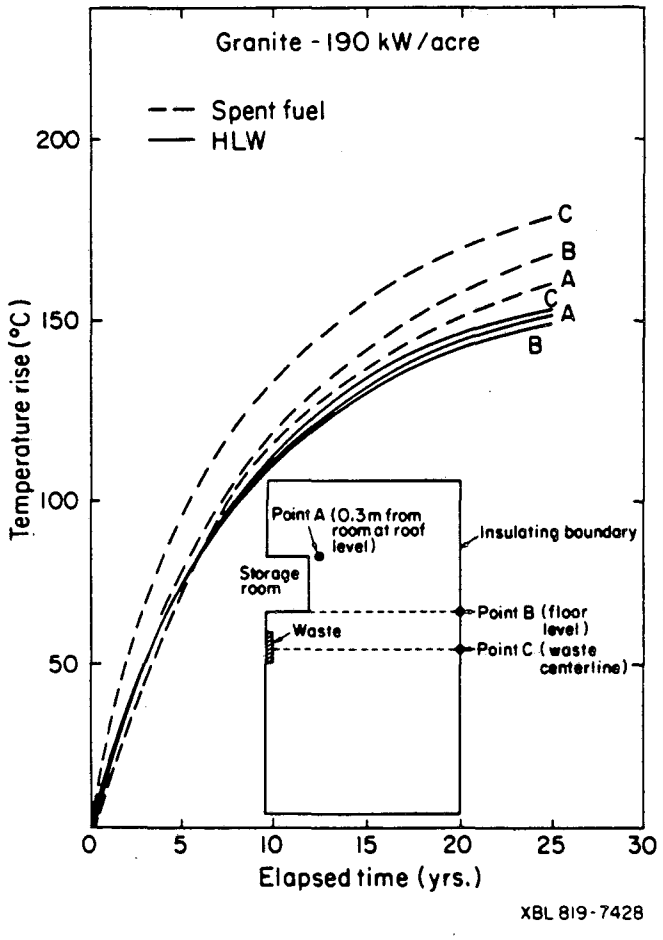

Figure 2.9 Near-field temperature histories for a 47-W/m^2 (190-kW/acre) SF and HLW repository in granite (Science Applicatons Inc 1978).

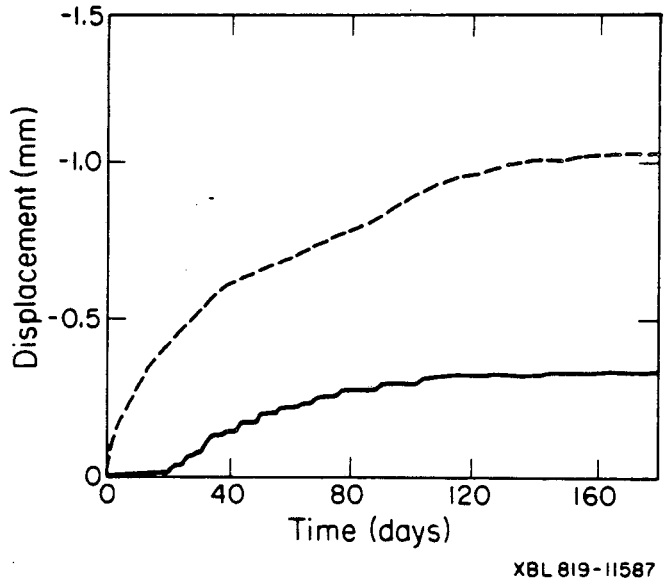

Figure 2.10 Predicted and measured vertical displacements between anchor points 3 m above and 3 m below heater midplane (Hood and others 1979).

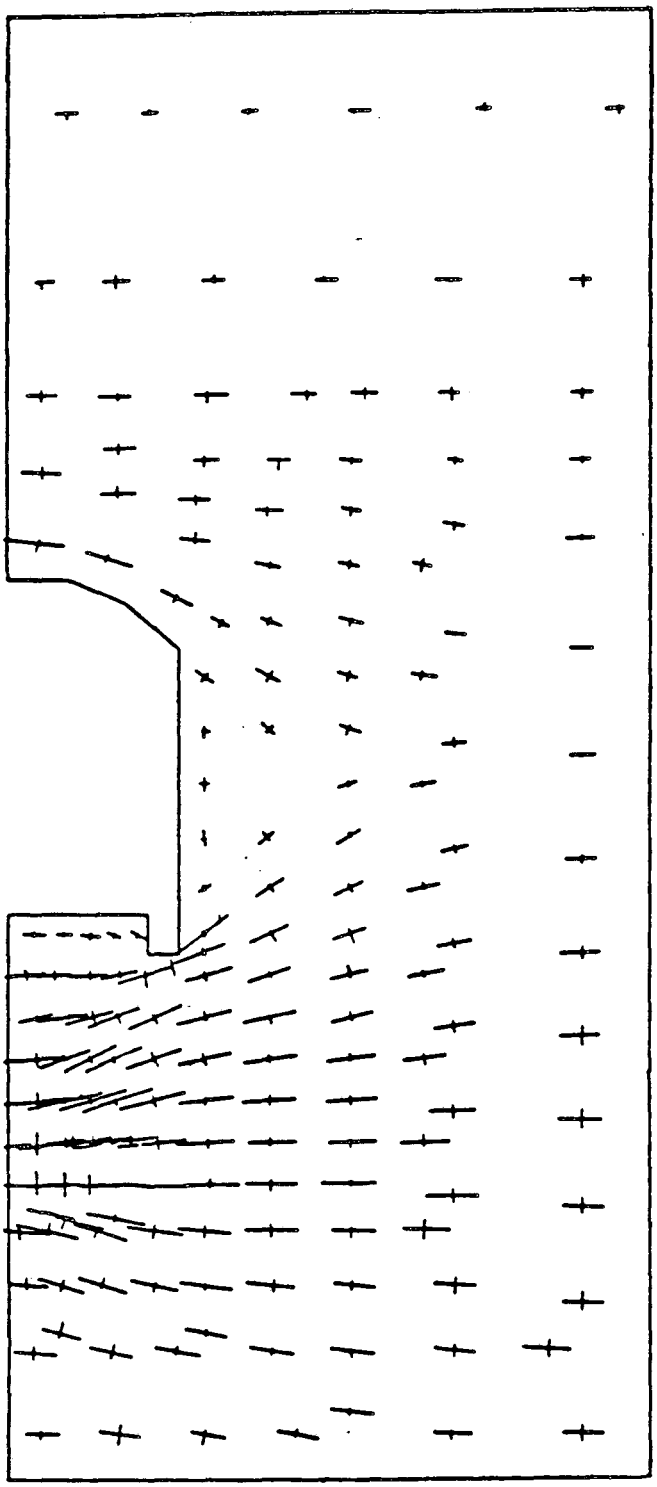

Figure 2.11 Stresses at 5 years after emplacement in granite at a depth of 580 m (1900 ft) for an HLW repository loaded at 47 W/m^2 (190 kW/acre) (Dames and Moore 1978a).

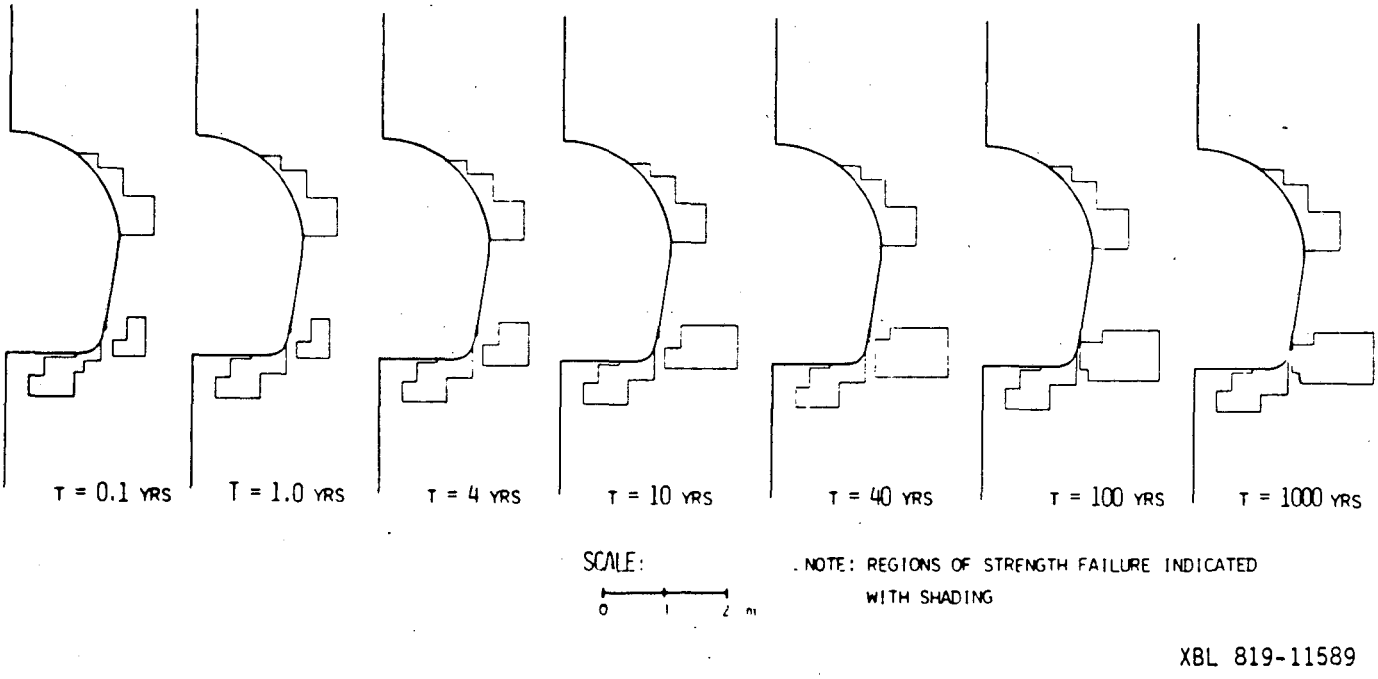

Figure 2.12 Progressive strength failure due to excavation and thermomechanical stresses with joints at 0° and 90° (Ratigan 1977).

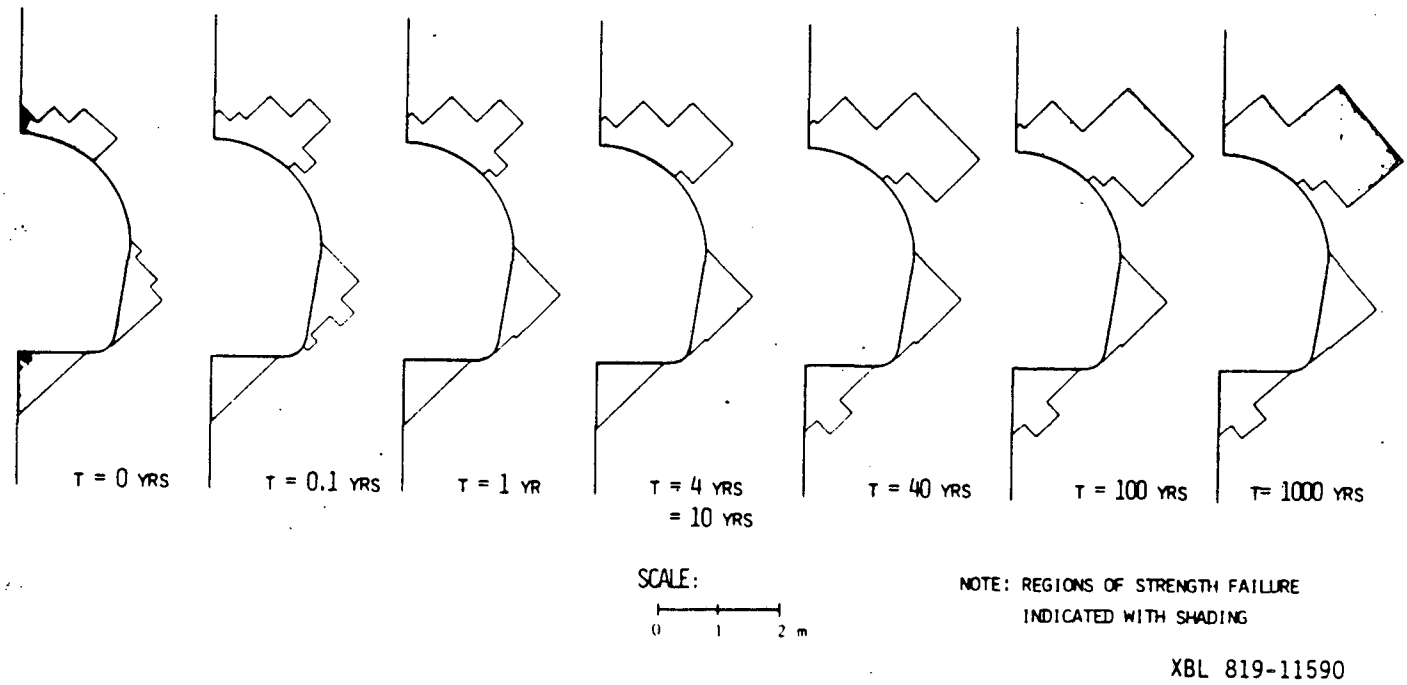

Figure 2.13 Progressive strength failure due to excavation and thermomechanical stresses with joints at 45° and -45° (Ratigan 1977).

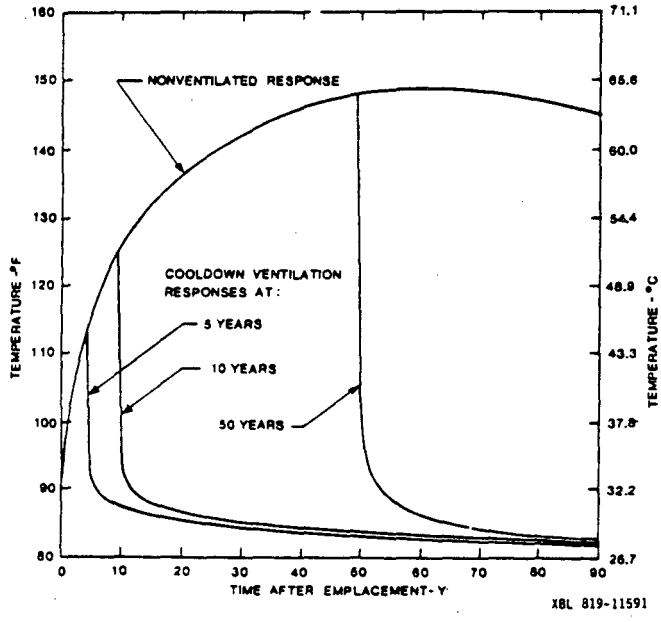

Figure 2.14 Storage room floor temperature histories representing cool-down by 4.72 m^3/s (10,000 ft^3/min) of air from an unventilated state after 5, 10, and 50 years (Altenbach and Lowry 1980).

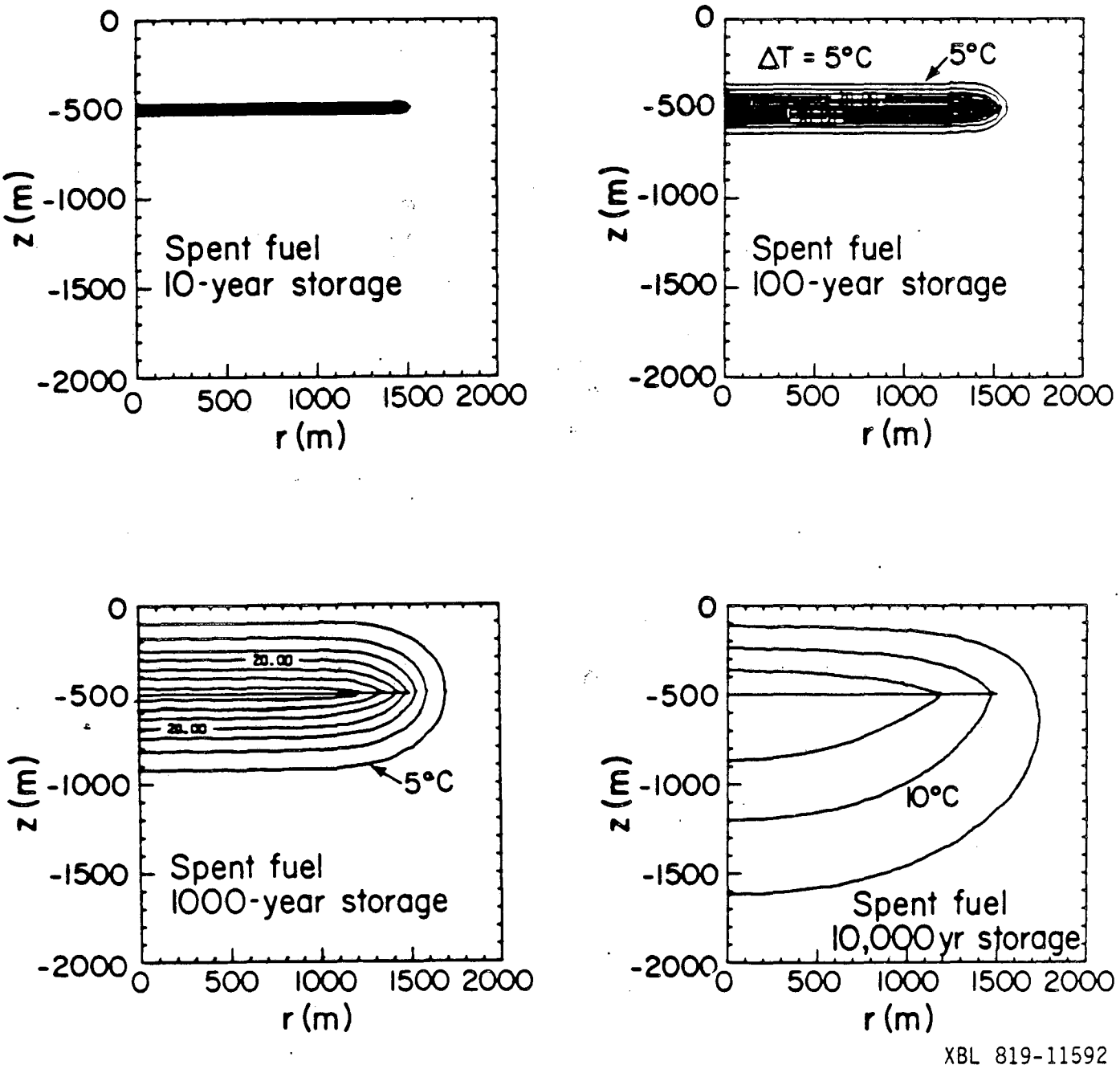

Figure 2.15 Isotherms and profiles of the temperature rise around an SF repository in granite after 10, 10^2, 10^3, and 10^4 years (Wang and others 1981).

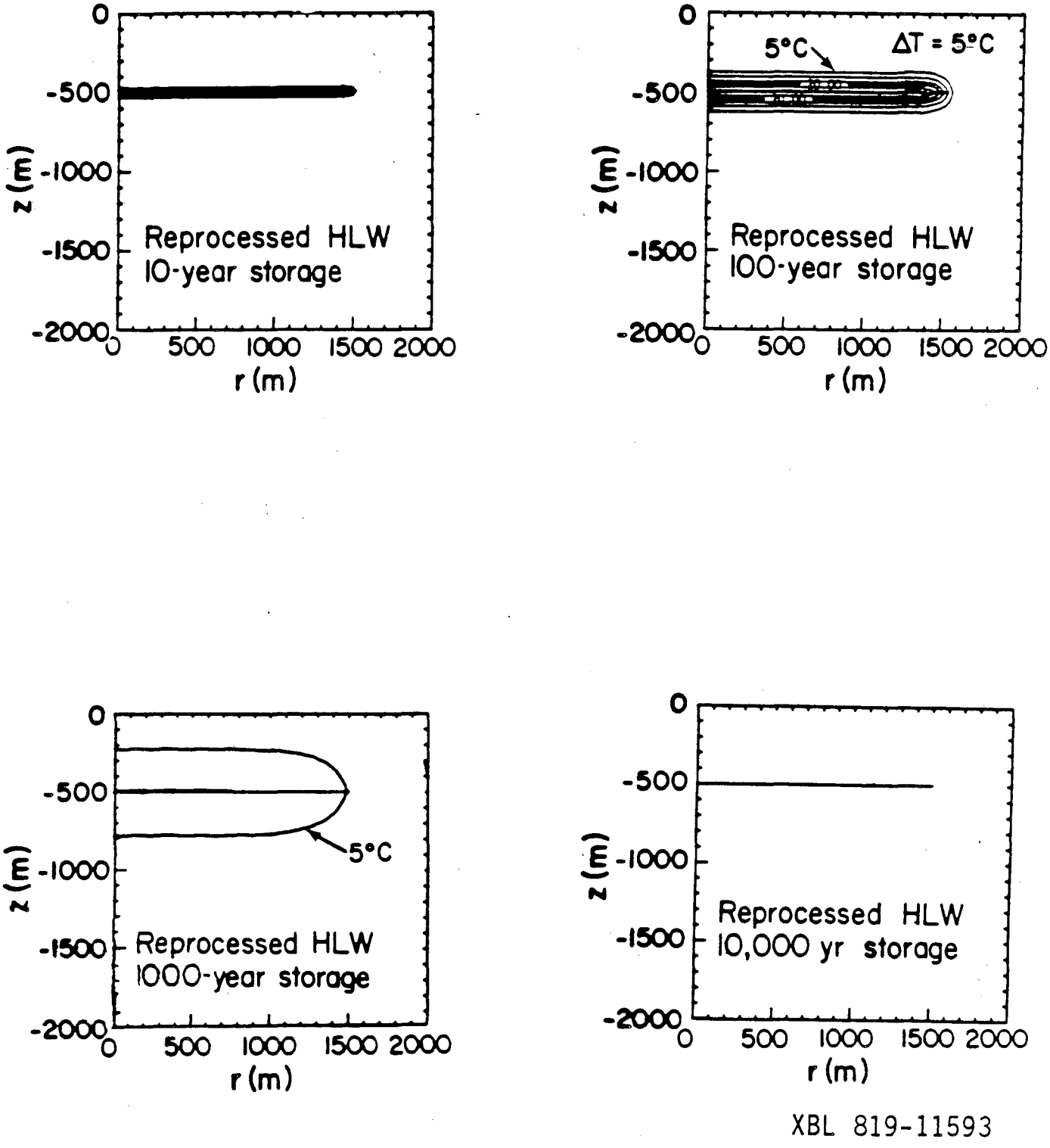

Figure 2.16 Isotherms and profiles of the temperature rise around an HLW repository in granite after 10, 10^2, 10^3, and 10^4 years (Wang and others 1981).

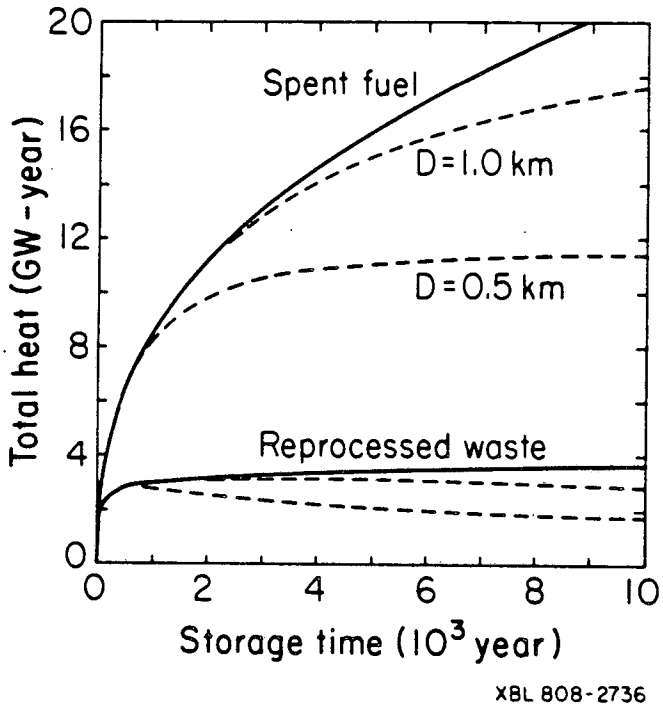

Figure 2.17 Heat released by the buried wastes and heat remaining in the granite formation for a disk-shaped repository 3 km in diameter at different depths (Wang and others 1981).

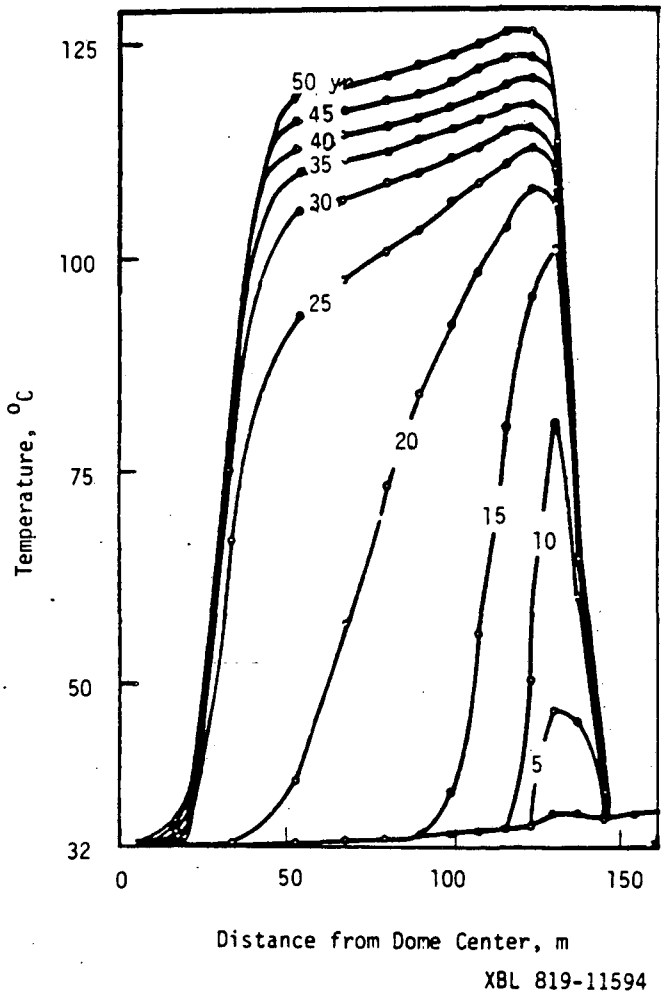

Figure 2.18 Evolution of the temperature distribution for a repository in domed salt loaded sequentially from the outermost boundary toward the dome center (Stearns-Roger Engineering and Woodward-Clyde Consultants 1978).

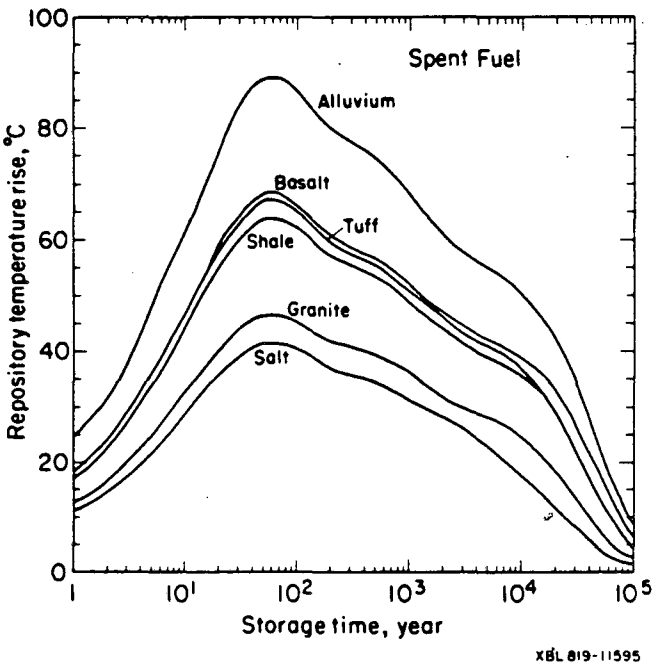

Figure 2.19 History of average SF repository temperature for six major rock types.

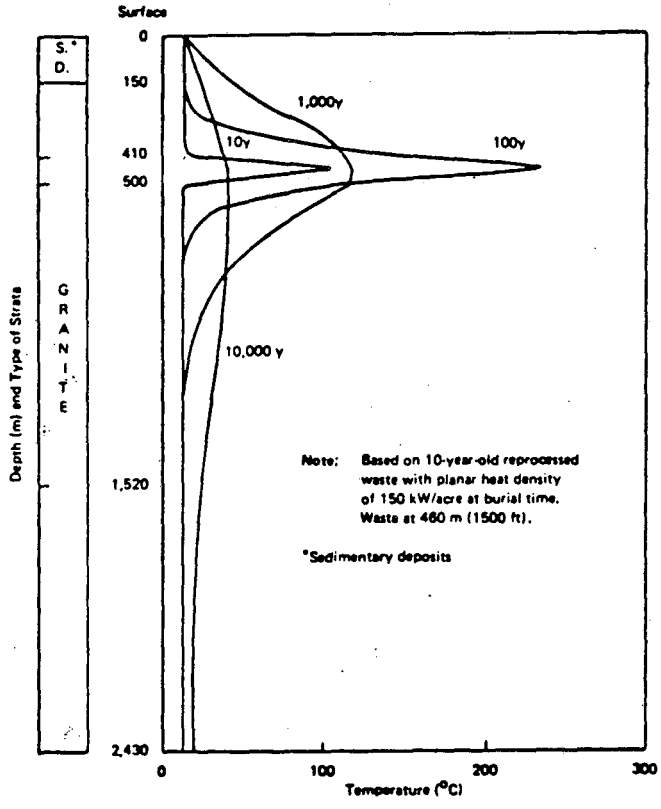

XBL 819-11596

Figure 2.20 Vertical temperature distribution for a repository at 460 m depth in granite, loaded at 37 W/m^2 (150 kW/acre) (EPA 1977).

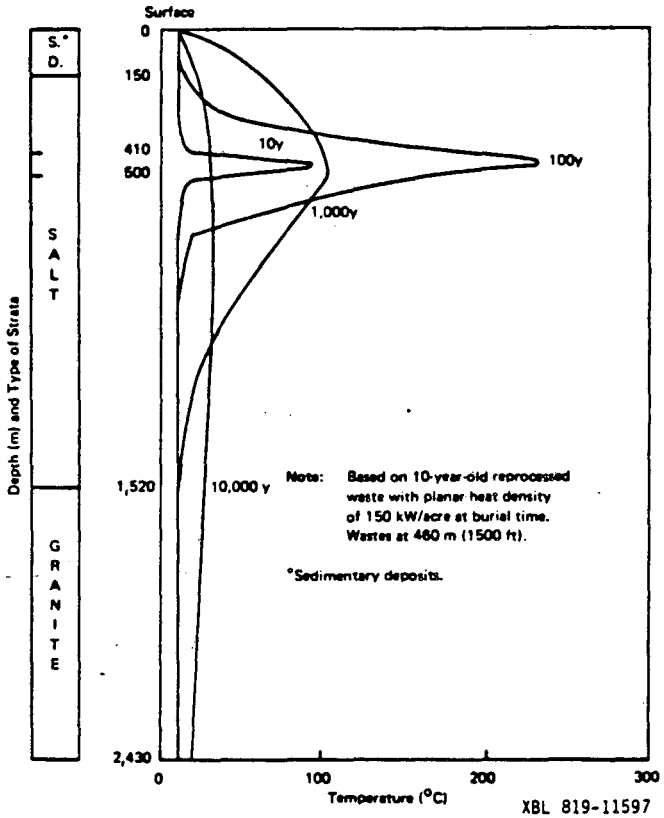

Figure 2.21 Vertical temperature distribution for a repository at 460 m depth in domed salt, loaded at 37 W/m^2 (150 kW/acre) (EPA 1977).

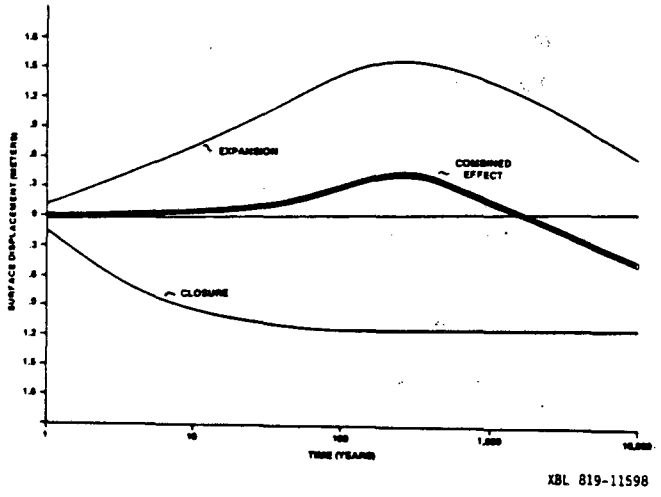

Figure 2.22 Comparison of repository closure and thermal expansion for an HLW repository in salt (INFCE 1980).

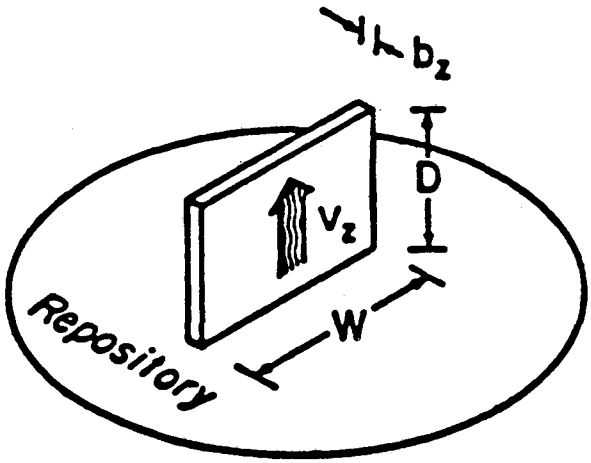

XBL 819-11599

Figure 2.23 Sketch of a vertical fracture from within the repository to the surface (Wang and others 1981).

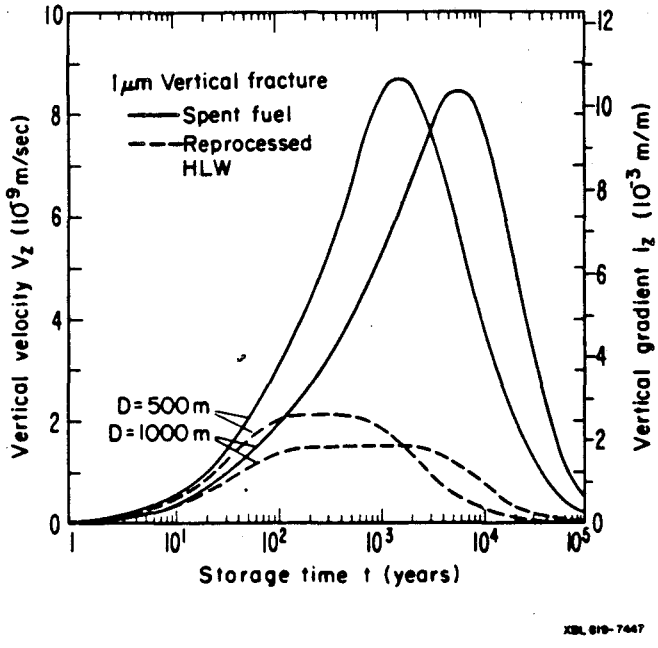

Figure 2.24 Effect of fuel cycle and depth of a repository on the flow velocities, hydraulic gradients, and water movement along a vertical fracture from the repository to the surface (Wang and others 1981).

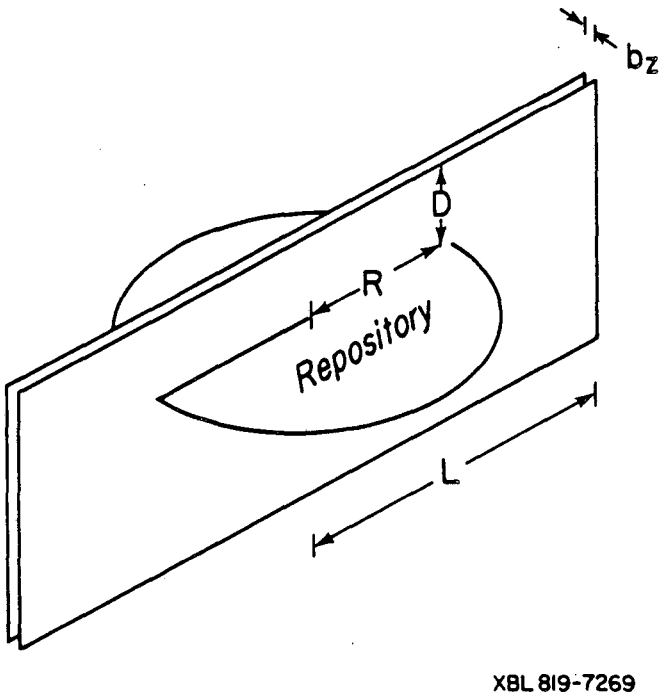

Figure 2.25 Sketch of a vertical fracture through the repository to the surface (Wang and others 1980).

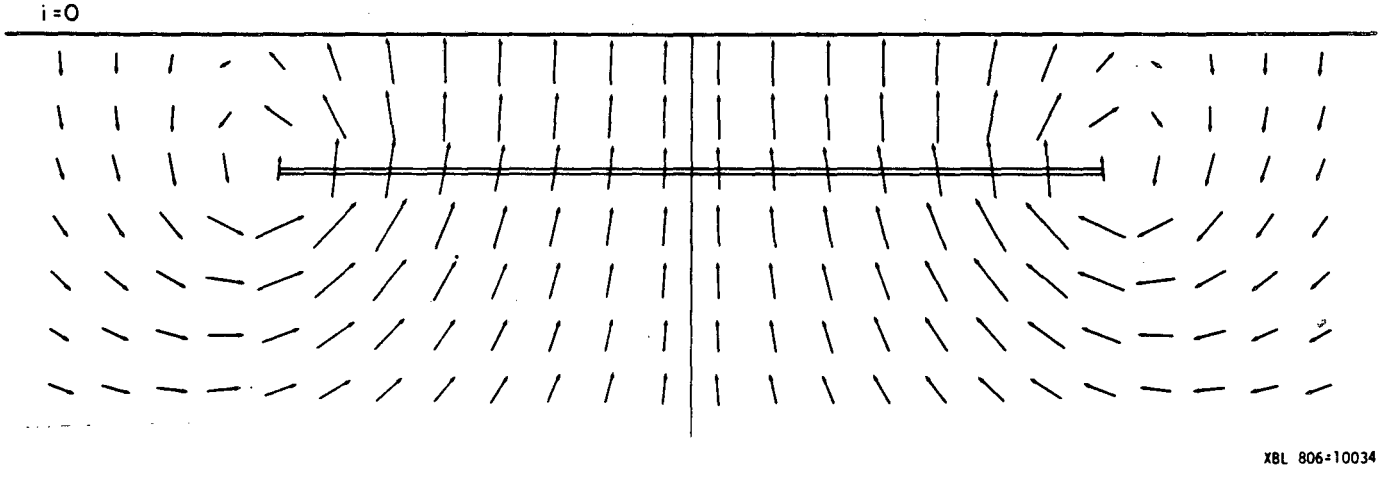

Figure 2.26 Convection cell in an extended vertical fracture around a repository; horizontal gradient = 0.0 m/m (Wang and Tsang 1980).

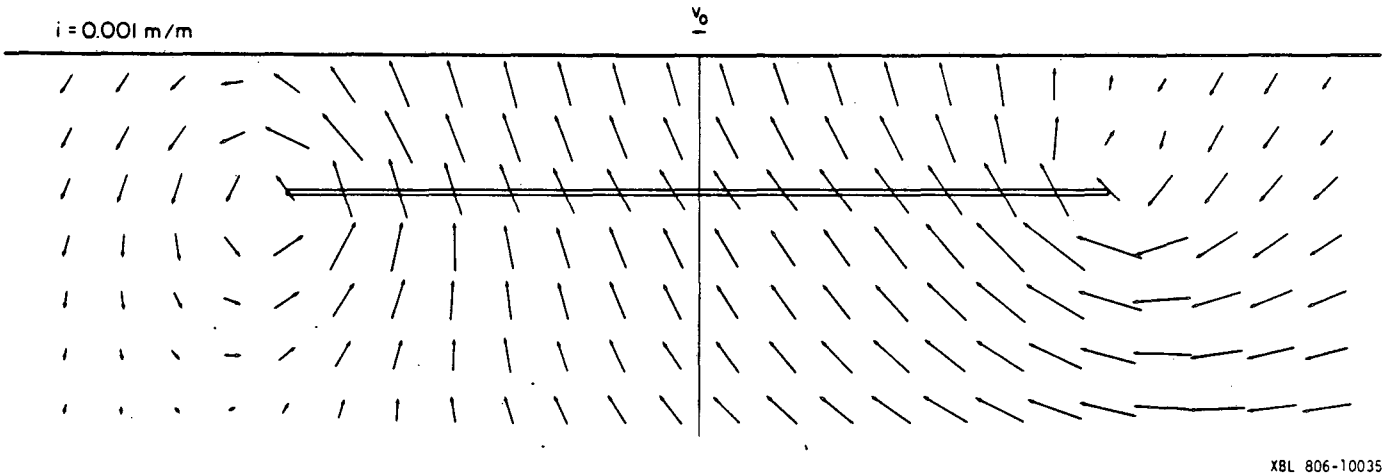

Figure 2.27 Convection cell in an extended vertical fracture around a repository; horizontal gradient = 0.001 m/m (Wang and Tsang 1980).

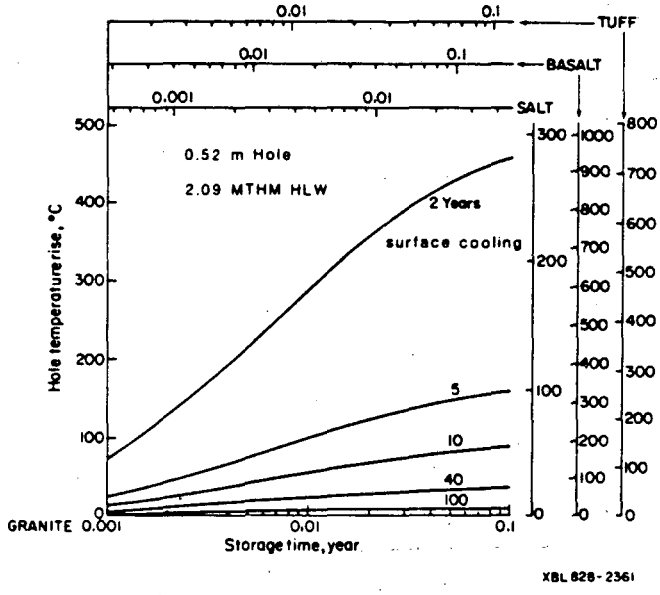

Figure 4.1 Temperature rise at the borehole as a function of surface cooling period.

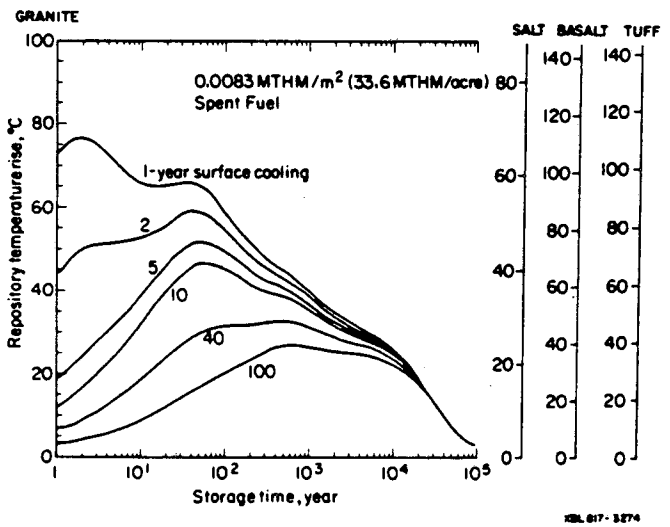

Figure 4.2 Temperature rise in an SF repository as a function of of surface cooling period; constant waste density loading.

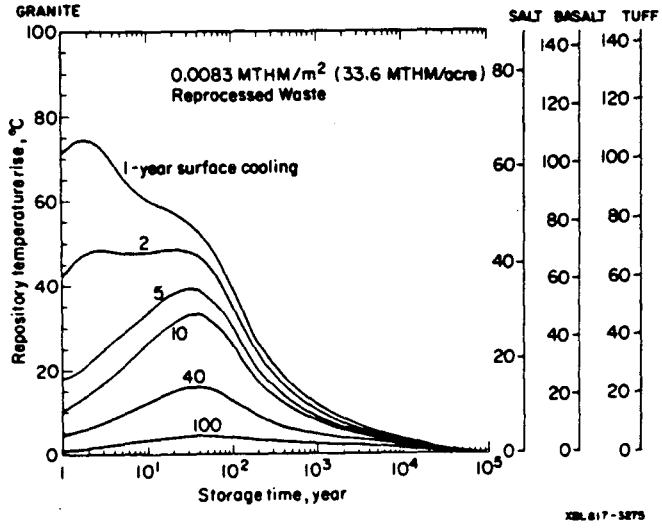

Figure 4.3 Temperature rise in an HLW repository as a function of surface cooling period; constant waste density loading.

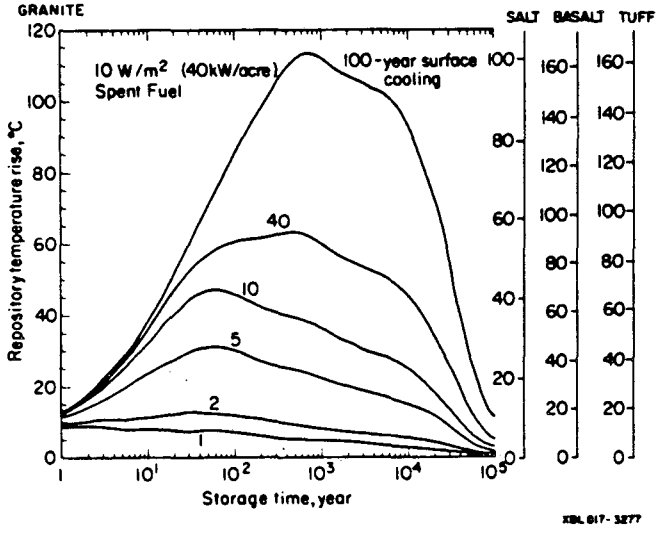

Figure 4.4 Temperature rise in an SF repository as a function of surface cooling period; constant emplacement power density loading.

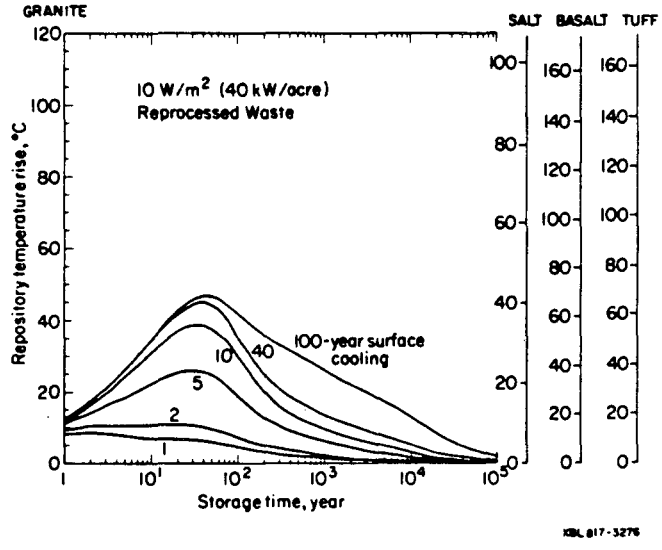

Figure 4.5 Temperature rise in an HLW repository as a function of surface cooling period; constant emplacement power density loading.

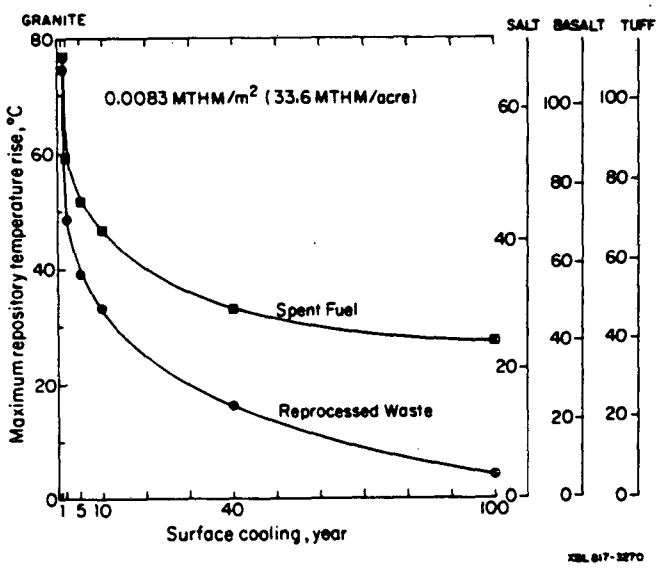

Figure 4.6 Maximum repository temperature rise as a function of surface cooling period; constant waste density loading for SF and HLW.

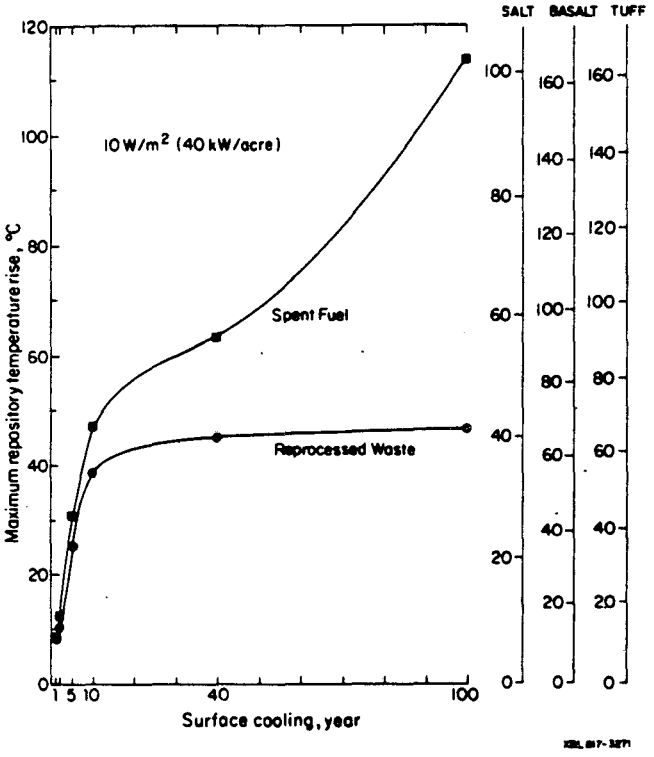

Figure 4.7 Maximum repository temperature rise as a function of surface cooling period; constant emplacement power density loading for SF and HLW.

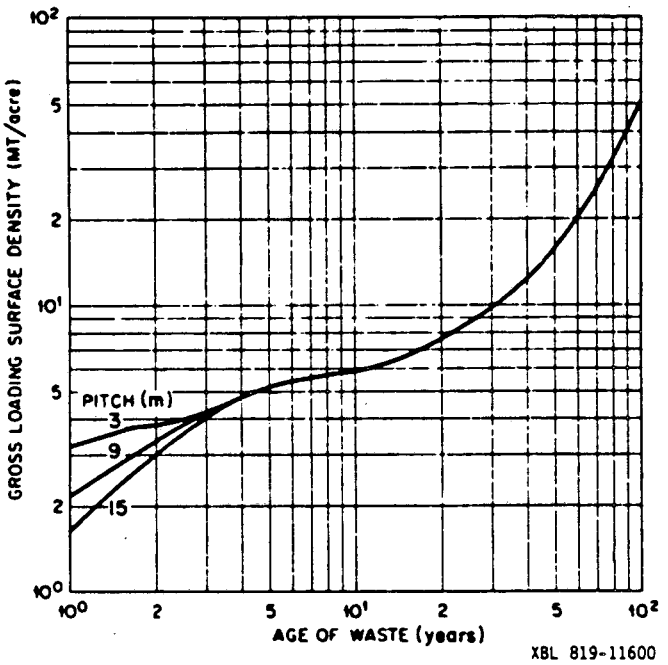

Figure 4.8 Maximum permissible gross loading surface density for a 4.6-m (15-ft) room versus age of waste, based on salt temperature criteria (Cheverton and Turner 1972).

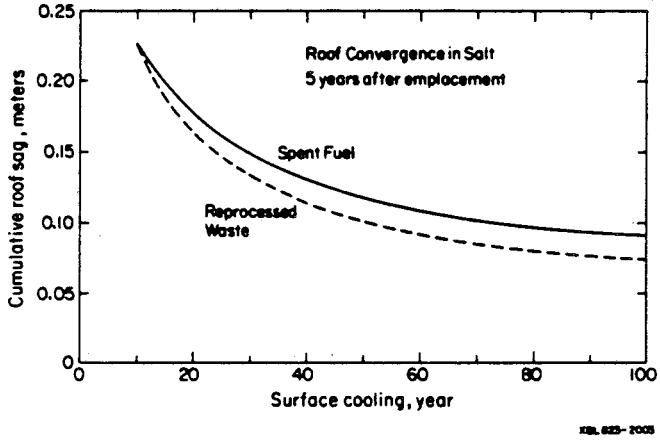

Figure 4.9 Roof convergence in salt as a function of surface cooling period in SF and HLW repositories.

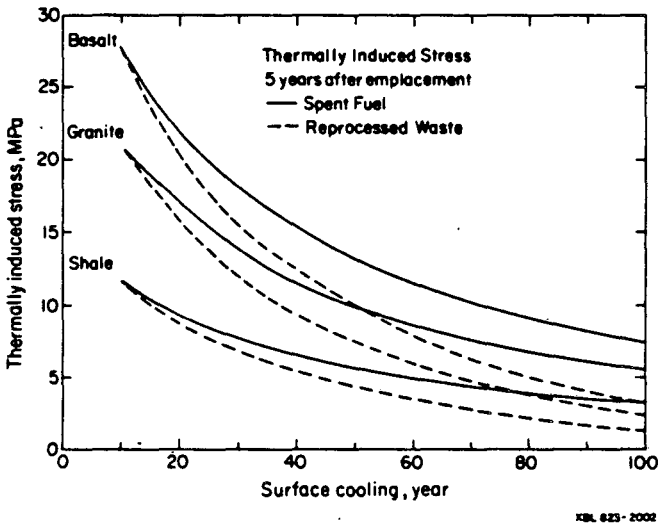

Figure 4.10 Thermally induced stress in granite at 47 W/m^2 (190 kW/acre), basalt at 47 W/m^2 (190 kW/acre), and shale at 30 W/m^2 (120 kW/acre) as a function of surface cooling period in SF and HLW repositories.

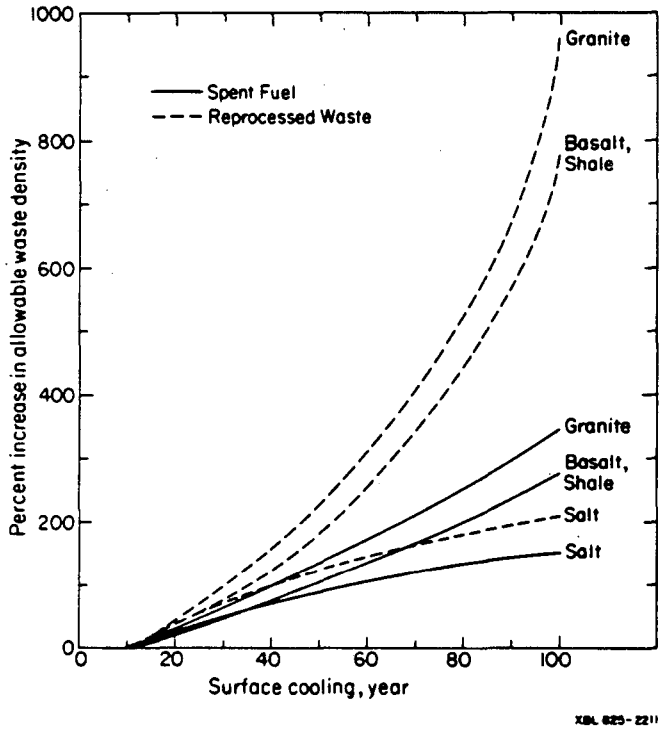

Figure 4.11 Percent increase in allowable waste density in four major rock types as a function of surface cooling period for SF and HLW repositories.

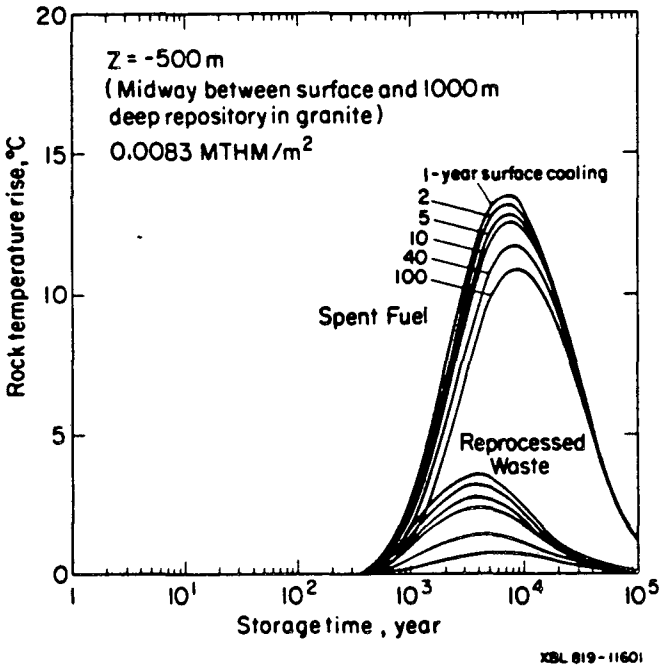

Figure 4.12 Temperature rise at a point midway between the repository and the surface as a function of surface cooling period; constant waste density loading for SF and HLW.

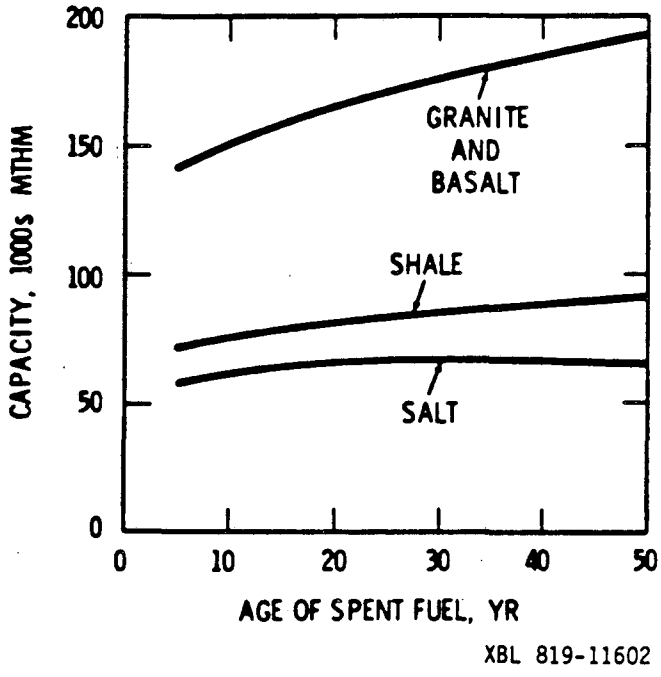

Figure 4.13 Repository capacity as a function of SF age (DOE 1980a).

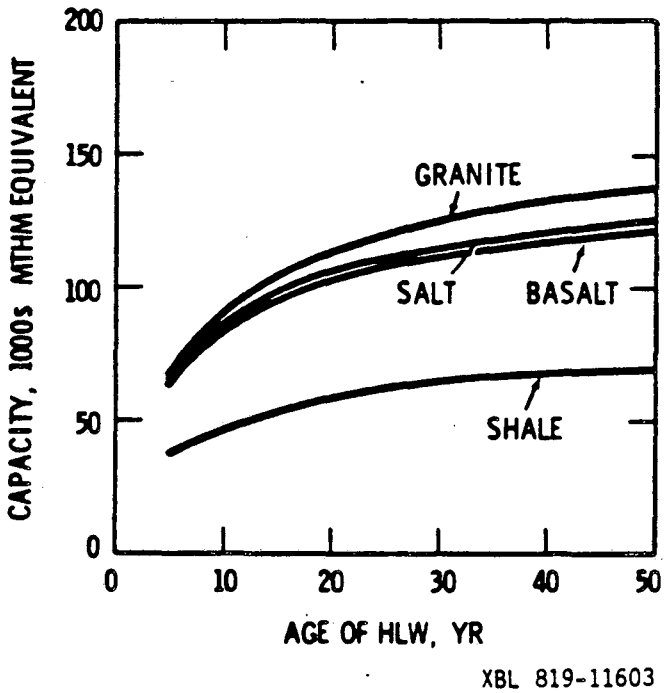

Figure 4.14 Repository capacity as a function of HLW age (DOE 1980a).

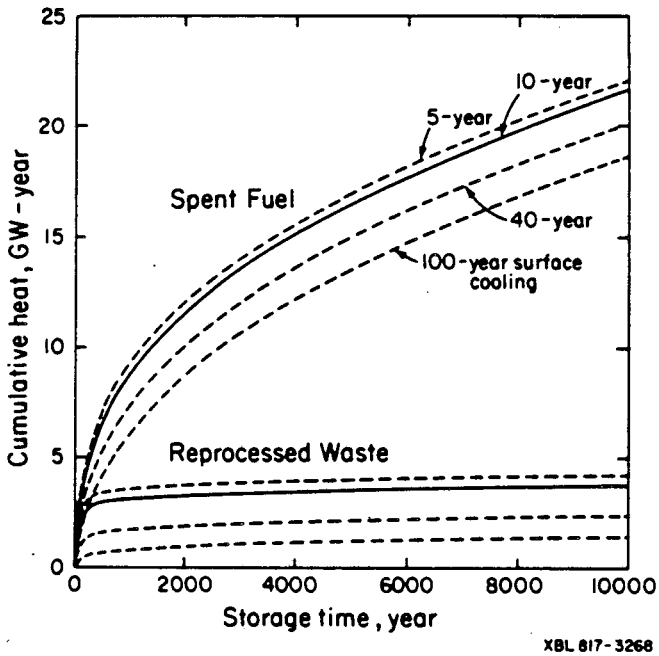

Figure 4.15 Cumulative heat released by SF and HLW as a function of surface cooling period.

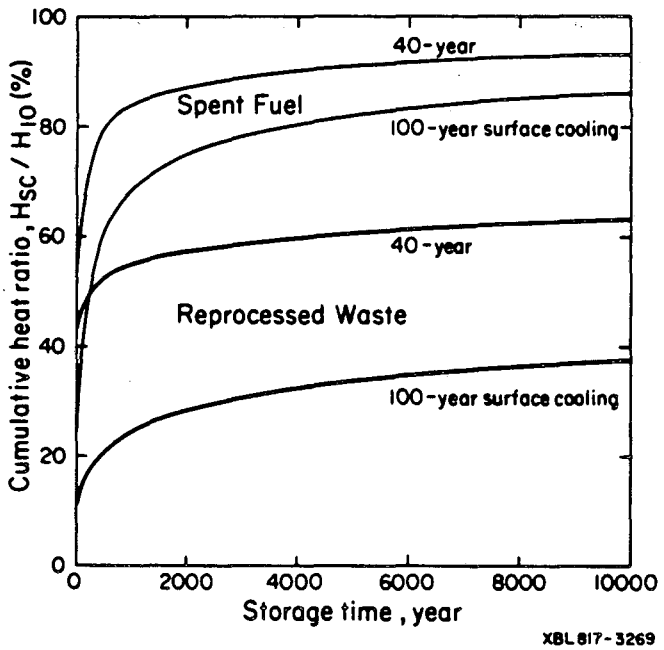

Figure 4.16 Ratio of cumulative heat released by 40-year-old and 100-year-old wastes to that released by 10-year-old wastes.

This report was done with support from the Department of Energy. Any conclusions or opinions expressed in this report represent solely those of the author(s) and not necessarily those of The Regents of the University of California, the Lawrence Berkeley Laboratory or the Department of Energy.

Reference to a company or product name does not imply approval or recommendation of the product by the University of California or the U.S. Department of Energy to the exclusion of others that may be suitable.

LAWRENCE BERKELEY LABORATORY
TECHNICAL INFORMATION DEPARTMENT
UNIVERSITY OF CALIFORNIA
BERKELEY, CALIFORNIA 94720